CELL SURFACE ADHESINS, EXOPOLYSACCHARIDES AND THE POR (TYPE IX) SECRETION SYSTEM OF *FLAVOBACTERIUM JOHNSONIAE*

by

Abhishek Shrivastava

A Dissertation Submitted in

Partial Fulfillment of the

Requirements for the Degree of

Doctor of Philosophy

in Biological Sciences

at

The University of Wisconsin-Milwaukee

May 2013

ABSTRACT

CELL SURFACE ADHESINS, EXOPOLYSACCHARIDES AND THE POR (TYPE IX) SECRETION SYSTEM OF *FLAVOBACTERIUM JOHNSONIAE*

by

Abhishek Shrivastava

The University of Wisconsin-Milwaukee, 2013
Under the Supervision of Dr. Mark J. McBride

Flavobacterium johnsoniae, a member of the phylum *Bacteroidetes*, crawls rapidly over surfaces. Cell movement is thought to result from the action of the gliding motor, composed of Gld proteins, on the cell-surface adhesin SprB. Cells lacking SprB are partially defective in motility. Transposon mutagenesis of an *sprB* mutant resulted in the identification of *remA*, which encodes a motility adhesin that is partially redundant with SprB. Cells lacking SprB and RemA had more severe motility defects than did cells lacking just SprB. RemA moves on the cell-surface with a speed of 1 to 2 μm per sec, similar to SprB. RemA contains a lectin domain that enables it to interact with exopolysaccharides secreted by the cells. RemA-exopolysaccharide interaction resulted in the formation of cell-aggregates. Cells lacking polysaccharide biosynthesis and transport proteins RemC, Wza and Wzc failed to form aggreagates. It appears that as cells move, they pave their own 'roads' with exopolysaccharide. Mobile cell-surface adhesins like RemA adhere to these 'roads' and help in motility of the cell. Recent results suggest that some proteins required for gliding are components of a novel protein secretion system, the Type IX

Bacterial Protein Secretion System (T9SS). The T9SS was initially called the Por Secretion System. T9SSs are found in all gliding bacteroidetes, and in many nongliding bacteroidetes, such as the periodontal pathogen *Porphyromonas gingivalis*, but they are apparently not found outside of the phylum *Bacteroidetes*. GldN, SprE, and SprT were previously shown to be components of the *F. johnsoniae* T9SS. Here we show that GldK, GldL, GldM, and SprA, are also components of this secretion system. The *F. johnsoniae* T9SS is required for secretion of SprB and RemA, and is thus needed for motility. Other proteins required for *F. johnsoniae* gliding, such as GldA, GldF, GldG (which form an ABC transporter complex), and GldB, GldD, GldH, GldI, and GldJ, may interact with the T9SS. Mutations in the genes encoding any of these proteins resulted in apparent instability of the T9SS protein GldK, and thus loss of T9SS function. The gliding motility proteins and the T9SS of *F. johnsoniae* appear to be intertwined. Strains that produced truncated GldJ proteins were isolated that had normal T9SS function but were defective in motility. Further analysis of these strains may enable us to untangle gliding motility from protein secretion.

TABLE OF CONTENTS

LIST Of FIGURES

Chapter 1

Chapter 2

Chapter 3

Chapter 4

Appendix 1

LIST OF TABLES

Chapter 2

Chapter 3

Chapter 4

Appendix 1

Appendix 2

ACKNOWLEDGMENTS

This work could not have been completed without the help of my advisor Dr. Mark J. McBride, my thesis committee members, colleagues in the laboratory and the support of my friends and family.

Dr. Mark J. McBride and Dr. Ryan G. Rhodes had major contributions towards generating the strains used in chapter 2. Dr. Mark J. McBride performed the transposon mutagenesis screen to isolate *remA*, *remB, remC, wza* and *wzc* gene mutants. Dr. Ryan G. Rhodes generated *remA::myc-tag-1, remA::myc-tag-3*, *remA::myc-tag-4* and *remA::myc-tag-5* containing strains and the Δ*remA* and Δ*remA*Δ*sprB* mutant strains CJ2083, CJ2077, C2112, CJ2073, CJ1984 and CJ1985 respectively. Soumya Pochiraju and Dr. Ryan G. Rhodes generated the antiserum against RemA.

Joseph J. Johnston generated the *gldK* and *gldM* deletion strains CJ2122 and CJ2262 described in chapter 3. Jessica van Barren generated the antiserum against GldK, GldL, GldM and GldN described in chapter 3.

Dr. Sreelekha Bollampalli generated the plasmids used to isolate *remC* and *wzc* gene mutants described in Appendix 2.

Working towards a Ph.D at UW-Milwaukee has been a very fulfilling experience for me. I travelled half way around the world, searching for an exciting Ph.D project and I am glad that I found Dr. Mark J. McBride's lab. I have learnt valuable laboratory and life skills from Dr. Mark J. McBride. He has been a constant motivation throughout my Ph.D and his scientific humor is very efficient in reducing the disappointment of failed experiments. I really appreciate the way Dr. Mark J. McBride has developed the field of

Flavobacterium johnsoniae. Thank you Mark, for introducing me to *F. johnsoniae* gliding and to the exciting world of phylum *Bacteroidetes*.

I would also like to thank Dr. Daad A. Saffarini for her inputs towards my projects during our common lab meetings and for letting me use her lab's equipments. Our lab collaborates with Dr. Daad A. Saffarini's lab on a daily basis and I have used a lot of equipments from her lab for my research. I would also like to thank my committee members Dr. Sonia L. Bardy, Dr. Ching-Hong Yang and Dr. Sergei Kuchin for their inputs during my committee meetings and for their constant direction and support towards my projects.

This project could not have been completed without the help of my previous and current lab members and the members of the Saffarini lab. Dr. Yongtao Zhu, Sampada S. Kharade, Joseph J. Johnston and Surashree Kulkarni, thank you for being good 'gliders'. I wish you the very best for your future.

I have been blessed with wonderful friends here in Milwaukee. Hitting the gym in the evening after lab with my friends was a great stress buster. I would like to thank my friends in my tennis and racquetball groups. You guys are awesome and I really thank you guys for helping me recharge my batteries.

The role of my family towards supporting me through my Ph.D has been very important. Thank you mom for supporting me in my initial decision of choosing a career in science. You have very selfelessly motivated me to attain the highest academic degree possible. I would also like to thank my wife Dhara for being a great friend, colleague and chef. Thank you for patiently listening to my research talks and for making grad school a lot more interesting.

Chapter 1: Introduction

Flavobacterium johnsoniae is a Gram negative, rod shaped bacterium that belongs to the phylum *Bacteroidetes*. Like many members of the phylum *Bacteroidetes, F. johnsoniae* is capable of secreting extracellular enzymes that help digest macromolecules such as polysaccharides and proteins (14, 33). *F. johnsoniae* is a nonpathogenic soil bacterium but some of its close relatives are important fish pathogens. Of particular concern for fish are *Flavobacterium columnare, Flavobacterium psychrophilum*, and *Flavobacterium branchiophilum* (2). Because of ease of growth and efficient genetic techniques developed by our lab, *F. johnsoniae* has emerged as a very good model organism to study processes that are common among members of the phylum *Bacteroidetes*, including the recently described bacterial Type IX secretion system (T9SS). T9SSs are important for secretion of extracellular enzymes, virulence factors and cell surface adhesins (15, 23, 25, 27).

Gliding motility

Many members of the phylum *Bacteroidetes* crawl over a wide range of surfaces by a process called gliding motility (15). Bacterial gliding motility is loosely defined as movement of a cell without the help of a flagellum or pilus. Examples of bacteria that exhibit gliding motility are found in many bacterial phyla (Figure 1). In most gliders, the mechanism of movement is very poorly understood. Study of *F. johnsoniae* gliding has been a focus of our lab for many years. We recently discovered that the *F. johnsoniae* gliding motility machinery is intertwined with the T9SS (Shrivastava et al. in

preparation). Study of *F. johnsoniae* gliding and protein secretion can help us understand the function of a large set of proteins that are present in many members of the phylum *Bacteroidetes*.

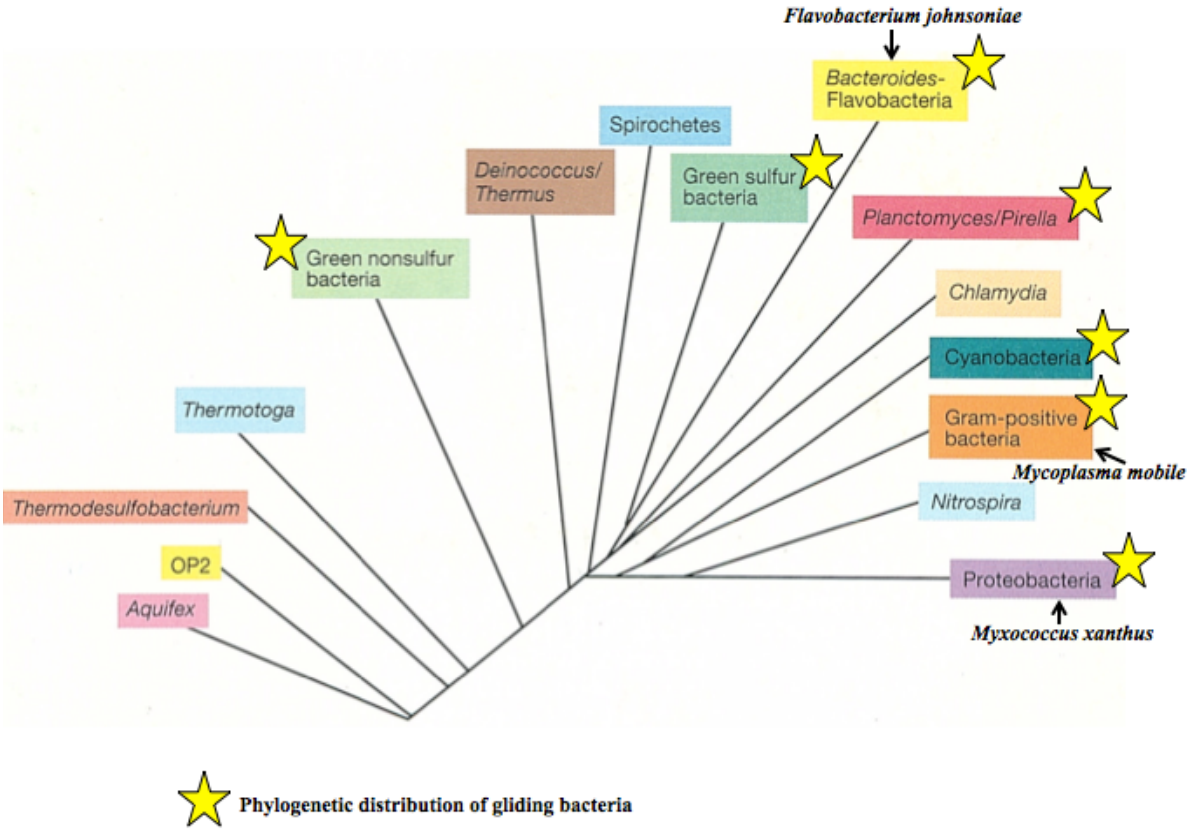

Figure 1. Phylogenetic tree of bacteria. Adapted from : Brock Biology of Microorganisms. Madigan, Martinko, Parker (Ninth edition). Branches with yellow stars are known to have some members that exhibit gliding motility.

F. johnsoniae forms thin spreading colonies on agar surfaces. *F. johnsoniae* cells attach to and move over glass or Teflon surfaces at a speed of approximately 2 μm/sec. The types of movement observed include (i) movement along a straight path (ii) back and

forth motion (iii) flipping and looping and (iv) attaching at one pole and rotating (Figure 2)

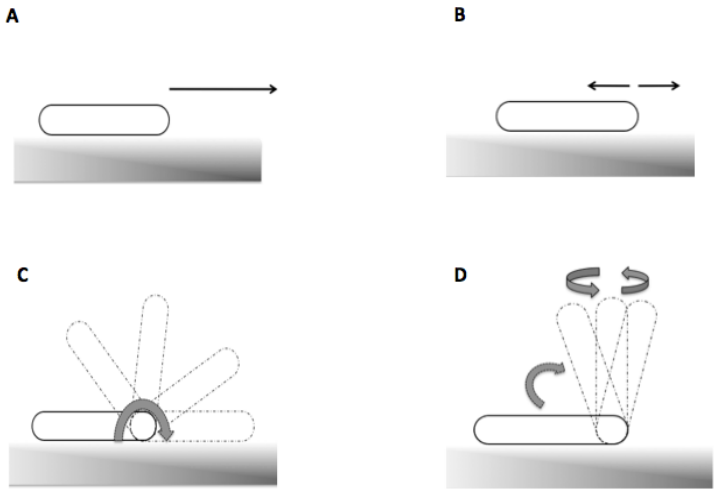

Figure 2. *F. johnsoniae* movement (A) Forward motion (B) Back and forth motion (C) Flipping and looping (D) Attaching at one pole and rotating

F. johnsoniae, *Myxococcus xanthus* (δ proteobacteria) and *Mycoplasma mobile* (firmicutes) are the three most extensively studied gliding bacteria. No similarity in the motility related genes and proteins is found among these three bacteria. *M. mobile* is flask shaped while *F. johnsoniae* and *M. xanthus* are both rod shaped. *M. mobile* and *F. johnsoniae* glide on surfaces at speeds of 2-5 μm/sec (10, 17) while *M. xanthus* cells glide at comparatively much slower speeds of approximately 4 μm/min (18).

M. mobile has a neck region and its gliding machinery exists at the base of its neck region. It is thought that many flexible legs project outside the cell and are supported by cytoskeletal structures from inside the cell. The cell is thought to move in a centipede like fashion. The legs bind to various surfaces and the cells are propelled by repeated binding

and releasing of the legs (17). The motor which causes the legs to move and the mechanisms that lead to the binding and releasing of the legs are not known. Because of the flask like shape of *M. mobile* and specific localization of its motility adhesins in the neck region, it does not appear that *M. mobile* and *F. johnsoniae* gliding are mechanistically similar. Further, *M. mobile* gliding is powered by ATP hydrolysis (17, 30) whereas *F. johnsoniae* gliding is apparently powered by the proton gradient across the membrane (32).

M. xanthus has two types of motility systems: the Social 'S' motility system which is a term used to define coordinated group movements and the Adventurous 'A' motility system which is a term used to define single cell movement (34). The Social motility system requires interaction between Type 4 pili and exopolysaccharide and is essentially the same as twitching motility (5). The 'A' motility system is a true gliding motility system. The most widely accepted model of 'A' motility is the 'Focal adhesion complex' model (16). According to this model, soluble proteins form clusters that are regularly distributed along the body of the rod shaped cell. These clusters are called focal adhesion complexes. A motor comprised of AglR, AglQ and AglS is thought to enable the movement of these complexes (28). The movement of the focal adhesion complex is thought to drive the movement of unknown cell-surface adhesins. This movement of cell-surface adhesins results in movement of the cell. While the identification of moving cell-surface adhesins is still a big challenge for the *M. xanthus* field, movement of latex spheres on the cell surface provides support to this model (28). This recent model for *M. xanthus* movement appears to be very similar to the one proposed for *F. johnsoniae* (11,

27). It is possible that despite having different proteins, these two rod-shaped bacteria follow similar physical principles to crawl over various surfaces.

We used genetic and genomic approaches to identify moving *F. johnsoniae* cell-surface adhesins involved in cell movement. SprB is the major mobile *F. johnsoniae* cell-surface adhesin (19). SprB is an unusually large protein and has an approximate molecular mass of 669 kDa. *sprB* homologs are found in many members of the phylum *Bacteroidetes*. Cryo-electron tomography of *F. johnsoniae* has revealed thin filaments extending from its outer membrane (10). Similar filaments were observed by electron microscopy of negatively stained cells, and these filaments were not observed in an *sprB* mutant suggesting that the filaments are made of SprB (Nakane et al. unpublished). Anti-SprB coated latex spheres and immunofluorescence microscopy (19); (Nakane et al. unpublished) were used to reveal that SprB moves along the length of the cell in a semi-helical fashion. Disruption of *sprB* results in the formation of nonspreading colonies, in contrast to the thin spreading colonies produced by wild-type cells (Figure 3). However, *sprB* mutant cells retain some ability to crawl on glass surfaces (Figure 4). This suggests that other mobile SprB-like proteins might be present on the surface of *F. johnsoniae*.

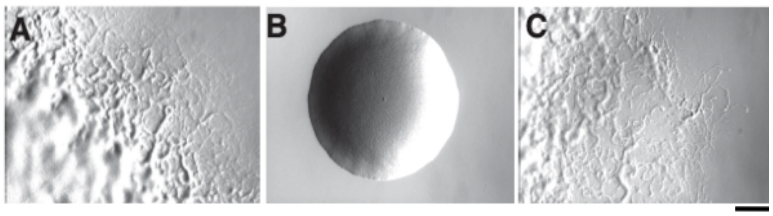

Figure 3. Photomicrographs of *F. johnsoniae* colonies. (A) wild-type *F. johnsoniae* FJ1 (B) *sprB* mutant FJ156 (C) FJ156 complemented with pSN60 which carries *sprB*. Bar in panel C = 0.5 mm (applies to all panels). (19)

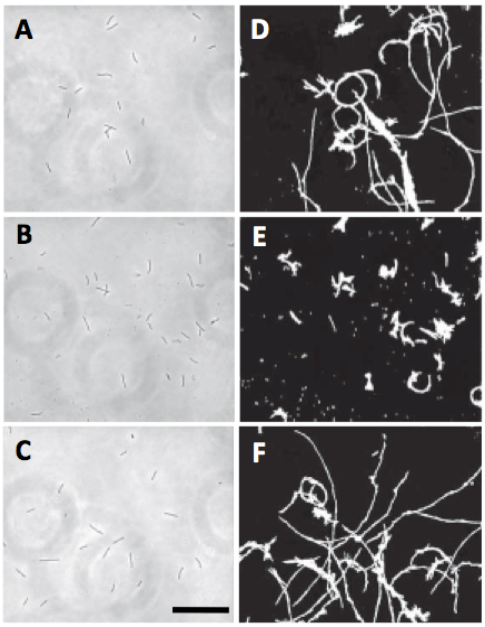

Figure 4. Effects of mutations in *sprB* on gliding of cells on glass. (A) Wild-type strain FJ1, (B) *sprB* mutant FJ156, (C) FJ156 complemented with pSN60. Tracks illustrating the movements of the cells shown in panel A to C over a 106-s period were obtained by superimposing individual digital video frames of (D) wild-type strain FJ1, (E) *sprB* mutant FJ156 and (F) FJ156 complemented with pSN60. Bar in panel C = 75 μm (applies to all panels). Nelson S.S., Bolampalli S and McBride M.J., Journal of Bacteriology 2008, 190(8):2851.

Analysis of the *F. johnsoniae* genome sequence revealed many *sprB* paralogs, any of which might explain the residual motility exhibited by the *sprB* mutants. In this thesis, I describe a mobile cell-surface adhesin RemA and its effect on the motility and physiology of *F. johnsoniae*. RemA and SprB show regions of sequence similarity. RemA also has a SUEL-like lectin domain. The lectin domain enables protein-polysaccharide interactions that contribute to cell-aggregation and group motility. We also show that SprB and RemA move rapidly on the cell surface independent of each other (27). However, the proteins that comprise the motors that propel SprB and RemA remain unknown (Figure 5).

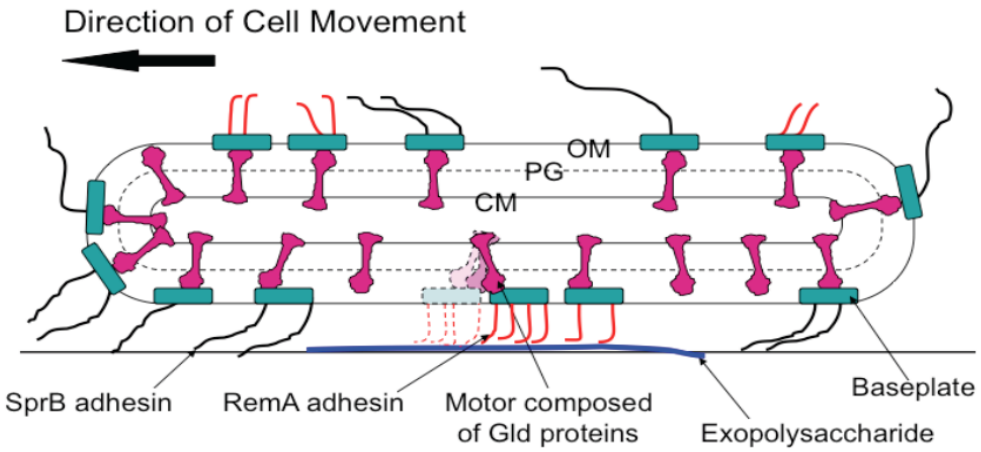

Figure 5. Model of *F. johnsoniae* gliding motility. Gld proteins anchored in the cell envelope form the motors (pink) that propel baseplates (turquoise) attached to adhesins such as SprB (black) and RemA (red) along the cell surface until they can be picked up by the next motor. Exopolysaccharides (blue) enhance motility by coating the substratum and interacting with specific adhesins such as RemA. In this model, the motors remain fixed with respect to the cell, and propel the adhesins along the length of the cell. Attachment of the adhesins to the substratum (directly or via exopolysaccharide) allows the motors to transmit the force that propels the cell along the substratum. CM cytoplasmic membrane; OM- outer membrane; PG- peptidoglycan (27).

Bacteroidetes-specific gliding motility is quite common but its exact mechanism is very poorly understood. *F. johnsoniae* is the most extensively studied gliding member of the phylum *Bacteroidetes*. Nineteen *F. johnsoniae* genes have been discovered so far, mutants of which are defective in gliding. These genes are divided into two categories, *gld* and *spr*. *F. johnsoniae* cells with mutations in the *gld* genes are completely nonmotile while the *spr* gene mutants show reduced but still noticeable movements (1, 3, 4, 6-8, 12, 13, 19, 20). Some of the Gld and Spr proteins may be components of the machinery that propels SprB and RemA along the cell-surface.

Bacterial protein secretion systems

Some of the Gld and Spr proteins are also essential components of the newly discovered T9SS, which has previously been referred to as the PorSS. Bacteria employ diverse strategies to secrete proteins. Transport of virulence factors and enzymes that degrade complex macromolecules gives obvious competitive advantages to bacteria. Secretion of proteins through bacterial membranes often involves a set of proteins that form specialized protein secretion systems. Eight bacterial protein secretion systems have been classified as Type I to Type VIII secretion systems (15, 29) and (Figure 6). The Type I to Type VI secretion systems and the Type VIII secretion system (also known as the extracellular nucleation-precipitation (ENP) pathway involved in secretion and assembly of curly amyloid fibers) are present in Gram negative bacteria. Type I, Type III, Type IV and Type VI Secretion System are used for transport of proteins across the inner and outer membranes in a single step. In contrast, the Type II, Type V and Type VIII secretion systems function in conjunction with the Sec or Tat protein export pathways (9). The Sec or Tat protein export pathways transport proteins across the inner membrane into the periplasm. These proteins are then transported across the outer membrane via the Type II, Type V or TypeVIII Secretion Systems. The Type VII secretion system is found in the Gram positive mycobacteria. The exact mechanism of transport of proteins via the Type VII Secretion System is not known.

T9SS proteins are not similar to any of the components of Type I to Type VIII protein secretion systems. T9SSs are common among members of the phylum *Bacteroidetes* and are not found outside of this phylum (15) and (Figure 7). The gliding motility machinery and T9SS appear to be intertwined in many cases. Among the gliding

members, T9SSs are involved in secretion of gliding motility related cell-surface adhesins such as SprB. Members of the phylum *Bacteroidetes* also secrete enzymes to digest complex macromolecules via the T9SS. In the nonmotile pathogenic bacterium *Porphyromonas gingivalis*, gingipain proteases are secreted via the T9SS (25, 26). *F. johnsoniae* and *P. gingivalis* were the first bacteria in which T9SSs were discovered (25). Because of efficient genetic manipulation techniques and ease of cultivation, *F. johnsoniae* has emerged as a model system to study the T9SS. Since most of the *F. johnsoniae* motility gene mutants are also deficient in secretion via the T9SS, a complete understanding of the mechanism of *F. johnsoniae* gliding requires knowledge of the T9SS.

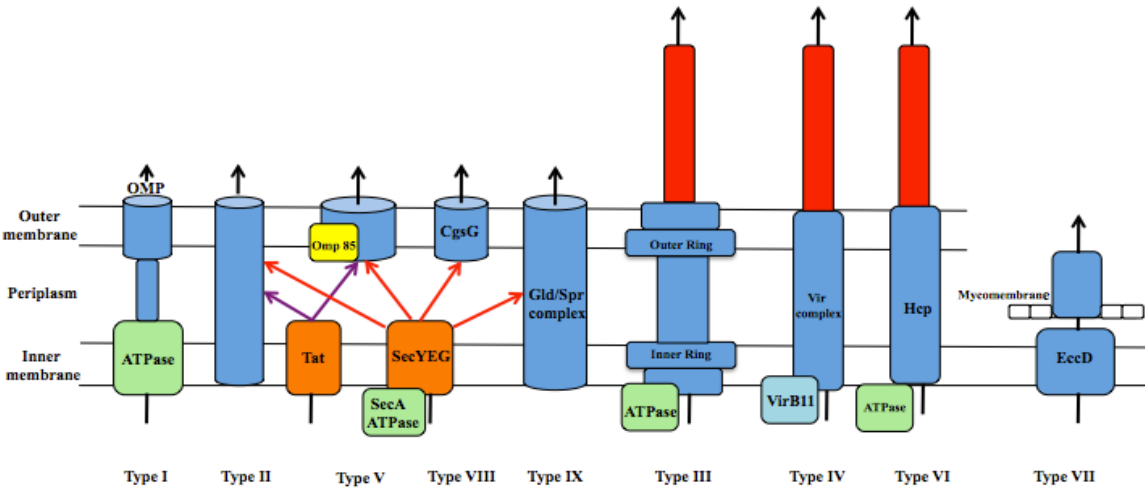

Figure 6. Bacterial Type I – Type IX protein secretion systems. Type II, TypeV, Type VIII and Type IX secretion systems function in association with the Sec or Tat protein export pathways. Type I secretion system is composed of an ABC transporter which transports proteins from the cytoplasm. The ABC transporter is connected to an outer membrane protein. Type III, Type IV and Type VI secretion systems transport proteins from the cytoplasm via needle like structures.

These needles can sometimes puncture host cell membranes and deliver toxins. Type VII secretion system is found in Gram positive mycobacteria.

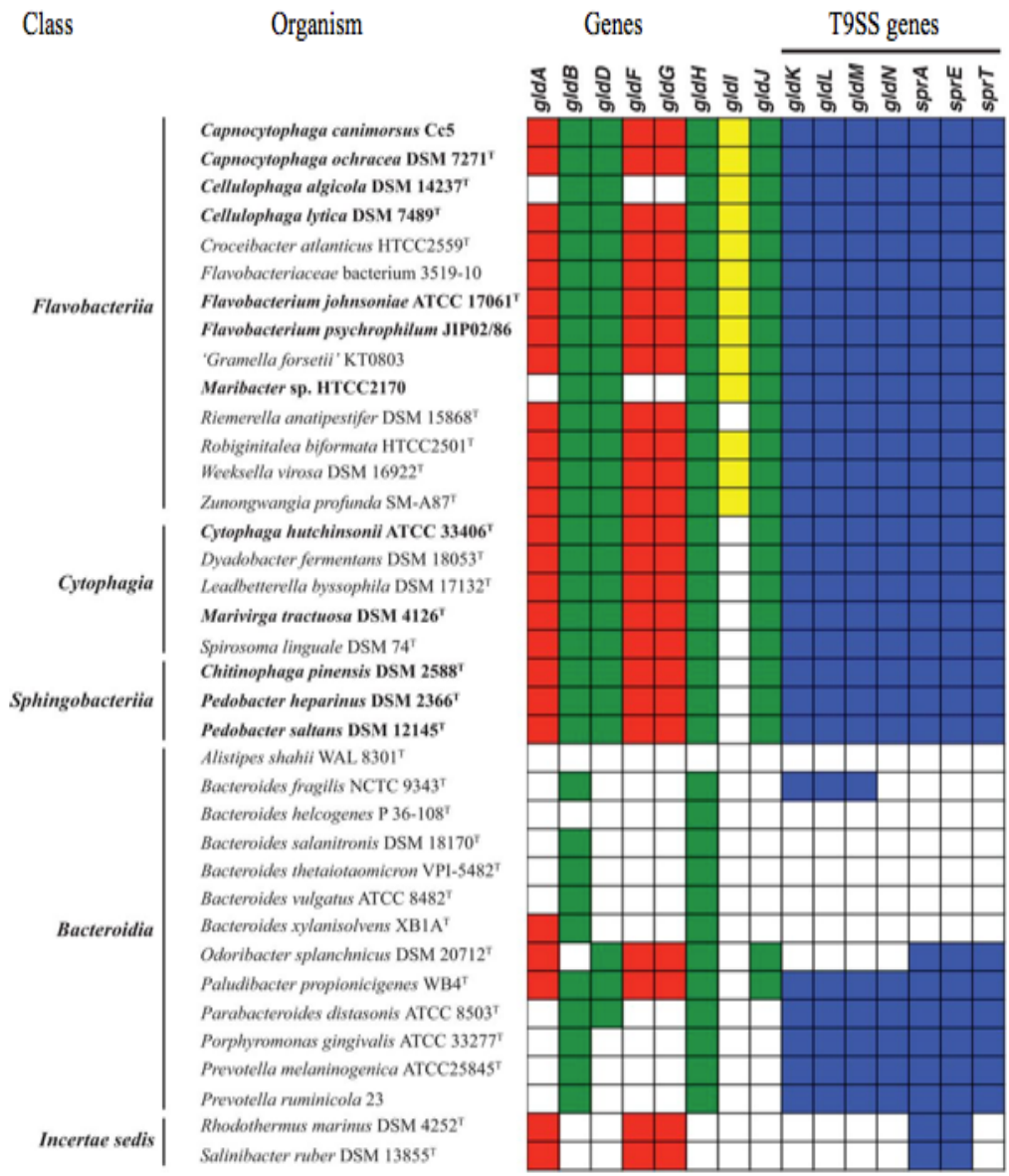

Figure 7. Distibution of T9SS proteins among members of phylum *Bacteroidetes* (15). A colored square indicated the presence of an ortholog and a white square indicates the absence of an ortholog. Blue boxes represent T9SS proteins. Red boxes represent ABC transporter components; yellow boxes, peptidylprolylisomerase; green boxes, additional proteins required for gliding (15).

Interconnection between gliding motility and T9SS

In this thesis I present evidence that *F. johnsoniae* GldK, GldL, GldM, GldN, SprA, SprE and SprT are required for secretion of the mobile cell surface adhesins SprB and RemA (23-25), Shrivastava et al. in review. These proteins are also required for chitin utilization, possibly by secretion of a novel chitinase. GldK, GldL, GldM, and GldN are novel proteins, and their exact functions are not known. Analysis of genome sequences revealed orthologs to the genes encoding each of these proteins in many members of the phylum *Bacteroidetes*, but not in other bacteria. The genetic organization of *gldK*, *gldL*, *gldM* and *gldN* is highly conserved with these four genes found next to each other in the same order in nearly every case. In this thesis I present evidence that *F. johnsoniae gldK*, *gldL*, *gldM* and *gldN* are cotranscribed. I also present evidence suggesting that GldK, GldL, GldM and GldN might interact and form the core of the T9SS.

SprA, SprE and SprT are also thought to be part of the T9SS complex. Wild-type *F. johnsoniae* is sensitive to bacteriophage ϕCj1, ϕCj13, ϕCj23, ϕCj28, ϕCj29, ϕCj42, ϕCj48 and ϕCj54 but cells with mutations in *gldK*, *gldL*, *gldM* and *gldN* are resistant to infection by these bacteriophages (23) Shrivastava et al. in review. It appears that SprB is a receptor for *F. johnsoniae* bacteriophages ϕCj1, ϕCj13, ϕCj23 and ϕCj29 (19, 22) and RemA appears to be a receptor for phages ϕCj42, ϕCj48 and ϕCj54 (27). The receptor for phage ϕCj28 is not known (Figure 8). *F. johnsoniae* cells with mutations in *sprA*, *sprE* and *sprT* are resistant to some but not all bacteriophages (24) and Shrivastava et al. in review. This suggests that SprA, SprE and SprT are involved in secretion of some but not

all proteins secreted by T9SS. *F. johnsoniae* cells with mutations in *sprA*, *sprE* and *sprT* show severe motility defects (20, 24, 25).

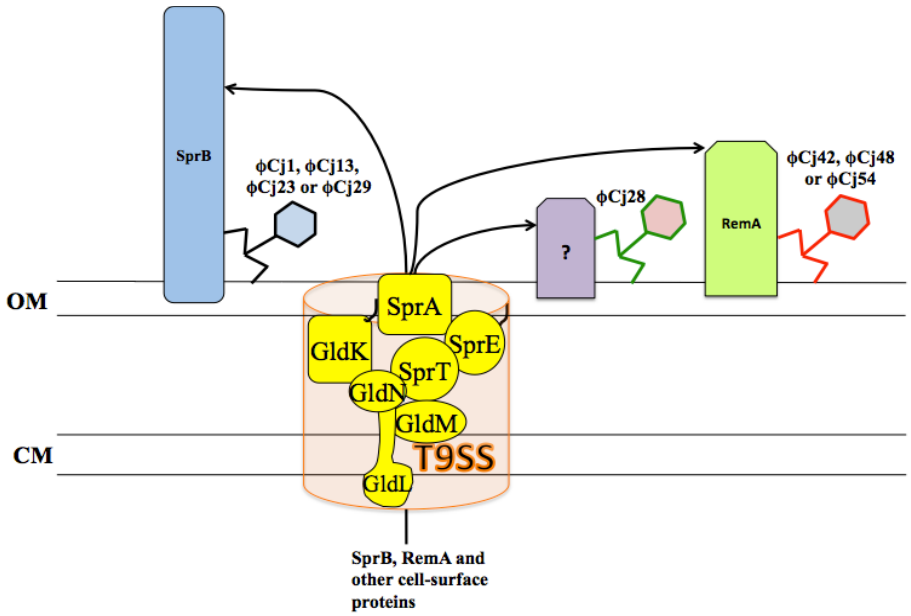

Figure 8. *F. johnsoniae* bacteriophage receptors. SprB, RemA and unknown protein/s represented with '?' are secreted via the T9SS. SprB is the receptor for ϕCj1, ϕCj13, ϕCj23 and ϕCj29 and RemA is a receptor for ϕCj42, ϕCj48 and ϕCj54. The receptor for ϕCj28 is not known.

SprA is similar in sequence to the *P. gingivalis* T9SS protein Sov. SprA appears to have an amino-terminal hydrophobic signal peptide, but the bulk of the protein is predicted to be hydrophilic. SprA is not predicted to have an extensive β sheet structure. PSORTb analysis suggests that it is an outer membrane protein. Proteinase K treatment of *F. johnsoniae* cells indicates that part of SprA is exposed on the cell surface (20).

F. johnsoniae SprE is a membrane associated liporotein (24). SprE displays six tetratricopeptide repeats (TPRs) as determined by TPRpred. A TPR domain containing protein 'Tgl' has been shown to be important in coordinating *M. xanthus* social motility (31).

SprT is a homolog of *P. gingivalis* PorT. PorT is an integral outer membrane protein. Structural modeling shows that PorT contains eight anti-parallel, amphipathic, membrane traversing *β*-strands (21). *F. johnsoniae* SprT is thought to be similarly localized. However, biochemical data to support this is still lacking.

In addition to the T9SS proteins, GldA, GldB, GldD, GldF, GldG, GldH, GldI and GldJ have also been identified as proteins that are required for gliding motility of *F. johnsoniae* (Figure 9). Cells with mutations in the genes encoding any of these proteins exhibit defects in chitin utilization and complete resistance to previously reported *F. johnsoniae* bacteriophages ϕCj1, ϕCj13, ϕCj23, ϕCj28, ϕCj29, ϕCj42, ϕCj48 and ϕCj54 (1, 3, 4, 6-8, 12, 13, 19, 20). This evidence suggests that the T9SS is not functional in the mutant cells. Bioinformatic analysis suggests that GldA, GldB, GldD, GldF, GldG, GldH, GldI and GldJ are not essential components of a T9SS. The periodontal pathogen *P. gingivalis* does not have any of these proteins but it has a functional T9SS. Why *F. johnsoniae gldA*, *gldB*, *gldD*, *gldF*, *gldG*, *gldH*, *gldI* and *gldJ* mutant cells lack a functional T9SS has been a mystery. To explain this pleiotropy, I present evidence that GldA, GldB, GldD, GldF, GldG, GldH, GldI and GldJ are required for the stability of the T9SS protein GldK. Absence of any of these proteins thus results in a defective T9SS. Interestingly, with few exceptions, GldA, GldB, GldD, GldF, GldG, GldH, GldI and GldJ are present in motile members of the phylum *Bacteroidetes* while GldK, GldL, GldM, GldN, SprA, SprE and SprT are present in both motile and nonmotile members of the phylum *Bacteroidetes* (15). It appears that besides stabilizing the T9SS; GldA, GldB, GldD, GldF, GldG, GldH, GldI and GldJ might be involved more directly in movement of cell surface adhesins and thus in gliding. In this thesis, we probe the effect of truncated

GldJ on T9SS function and on the movement of cell surface adhesins as a first attempt to separate gliding motility from secretion.

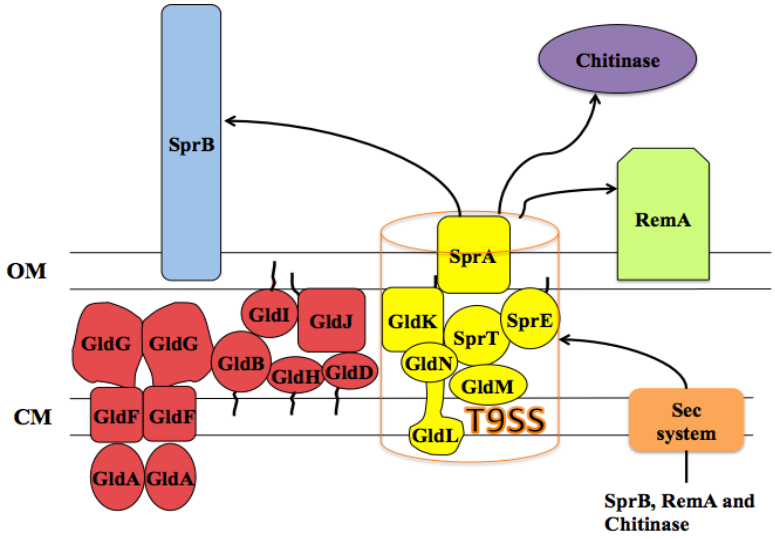

Figure 9. *F. johnsoniae* motility and T9SS proteins. Gliding motility related proteins are colored red. T9SS proteins are colored yellow. T9SS is required for secretion of motility adhesins SprB and RemA. T9SS is also required for secretion a chitinase. The sec protein export system translocates SprB, RemA and chitinase to the periplasm. T9SS is required for transport of SprB, RemA and chitinase across the outer membrane.

This thesis is focused on cell-surface adhesins, gliding motility related proteins and the T9SS of *F. johnsoniae*. Chapter 2 covers the mobile cell surface adhesin RemA and it's effect on the physiology of *F. johnsoniae*. Data from Chapter 2 was published in the Journal of Bacteriology (27). Chapter 3 covers a detailed description of the T9SS proteins and their involvement in secretion of cell surface adhesins. Data from Chapter 3 has been submitted to the Journal of Bacteriology and is currently under review. Chapter 4 is focused on untangling the gliding motility and T9SS machineries. Two appendices follow the main text. Appendix 1 describes the phenotypes associated with *F. johnsoniae* cells

carrying mutations in *porX*, *porY* and *porQ*. *P. gingivalis* PorX and PorY have been reported to be involved in a two component signal transduction pathway that regulates expression of T9SS genes, and *P. gingivalis* PorQ is another putative T9SS protein (25). Appendix 2 describes the effect of mutations in *F. johnsoniae* polysaccharide biosynthesis and transport genes on motility and protein secretion.

References

1. **Agarwal, S., D. W. Hunnicutt, and M. J. McBride.** 1997. Cloning and characterization of the *Flavobacterium johnsoniae* (*Cytophaga johnsonae*) gliding motility gene, *gldA*. Proc. Natl. Acad. Sci. USA **94:**12139-12144.
2. **Bernardet, J.-F.** 1997. Immunization with bacterial antigens: Flavobacterium and Flexibacter infections. Developments in biological standardization **90:**179-188.
3. **Braun, T. F., M. K. Khubbar, D. A. Saffarini, and M. J. McBride.** 2005. *Flavobacterium johnsoniae* gliding motility genes identified by *mariner* mutagenesis. J. Bacteriol. **187:**6943-6952.
4. **Braun, T. F., and M. J. McBride.** 2005. *Flavobacterium johnsoniae* GldJ is a lipoprotein that is required for gliding motility. J. Bacteriol. **187:**2628-2637.
5. **Gibiansky, M. L., W. Hu, K. A. Dahmen, W. Shi, and G. C. Wong.** 2013. Earthquake-like dynamics in *Myxococcus xanthus* social motility. Proc Natl Acad Sci U S A **110:**2330-2335.
6. **Hunnicutt, D. W., M. J. Kempf, and M. J. McBride.** 2002. Mutations in *Flavobacterium johnsoniae gldF* and *gldG* disrupt gliding motility and interfere with membrane localization of GldA. J. Bacteriol. **184:**2370-2378.
7. **Hunnicutt, D. W., and M. J. McBride.** 2001. Cloning and characterization of the *Flavobacterium johnsoniae* gliding motility genes *gldD* and *gldE*. J. Bacteriol. **183:**4167-4175.
8. **Hunnicutt, D. W., and M. J. McBride.** 2000. Cloning and characterization of the *Flavobacterium johnsoniae* gliding motility genes, *gldB* and *gldC.* J. Bacteriol. **182:**911-918.
9. **Kostakioti, M., C. L. Newman, D. G. Thanassi, and C. Stathopoulos.** 2005. Mechanisms of protein export across the bacterial outer membrane. J Bacteriol **187:**4306-4314.
10. **Liu, J., M. J. McBride, and S. Subramaniam.** 2007. Cell-surface filaments of the gliding bacterium *Flavobacterium johnsoniae* revealed by cryo-electron tomography. J. Bacteriol. **189:**7503-7506.
11. **McBride, M. J.** 2001. Bacterial Gliding Motility: Multiple mechanisms for cell movement over surfaces. Annu. Rev. Microbiol. **55:**49-75.
12. **McBride, M. J., and T. F. Braun.** 2004. GldI is a lipoprotein that is required for *Flavobacterium johnsoniae* gliding motility and chitin utilization. J. Bacteriol. **186:**2295-2302.
13. **McBride, M. J., T. F. Braun, and J. L. Brust.** 2003. *Flavobacterium johnsoniae* GldH is a lipoprotein that is required for gliding motility and chitin utilization. J. Bacteriol. **185:**6648-6657.
14. **McBride, M. J., G. Xie, E. C. Martens, A. Lapidus, B. Henrissat, R. G. Rhodes, E. Goltsman, W. Wang, J. Xu, D. W. Hunnicutt, A. M. Staroscik, T. R. Hoover, Y. Q. Cheng, and J. L. Stein.** 2009. Novel features of the polysaccharide-digesting gliding bacterium *Flavobacterium johnsoniae* as revealed by genome sequence analysis. Appl. Environ. Microbiol. **75:**6864-6875.

15. **McBride, M. J., and Y. Zhu.** 2013. Gliding motility and Por secretion system genes are widespread among members of the phylum Bacteroidetes. J. Bacteriol. **195:**270-278.
16. **Mignot, T., J. W. Shaevitz, P. L. Hartzell, and D. R. Zusman.** 2007. Evidence that focal adhesion complexes power bacterial gliding motility. Science **315:**853-856.
17. **Miyata, M.** 2010. Unique centipede mechanism of *Mycoplasma* gliding. Annu. Rev. Microbiol. **64:**519-537.
18. **Nan, B., and D. R. Zusman.** 2011. Uncovering the mystery of gliding motility in the myxobacteria. Annual review of genetics **45:**21-39.
19. **Nelson, S. S., S. Bollampalli, and M. J. McBride.** 2008. SprB is a cell surface component of the *Flavobacterium johnsoniae* gliding motility machinery. J. Bacteriol. **190:**2851-2857.
20. **Nelson, S. S., P. P. Glocka, S. Agarwal, D. P. Grimm, and M. J. McBride.** 2007. *Flavobacterium johnsoniae* SprA is a cell-surface protein involved in gliding motility. J. Bacteriol. **189:**7145-7150.
21. **Nguyen, K. A., J. Zylicz, P. Szczesny, A. Sroka, N. Hunter, and J. Potempa.** 2009. Verification of a topology model of PorT as an integral outer-membrane protein in *Porphyromonas gingivalis*. Microbiol. **155:**328-337.
22. **Rhodes, R. G., S. S. Nelson, S. Pochiraju, and M. J. McBride.** 2011. *Flavobacterium johnsoniae sprB* is part of an operon spanning the additional gliding motility genes *sprC*, *sprD*, and *sprF*. J. Bacteriol. **193:**599-610.
23. **Rhodes, R. G., M. N. Samarasam, A. Shrivastava, J. M. van Baaren, S. Pochiraju, S. Bollampalli, and M. J. McBride.** 2010. *Flavobacterium johnsoniae gldN* and *gldO* are partially redundant genes required for gliding motility and surface localization of SprB. J. Bacteriol. **192:**1201-1211.
24. **Rhodes, R. G., M. N. Samarasam, E. J. Van Groll, and M. J. McBride.** 2011. Mutations in *Flavobacterium johnsoniae sprE* Result in Defects in Gliding Motility and Protein Secretion. Journal of bacteriology **193:**5322-5327.
25. **Sato, K., M. Naito, H. Yukitake, H. Hirakawa, M. Shoji, M. J. McBride, R. G. Rhodes, and K. Nakayama.** 2010. A protein secretion system linked to bacteroidete gliding motility and pathogenesis. Proc. Natl. Acad. Sci. USA **107:**276-281.
26. **Shoji, M., K. Sato, H. Yukitake, Y. Kondo, Y. Narita, T. Kadowaki, M. Naito, and K. Nakayama.** 2011. Por secretion system-dependent secretion and glycosylation of *Porphyromonas gingivalis* hemin-binding protein 35. PLOS One **6:**e21372.
27. **Shrivastava, A., R. G. Rhodes, S. Pochiraju, D. Nakane, and M. J. McBride.** 2012. *Flavobacterium johnsoniae* RemA is a mobile cell-surface lectin involved in gliding. J. Bacteriol. **194:**3678-3688.
28. **Sun, M., M. Wartel, E. Cascales, J. W. Shaevitz, and T. Mignot.** 2011. Motor-driven intracellular transport powers bacterial gliding motility. Proc. Natl. Acad. Sci. USA **108:**7559-7564.
29. **Tseng, T. T., B. M. Tyler, and J. C. Setubal.** 2009. Protein secretion systems in bacterial-host associations, and their description in the Gene Ontology. BMC Microbiol **9 Suppl 1:**S2.

30. **Uenoyama, A., and M. Miyata.** 2005. Gliding ghosts of *Mycoplasma mobile*. Proc. Natl. Acad. Sci. USA **102:**12754-12758.
31. **Wall, D., S. S. Wu, and D. Kaiser.** 1998. Contact stimulation of Tgl and type IV pili in *Myxococcus xanthus*. J. Bacteriol. **180:**759-761.
32. **Wolkin, R. H., and J. L. Pate.** 1986. Phage adsorption and cell adherence are motility-dependent characteristics of the gliding bacterium *Cytophaga johnsonae*. J. Gen. Microbiol. **132:**355-367.
33. **Xie, G., D. C. Bruce, J. F. Challacombe, O. Chertkov, J. C. Detter, P. Gilna, C. S. Han, S. Lucas, M. Misra, G. L. Myers, P. Richardson, R. Tapia, N. Thayer, L. S. Thompson, T. S. Brettin, B. Henrissat, D. B. Wilson, and M. J. McBride.** 2007. Genome sequence of the cellulolytic gliding bacterium *Cytophaga hutchinsonii*. Appl. Environ. Microbiol. **73:**3536-3546.
34. **Zhang, Y., A. Ducret, J. Shaevitz, and T. Mignot.** 2012. From individual cell motility to collective behaviors: insights from a prokaryote, *Myxococcus xanthus*. FEMS Microbiol. Rev. **36:**149-164.

Chapter 2. *Flavobacterium johnsoniae* RemA is a mobile cell-surface lectin involved in gliding

Abstract

Cells of *Flavobacterium johnsoniae* move rapidly over surfaces by a process known as gliding motility. Gld proteins are thought to comprise the motor that propels the cell surface adhesin SprB. Cells with mutations in *sprB* are partially defective in motility and are also resistant to some bacteriophages. Transposon mutagenesis of a strain carrying a deletion spanning *sprB* identified eight mutants that were resistant to additional phages and exhibited reduced motility. Four of the mutants had transposon insertions in *remA*, which encodes a cell-surface protein that has a lectin domain and appears to interact with polysaccharides. Three other genes identified in this screen (*remC*, *wza*, *wzc*) encode proteins predicted to be involved in polysaccharide synthesis and secretion. Myc-tagged versions of RemA localized to the cell surface, and were propelled rapidly along the cell at speeds of 1 to 2 μm per sec. Deletion of *gldN* and *gldO*, which encode components of a bacteroidete protein secretion system, blocked transport of RemA to the cell surface. Overexpression of RemA resulted in the formation of cell aggregates that were dispersed by the addition of galactose or rhamnose. Cells lacking RemC, Wza and Wzc failed to aggregate. Cells of a *remC* mutant, and cells of a *remA* mutant, neither of which formed aggregates in isolation, aggregated when they were mixed together, suggesting that polysaccharides secreted by one cell may interact with RemA on another cell. Fluorescently labeled lectin *Ricinus communis* Agglutinin I detected polysaccharides secreted by *F. johnsoniae*. The polysaccharides bound to cells

expressing RemA, and were rapidly propelled on the cell surface. RemA appears to be a mobile cell surface adhesin, and secreted polysaccharides may interact with the lectin domain of RemA and enhance motility.

Introduction

Cells of *Flavobacterium johnsoniae* and of many other members of the phylum *Bacteroidetes*, translocate rapidly over surfaces in a process called gliding motility (19). These cells do not have well-studied bacterial motility organelles such as flagella or pili. Instead they rely on a novel motility apparatus composed of proteins that are unique to the phylum *Bacteroidetes*. Nineteen proteins involved in motility have been identified (2, 3, 20, 26, 27, 31, 34). SprB is a cell surface protein that appears to be propelled rapidly by the motility machinery (26). Some of the motility proteins (GldK, GldL, GldM, GldN, SprA, SprE, SprT) are thought to comprise a protein secretion system, the T9SS, that is needed for delivery of SprB to the cell surface and for secretion of an extracellular chitinase (33-35). The T9SS is not related to the Type I –Type VI protein secretion systems. Other Gld proteins are likely components of the motors that propel SprB along the cell surface.

Disruption of *sprB* results in the formation of nonspreading colonies, in contrast to the thin spreading colonies produced by wild-type cells. However, *sprB* mutant cells retain some ability to crawl on glass surfaces (26). This suggested the possibility that SprB is a semi-redundant component of the motility machinery. Analysis of the genome

sequence revealed many *sprB* paralogs, any of which might explain the residual motility exhibited by *sprB* mutants (24).

Disruption of *F. johnsoniae* motility genes results not only in motility defects, but also in resistance to bacteriophages that infect wild-type cells. Completely nonmotile *gld* mutants are resistant to infection by all bacteriophages, whereas most mutants with partial motility defects are resistant to some but not all phages (33). *sprB* mutants display increased resistance to *F. johnsoniae* phages ϕCj1, ϕCj13, ϕCj23, and ϕCj29, but are sensitive to ϕCj28, ϕCj42, ϕCj48 and ϕCj54 (26). SprB may function as a phage receptor, and other cell-surface components of the motility machinery may also interact with specific phages.

In this study we conducted *HimarEm1* mutagenesis of an *sprB* mutant and identified eight mutants that exhibited resistance to additional bacteriophages. Cells of the mutants exhibited more severe motility defects than did the parent strain, suggesting that the disrupted genes encode proteins involved in cell movement. The genes mutated included the *sprB*-like gene *remA*, which encodes a cell-surface protein with a lectin domain, and genes likely to be involved in polysaccharide synthesis or export. The results support the hypothesis that there is redundancy in the cell surface components of the motility machinery, and that multiple cell-surface proteins, such as RemA and SprB, may function as mobile adhesins to allow interaction with and movement over diverse surfaces.

Materials and Methods

Bacterial strains, bacteriophage, plasmids, and growth conditions. *F. johnsoniae* UW101, which is derived from the type strain ATCC 17061, was the wild-type strain used in this study (4, 22, 24). The streptomycin resistant *rpsL* mutant of UW101 (CJ1827) was used to construct strains with unmarked deletions and gene replacements (32). *F. johnsoniae* strains were grown in Casitone-yeast extract (CYE) medium at 30^{o}C, as previously described (23). To observe colony spreading, *F. johnsoniae* was grown at 25^{o}C on PY2 medium (1) or EC medium (4) supplemented with 10 g of agar per L. Motility medium (MM) (17) and EC medium were used to observe movement of individual cells in wet mounts. The bacteriophages active against *F. johnsoniae* that were used in this study were ϕCj1, ϕCj13, ϕCj23, ϕCj28, ϕCj29, ϕCj42, ϕCj48 and ϕCj54 (4, 28, 43). Sensitivity to bacteriophages was determined essentially as previously described by spotting 5 μl of phage lysates (10^9 plaque forming units/ml) onto lawns of cells in CYE overlay agar (11). The plates were incubated for 24 h at 25^{o}C to observe lysis. Strains and plasmids used in this study are listed in Table 1. The plasmids used for complementation were all derived from pCP1 and have copy numbers of approximately 10 in *F. johnsoniae* (1, 13, 23). Antibiotics were used at the following concentrations when needed: ampicillin, 100 μg/ml; cefoxitin, 100 μg/ml; chloramphenicol, 30 μg/ml; erythromycin, 100 μg/ml; kanamycin, 35 μg/ml; and tetracycline, 20 μg/ml.

Isolation of phage resistant mutants of *F. johnsoniae* CJ1584 [Δ(*sprC sprD sprB*)] by *HimarEm1* mutagenesis, and identification of sites of insertion. pHimarEm1 was introduced into *F. johnsoniae* CJ1584 by conjugation from *E. coli* S17-1 λ *pir* essentially as previously described (2). *HimarEm1* mutants were selected by plating cells on CYE agar containing erythromycin. Cells from 800 random erythromycin resistant colonies were transferred to CYE agar (master plate), and to CYE agar overlayed with 4 ml of CYE top agar containing approximately 10^9 plaque forming units of ϕCj42, and incubated for 24 h at 25°C. Colonies that grew in the presence of ϕCj42 were picked from the corresponding colonies on the master plate and streaked for isolation on CYE with erythromycin. Colonies were tested again for phage sensitivity, and those with increased resistance were selected for further analyses.

Chromosomal DNA was isolated from each of the phage resistant mutants, and the *HimarEm1* transposons and adjacent DNA from each were cloned in *E. coli* EC100D pir^+. Sequences of *F. johnsoniae* DNA disrupted by *HimarEm1* were determined as previously described (2).

Strain construction. Unmarked deletions were made as previously described (32). To delete *remA* a 1.8 kbp fragment spanning *fjoh_0809* and the final 72 bp of *remA* was amplified by PCR using primers 1061 (introducing a SalI site) and 760 (introducing a PstI site). The fragment was digested with SalI and PstI and ligated into pRR51 that had been digested with the same enzymes, to generate pRR76. A 2.1 kbp fragment spanning *fjoh_0807* and the first 150 bp of *remA* was amplified by PCR with primers 1059 (introducing a BamHI site) and 1060 (introducing a SalI site). The fragment was digested with BamHI and SalI and fused to the region downstream of *remA* by ligation with

pRR76 that had been digested with the same enzymes to generate the deletion construct pRR78. Plasmid pRR78 was introduced into the streptomycin resistant wild-type *F. johnsoniae* strain CJ1827 and into the *sprB* deletion mutant CJ1922 by triparental conjugation, and *remA* deletion mutants were isolated as previously described (32). Deletion of *remA* was confirmed by PCR amplification using primers 778 and 1062, which flank *remA*, and sequencing the resulting 1.8 kbp product. All other deletion strains listed in Table 1 except for CJ2089 [*rpsL2* Δ(*gldN gldO*) *remA::myc*-tag-1] and CJ2090 [*rpsL2* Δ(*gldN gldO*)] , were constructed in the same way, using the primers listed in Table 3 and the plasmids listed in Table 1. CJ2089 and CJ2090 were constructed as previously described (33) by introducing pNap3 into CJ2083 or CJ1827 respectively, selecting for antibiotic resistant colonies that had the plasmid inserted in the genome, and then selecting for resistance to ϕCj1 to obtain the *gldNO* deletions. The *sprF* mutant CJ2097 was constructed by integration of pRR47, which carries an internal fragment of *sprF*, into the chromosome of CJ2083 essentially as previously described (31).

To observe RemA on the cell surface, four strains expressing RemA containing the myc-tag sequence (EQKLISEEDL) at different locations were generated using the allelic exchange method previously described (32). As an example, to generate the strain carrying *remA::myc-tag-1* (CJ2083) primers 1059 (introducing a BamHI site) and 1112 (introducing the *myc*-tag) were used to amplify a 2.1 kbp fragment spanning *fjoh_0807* and the first 150 bp of *remA*. Similarly, primers 761 (introducing a SalI site) and 1110 (introducing the *myc*-tag) were used to amplify the 2.4 kbp fragment beginning at bp 151 of *remA*. The two PCR products were then used as the templates in a cross-over PCR

reaction with primers 761 and 1059. The resulting 4.5 kbp PCR product was digested with BamHI and SalI and ligated into the pRR51 suicide vector, to generate pRR92. Plasmid pRR92 was introduced into the streptomycin resistant wild-type strain CJ1827 and the *sprB* deletion mutant CJ1922 by triparental conjugation, and allelic exchange was performed as previously described (32). Replacement of wild-type *remA* with the *remA::myc-tag-1* allele was confirmed by PCR amplification using primers 1142 (*myc-tag* sequence) and 1063 (complementary to the *remA* sequence), and sequencing the resulting 0.6 kbp product. Four different *remA::myc-tag* strains were generated, with *remA::myc-tag-1*, *remA::myc-tag-3*, *remA::myc-tag-4*, and *remA::myc-tag-5*, inserted 150 bp, 2058 bp, 2286 bp and 2514 bp downstream of the 'A' in the start codon respectively.

Cloning of *remA* and complementation of *remA* mutants. Attempts to clone *remA* amplified by PCR were not successful so an alternative approach was used. The plasmids pMM332 and pMM336 that were used to sequence *remA HimarEm1* insertions served as raw material to reconstruct the intact *remA* gene. The 3' end of *remA* was obtained as a SphI-XbaI fragment from pMM336. This fragment was ligated into pUC18 that had been digested with the same enzymes to generate pRR36. The 5' end of *remA* and upstream sequences were obtained as a HindIII-SphI fragment from pMM332. This fragment was inserted into pRR36 that had been digested with HindIII and SphI to generate pRR37, which carries the intact *remA* gene. *remA* was transferred to pBC SK+ as a 4.9 kbp HindIII-XbaI fragment generating pRR38. This provided convenient restriction sites (KpnI, XbaI) to allow transfer of *remA* into the shuttle vector pCP23, generating pRR39. pRR39 was introduced into *remA* mutants by conjugation as

previously described (11, 21) except that pRK2013 (5) was used for triparental conjugations.

Expression of recombinant RemA in *E. coli* and generation of antibodies. A 1966 bp fragment encoding the 561 amino acid C-terminal region of RemA was amplified using Phusion DNA polymerase (New England BioLabs, Ipswich, MA) and primers 745 and 762. The PCR product was digested with BamHI and SalI and cloned into the pMAL-c2 expression vector (New England BioLabs) that had been digested with the same enzymes, generating pSP18. pSP18 was introduced into *E. coli* Rosetta 2 (DE3) cells (Novagen, Madison, WI), which expressed seven rare tRNAs required for the efficient expression of RemA. To isolate recombinant RemA, cells were grown to mid-log phase at 37°C in rich medium containing glucose (10 g tryptone, 5 g yeast extract, 5 g NaCl, 2 g glucose/liter), induced by the addition of 0.3 mM isopropyl-β-D-thiogalactopyranoside (IPTG), and incubated for 8 hr at 25°C. Cells were disrupted using a French press, and recombinant RemA was purified using an amylose resin column (New England Biolabs). Polyclonal antibodies against recombinant RemA were produced and affinity purified using the recombinant protein by ProteinTech Group, Inc. (Chicago, IL).

Immunodetection and localization of RemA. *F. johnsoniae* cells were grown to mid-log phase in CYE at 25°C. Whole cells were centrifuged at 4,000 x g, resuspended in SDS-PAGE loading buffer, and boiled for 5 minutes. Proteins were separated by SDS-PAGE and Western blot analyses were performed essentially as previously described (33) using affinity purified antisera against RemA (1:1000 dilution) or antisera against the *c-myc* epitope (1:10,000 dilution; AbCam, Cambridge, MA). To determine the localization

of RemA, cells were disrupted with a French press and fractionated into soluble and insoluble fractions as described previously by centrifugation at 352,900 x g for 30 min (34) and Western blotting was performed as described above.

Microscopic observations of cell movement. Wild-type and mutant cells of *F. johnsoniae* were examined for movement over glass by phase-contrast microscopy. Tunnel slides were prepared essentially as described (39) using Nichiban NW-5 double-sided tape (Nichiban Co., Tokyo, Japan) to hold a glass cover slip over a glass slide. Cells in MM were introduced into the tunnel slide, incubated for 5 min, and observed for motility using an Olympus BH-2 phase-contrast microscope with a heated stage set at 25^{o}C. Images were recorded using a Photometrics CoolSNAP$_{cf}^{2}$ camera, and were analyzed using MetaMorph software (Molecular Devices, Downingtown, PA).

Binding and movement of Protein G coated polystyrene spheres. Movement of surface localized myc-tagged RemA was detected essentially as previously described for movement of SprB (26). Cells were grown overnight at 25^{o}C in MM without shaking. Antibodies against myc-tag peptide (1 μl of a 1:10 dilution of 1 mg/ml stock), 0.5-μm-diameter protein G-coated polystyrene spheres (1 μl of a 0.1% stock preparation; Spherotech Inc., Libertyville, IL), and bovine serum albumin (1 μl of a 1% solution) were added to 7 μl of cells (approximately 5 x 10^{8} cells per ml) in MM. The presence of Protein-G on the spheres and the addition of bovine serum albumin eliminated nonspecific binding of spheres to cells as previously reported (26, 31-34). The cells were introduced into a tunnel slide and examined by phase-contrast microscopy at 25^{o}C. Samples were examined 2 min after introduction into a tunnel slide, and images were captured for 30 s.

Detection of RemA by immunofluorescence microscopy. Cells were grown overnight at 25^{o}C in MM without shaking. Antibodies specific for myc-tag peptide (1 μl of a 1:10 dilution of 1 mg/ml stock), F(ab') fragment of goat anti-rabbit IgG conjugated to Alexa-488 (1.5 μl of a 1:10 dilution of 2 mg/ml stock; Invitrogen, Carlsbad, CA), and bovine serum albumin (1 μl of a 1% solution) were added to 7 μl of cells (approximately 5 x 10^8 cells per ml) in MM. The cells were spotted on a glass slide, covered with a glass cover slip, and observed using a Nikon Eclipse 50i microscope. To observe the cells and the rapidly moving fluorescent signals at the same time a combination of low light phase contrast microscopy and fluorescence microscopy was used. Images were recorded using a Photometrics CoolSNAP$_{ES}$ camera and were deconvoluted and analysed using MetaMorph Software.

Detection of cell surface polysaccharides by immunofluorescence microscopy using the galactose/N-acetyl galactosamine-binding lectin RCA$_{120}$. 10 ml cultures were grown overnight in 150 mm x 25 mm test tubes at 23°C in EC media with appropriate antibiotics on a platform shaker set at 120 rpm. The cultures in test tubes were mixed gently and 7 μl of appropriate culture was mixed with Rhodamine-labeled RCA$_{120}$ (4 μl of 1:10 dilution of 2 mg/ml stock; Vector Laboratories, Burlingame, CA). 7 μl of the sample was introduced into tunnel slides. Samples were observed with epifluorescence illumination, and with epifluorescence in combination with phase contrast, using a Nikon Eclipse 50i microscope, and were recorded using a Photometrics CoolSNAP$_{ES}$ camera. Images were deconvoluted and analysed using MetaMorph Software.

Cell agglutination. 10 ml cultures were grown overnight in 150 mm x 25 mm test tubes at 23°C in EC media with appropriate antibiotics on a platform shaker set at 120 rpm. Strains displaying agglutination had the majority of the biomass at the bottom of the test tubes while strains not exhibiting agglutination were turbid throughout. The cultures in test tubes were mixed gently and 7 µl samples were introduced into tunnel slides and observed by phase-contrast microscopy using a Photometrics Coolsnap$_{cf}^{2}$ camera. To measure optical density, cultures were grown as described above, samples were collected from the top of the tubes, and optical density was measured at 600 nm. After initial measurements were taken, D-galactose was added to a concentration of 5 mM and incubated for 5 min to disperse aggregates, and optical density was determined again as a measure of total cell mass per tube. Strains that failed to agglutinate were also mixed with other nonagglutinating strains to determine if the combinations would agglutinate. Cells were grown as described above and 5 ml each of the appropriate cultures were mixed in 150 mm x 25 mm test tubes. The tubes were incubated at 23^{o}C with shaking for an additional 60 min, and cell aggregation was observed as described above.

The effect of various sugars on agglutination was determined. A 150 ml culture of wild-type *F. johnsoniae* CJ1827 carrying pRR39 was grown overnight at 23°C in EC medium with tetracycline on a tabletop shaker at 120 rpm in an erlenmyer flask. 9.5 ml of culture was transferred to test tubes containing 0.5 ml of appropriate 100 mM sugar stock solutions, or 0.5 ml of water. The tubes were incubated with shaking (120 rpm on a platform shaker) at 23°C for 60 minutes and cell aggregation was observed as described above.

Results

Isolation of bacteriophage resistant mutants and identification of sites of the mutations. In an attempt to identify novel motility genes, *HimarEm1* mutagenesis was conducted on *F. johnsoniae* mutant CJ1584, which has a deletion spanning *sprC*, *sprD*, and *sprB* (31). Cells of CJ1584 form nonspreading colonies on agar that are indistinguishable from those of completely nonmotile *gld* mutants, but individual cells exhibit some movement on glass surfaces (31). Cells of nonmotile *gld* mutants are resistant to all bacteriophages that infect the wild-type (2, 33). In contrast, cells of CJ1584 display increased resistance to some bacteriophages (ϕCj1, ϕCj13, ϕCj23, ϕCj29) but they remain sensitive to others (ϕCj28, ϕCj42, ϕCj48 and ϕCj54) (Figure 10). 800 randomly chosen erythromycin resistant colonies containing *HimarEm1* insertions were screened for resistance to ϕCj42 and eight mutants with partial or complete resistance were obtained. In addition to resistance to ϕCj42, the mutants exhibited increased resistance to other phages to which CJ1584 is susceptible (Figure 10). Microscopic examination revealed that each mutant also had a more severe motility defect than did the parent strain; see Movie S1 in the supplemental material of (36) and data not shown.

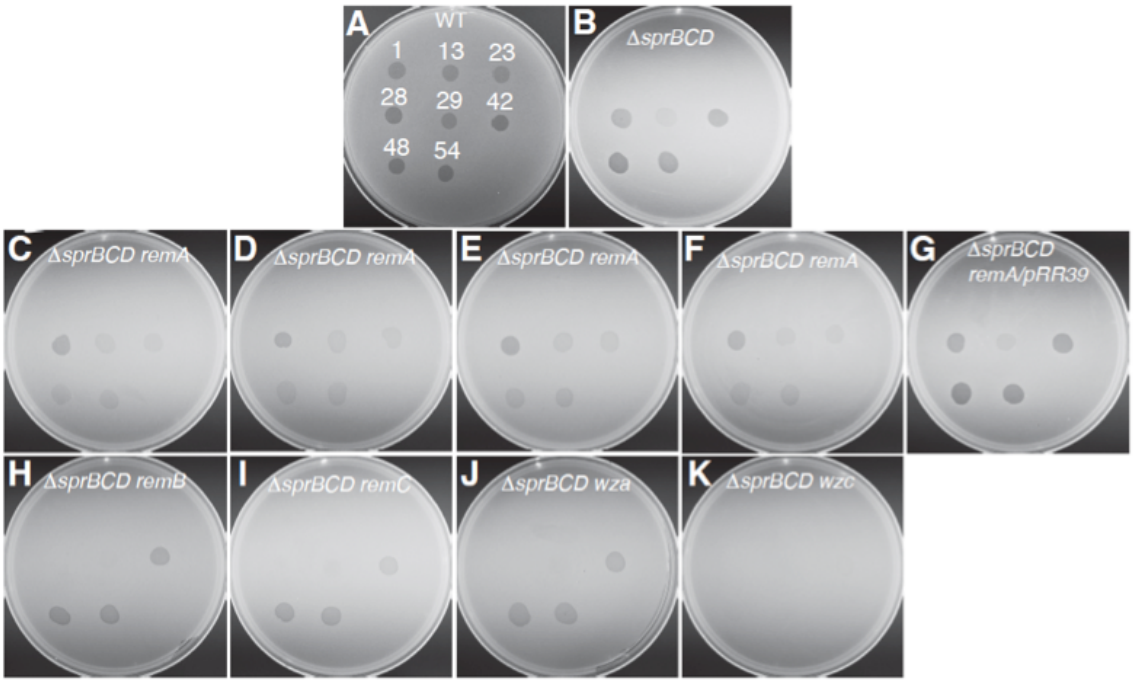

Figure 10. Effect of mutations on bacteriophage resistance. Bacteriophages (5 µl of lysates containing approximately 10^9 PFU/ml) were spotted onto lawns of cells in CYE overlay agar. The plates were incubated at 25°C for 24 h to observe lysis. Bacteriophages were spotted in the following order from left to right, as indicated also by the numbers in panel A: top row, ϕCj1, ϕCj13, and ϕCj23; middle row ϕCj28, ϕCj29, and ϕCj42; bottom row, ϕCj48 and ϕCj54. Panel A: Wild type *F. johnsoniae* UW101. Panel B: CJ1584 [Δ(*sprB sprC sprD*)]. Panel C: CJ1595 [Δ(*sprB sprC sprD*) *remA*::*HimarEm1*]. Panel D: CJ1596 [Δ(*sprB sprC sprD*) *remA*::*HimarEm1*]. Panel E: CJ1597 [Δ(*sprB sprC sprD*) *remA*::*HimarEm1*]. Panel F: CJ1601 [Δ(*sprB sprC sprD*) *remA*::*HimarEm1*]. Panel G: CJ1601 complemented with pRR39. Panel H: CJ1603 [Δ(*sprB sprC sprD*) *remB*::*HimarEm1*]. Panel I: CJ1600 [Δ(*sprB sprC sprD*) *remC*::*HimarEm1*]. Panel J: CJ1598 [Δ(*sprB sprC sprD*) *wza*::*HimarEm1*]. Panel K: CJ1602 [Δ(*sprB sprC sprD*) *wzc*::*HimarEm1*].

The sites of the transposon insertions were determined by cloning *HimarEm1* and adjacent DNA and sequencing across the junction. Four of the mutants had insertions in *fjoh_0808*, which we named *remA* (redundant motility gene A, Figure 11). *remA* encodes a predicted 152 kDa protein (after removal of its signal peptide) that exhibits limited

similarity to the much larger (669 kDa) cell-surface motility protein SprB (26). Similarity to SprB was confined to 5 regions of RemA (amino acids 158-225, 453-494, 580-642, 976-1022, and 1282-1370) and ranged from 26% to 43% identity. BlastP analysis also revealed similarity to two conserved domains of known function. The C-terminal 80 amino acids exhibited similarity to a Por secretion system C-terminal sorting domain (TIGR04183; E-value 6.93e-05), suggesting that like SprB, RemA may be secreted across the outer membrane by the *F. johnsoniae* T9SS. In addition, the region between amino acids 725 and 800 exhibited similarity to SUEL-related galactose/rhamnose-binding lectins (pfam02140; E-value 2.44e-17), suggesting that RemA may interact with sugars. The remaining four mutants had insertions in *fjoh_1657* (*remB*), *fjoh_0216* (*remC*), *fjoh_0361* (*wza*) and *fjoh_0360* (*wzc*). RemB is predicted to be an outer membrane protein of unknown function, RemC is a predicted glycosyltransferase, and Wza and Wzc are predicted components of a polysaccharide synthesis and secretion system. Secreted or cell-surface polysaccharides have previously been implicated in gliding of *F. johnsoniae* and of other bacteria (7, 8, 16, 18, 42, 44).

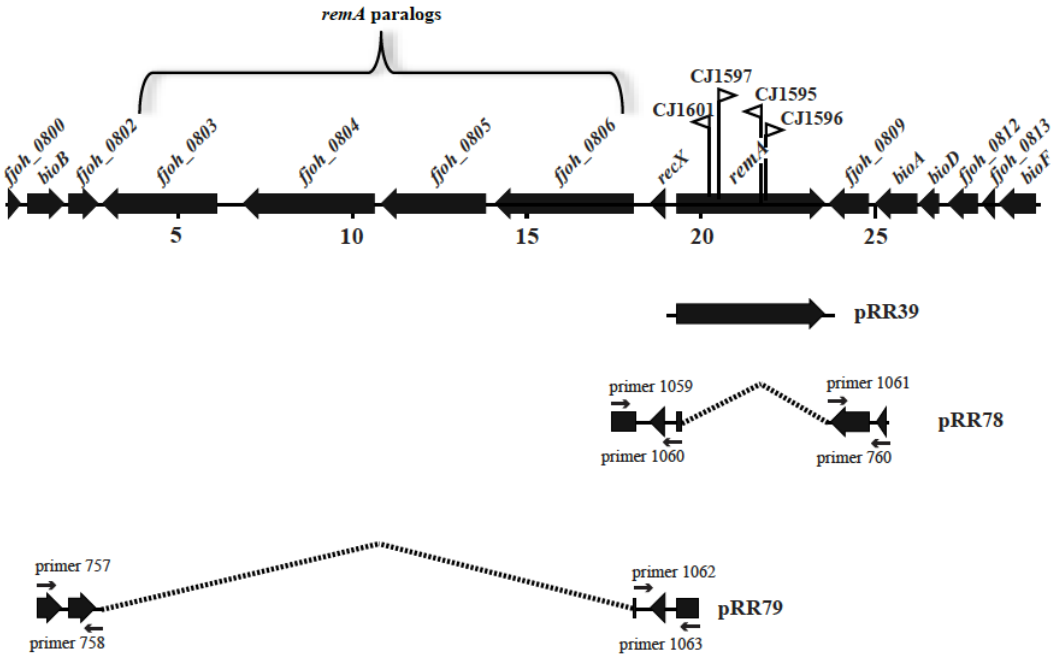

Figure 11. Map of the *remA* region. Numbers below the map refer to kilobase pairs of sequence. The sites of *HimarEm1* insertions in *remA* are indicated by triangles, with orientation indicated by the direction in which the triangle is pointing. Triangles pointing to the right in this diagram (CJ1597 for example) have IR2 on the right side and the kanamycin resistance gene of the transposon reading toward the right. The regions of DNA carried by plasmids used in this study are indicated beneath the map.

SprB, SprC, and SprD are each required for efficient motility on agar and for the formation of spreading colonies (26, 31). SprB is a mobile cell-surface adhesin, and SprC and SprD are thought to support SprB function. Disruption of *sprB* results in increased resistance to ϕCj1, ϕCj13, ϕCj23, and ϕCj29, whereas disruption of *sprC* and *sprD* does not result in resistance to phages that have been tested (31). CJ1985 (Δ*sprB* Δ*remA*) and CJ1984 (Δ*remA*) were constructed to simplify determination of the roles of *remA* and *sprB* in phage resistance and motility. Cells of CJ1985 (Δ*sprB* Δ*remA*) exhibited the same

phage resistance phenotypes as those of CJ1601 [Δ(*sprC sprD sprB*) *remA*::*HimarEm1*] (Figure 12 and Figure 10). Cells of CJ1984 (Δ*remA*) exhibited increased resistance to ϕCj42, ϕCj48, and ϕCj54, and introduction of *remA* on pRR39 restored sensitivity to these phages.

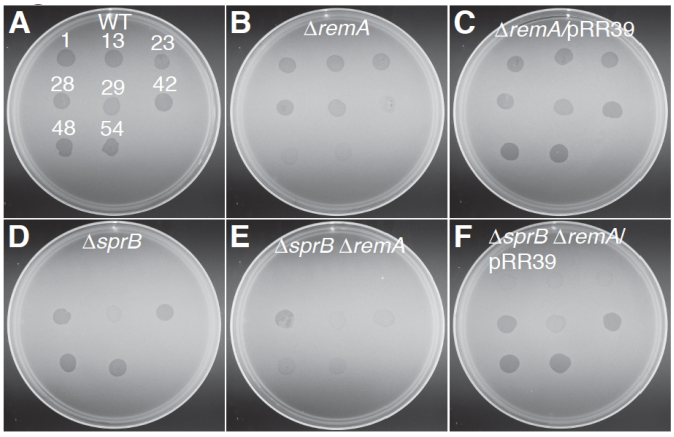

Figure 12. Effect of mutations on bacteriophage resistance. Bacteriophages (5 µl of lysates containing approximately 10^9 PFU/ml) were spotted onto lawns of cells in CYE overlay agar. The plates were incubated at 25°C for 24 h to observe lysis. Bacteriophages were spotted in the following order from left to right, as indicated also by the numbers in panel A: top row, ϕCj1, ϕCj13, and ϕCj23; middle row ϕCj28, ϕCj29, and ϕCj42; bottom row, ϕCj48 and ϕCj54. Panel A: Wild type *F. johnsoniae* CJ1827. Panel B: CJ1984 (Δ*remA*). Panel C: CJ1984 complemented with pRR39 which carries *remA*. Panel D: CJ1922 (Δ*sprB*). Panel E: CJ1985 (Δ*sprB* Δ*remA*). Panel F: CJ1985 complemented with pRR39.

Deletion of *remA* in an *sprB* mutant results in decreased motility. Cells of CJ1984 (Δ*remA*), CJ1922 (Δ*sprB*), and CJ1985 (Δ*sprB* Δ*remA*), were examined for motility; see Movies S2 and S3 in the supplemental material of (36). Cells of CJ1984 (Δ*remA*) were indistinguishable from wild-type cells, whereas cells of CJ1922 (Δ*sprB*) exhibited a partial motility defect similar to that of CJ1584 [Δ(*sprC sprD sprB*)], as previously reported (26, 31, 32). CJ1922 formed nonspreading colonies on agar, but

individual cells retained some ability to move on glass surfaces. Cells of CJ1985 (Δ*sprB* Δ*remA*) exhibited more dramatic motility defects, with most cells exhibiting little if any movement. The motility behavior of CJ1985 was similar to that of CJ1601 [Δ(*sprC sprD sprB*) *remA*::*HimarEm1*]; see Movie S1 in the supplemental material of (36). Complementation of CJ1985 (Δ*sprB* Δ*remA*) with pRR39, which carries *remA*, restored motility comparable to or exceeding that exhibited by the parent strain CJ1922 (Δ*sprB*). The decreased motility of CJ1985 (Δ*sprB* Δ*remA*) compared to CJ1922 (Δ*sprB*) suggests that SprB and RemA may be partially redundant components of the motility apparatus. *sprB* mutants form nonspreading colonies as a result of motility defects, but colonies of the *remA* deletion mutant CJ1984 (Δ*remA*) were indistinguishable from those of the wild type (Figure 13), indicating that unlike SprB, RemA is not required for movement of cells on agar.

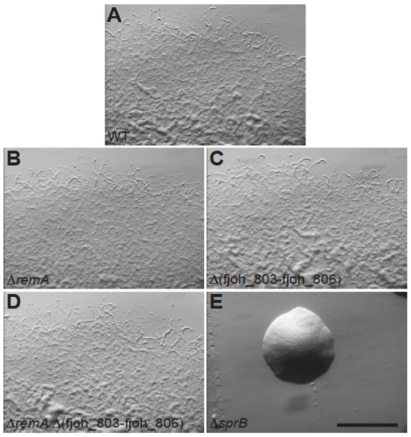

Figure 13. Deletion of *remA* or its paralogs have no effect on formation of spreading colonies on agar. Colonies were incubated at 25°C on PY2 agar medium for 48 h, and photomicrographs were taken with a Photometrics CoolSNAP$_{cf}^2$ camera mounted on an Olympus IMT-2 phase-contrast microscope. (A) Streptomycin resistant 'wild-type' strain CJ1827. (B) CJ1984 (Δ*remA*). (C) CJ1986 [Δ(Fjoh_0803-fjoh_0806)]. (D) CJ2098 [Δ*remA* Δ(Fjoh_0803-fjoh_0806)]. (E) CJ1922 (Δ*sprB*). Bar indicates 1 mm.

RemA moves rapidly along the cell surface. RemA was predicted to be a cell-surface-exposed outer membrane protein. Antiserum against recombinant RemA was used to detect RemA in *F. johnsoniae* cell extracts. RemA was found in the insoluble fraction of cell extracts, and migrated with an apparent molecular weight of approximately 150 kDa (Figure 14A), which is close to the size predicted for the mature protein. Antiserum against RemA detected denatured protein in Western blots, but failed to detect native RemA on the cell surface or in cell extracts. Four myc-tagged versions of *remA* were constructed and inserted into the genome in place of wild-type *remA*. Two of the strains, CJ2083 (*remA::myc*-tag-1; myc-tag inserted 150 bp downstream of the 'A' in the start codon) and CJ2112 (*remA::myc-tag-4*; myc-tag inserted 2286 bp downstream of the start codon), produced stable myc-tagged RemA protein as detected by western blot (Figure 14). These strains were sensitive to the same phages as were wild-type cells, suggesting that the myc-tagged versions of RemA localized properly and supported phage infection. Protein-G-coated latex spheres carrying antibodies against the myc-tag peptide bound specifically to cells of CJ2083 (*remA::myc-tag-1*) and CJ2112 (*remA::myc-tag-4*), indicating that RemA was exposed on the cell surface (Table 2). The bound spheres moved rapidly along the cell surface; see movie S4 in the supplemental material of (36), suggesting that RemA is propelled along the cell by the gliding 'motor', as previously suggested for SprB (26). As previously reported (26, 31-34), and as shown in Table 2 and in Movie S4 in the supplemental material of (36), Protein-G-coated spheres did not bind to cells unless specific antiserum was added. They also failed to bind to wild type cells that did not express Myc-tagged RemA. Cells of CJ2077 (*remA::myc-tag-3*; myc-tag inserted 2058 bp downstream of the start codon) and of CJ2073

(*remA::myc-tag-5*; myc-tag inserted 2514 bp downstream of the start codon) produced little if any RemA and failed to bind protein-G-coated latex spheres carrying antibodies against the myc-tag peptide. To eliminate potential artifacts resulting from the relatively large (0.5 μm) latex spheres, localization and movement of RemA-myc-tag-1 was also examined by immunofluorescence microscopy using antibodies against the myc-tag. Cells of CJ2083 expressed RemA-myc-tag-1 and were fluorescently labeled, whereas cells of CJ1827 (wild type) were not. The fluorescent antibodies moved smoothly along the cell surface at speeds of 1 to 2 μm/sec (Figure 15); see Movie S5 in the supplemental material of (36). The fluorescent signals traveled the length of the cell, looped around the pole, and returned to a location near the starting point, all within about 10 seconds. The movements of spheres and fluorescent antibodies are consistent with a model for gliding in which the gliding motor in the cell envelope propels cell-surface adhesins such as RemA. SprB, which also moves on the cell surface, was not required for RemA movement, since cells of CJ2072 (Δ*sprB remA::myc-tag-1*) also propelled fluorescently labeled anti-myc antibodies; see Movie S5 in the supplemental material of (36).

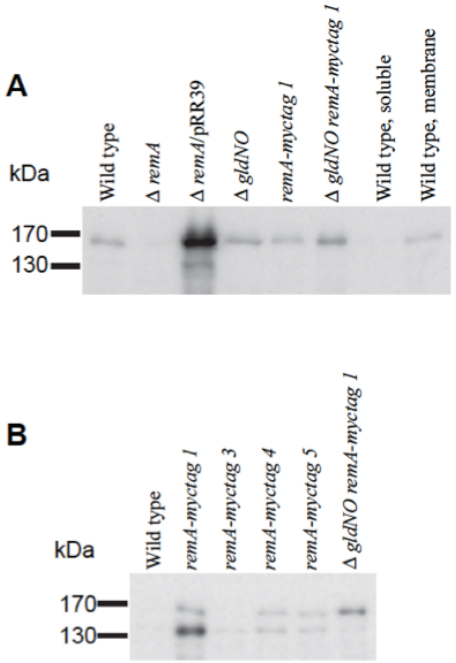

Figure 14. Immuno-detection of RemA and RemA-myc-tag. (A) Cell extracts (15 µg protein) were examined by Western blotting using antiserum against RemA. Lane 1, wild type *F. johnsoniae* CJ1827. Lane 2, CJ1984 (Δ*remA*). Lane 3, CJ1984 complemented with pRR39 which carries *remA*. Lane 4, CJ2090 [Δ(*gldN-gldO*)]. Lane 5, CJ2083 (*remA::myc-tag-1*). Lane 6, CJ2089 [Δ(*gldN-gldO*) *remA::myc-tag-1*]. Lane 7, soluble (cytoplasmic and periplasmic) fraction of wild-type cell extract. Lane 8, particulate (membrane) fraction of wild-type cell extract. (B) Cell extracts (20 µg protein) were examined by Western blotting using antiserum against myc-tag peptide. Lane 1, wild type *F. johnsoniae* CJ1827. Lane 2, CJ2083 (*remA::myc-tag-1*). Lane 3, CJ2077 (*remA::myc-tag-3*). Lane 4, CJ2112 (*remA::myc-tag-4*). Lane 5, CJ2073 (*remA::myc-tag-5*). Lane 6, CJ2089 [Δ(*gldN-gldO*) *remA::myc-tag-1*].

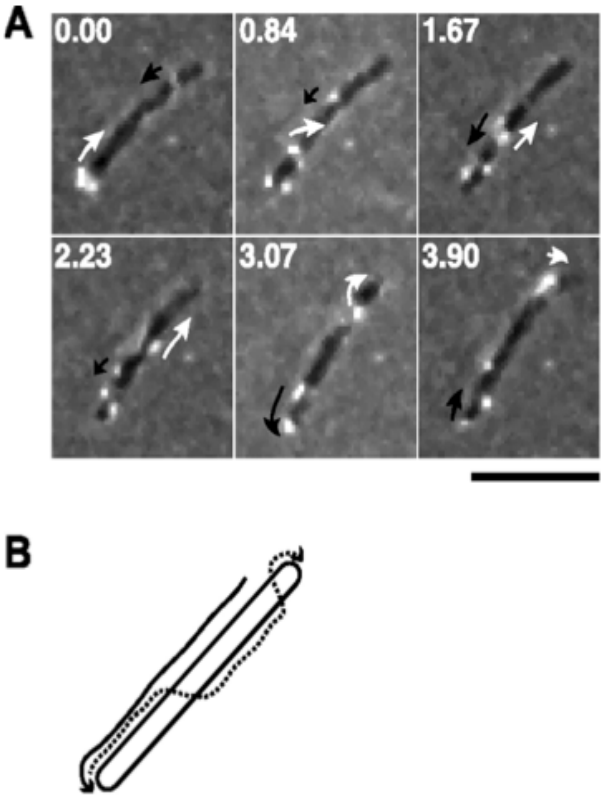

Figure 15. Movement of RemA on the cell surface. (A) Cells of CJ2083, which expressed RemA-myc-tag-1, were examined by a combination of immunofluorescence and phase contrast microscopy. Low light phase contrast was used to detect the cells, and antisera against the myc-tag peptide and goat anti-rabbit IgG conjugated to Alexa-488 were used to detect RemA-myc-tag-1. The sequence shown corresponds to the first 3.9 seconds of the third sequence [CJ2083, (RemA-myc-tag-1), with anti-myc-tag antibody] in Movie S5 of (36). The full movie includes controls demonstrating the specificity of the antiserum for the myc-tag peptide. Numbers in each panel indicate time in seconds. Arrows outline the apparent movements of two selected fluorescent signals. Bar indicates 5 μm. (B) Cartoon illustrating the apparent movements of the two selected fluorescent signals highlighted in panel A during 3.9 sec.

Mutations in T9SS genes disrupt secretion of RemA. A novel protein secretion system, the Type IX secretion system (T9SS), is required for delivery of SprB to the cell surface, and also for secretion of an extracellular chitinase (33-35). A strain carrying myc-tagged *remA*, and carrying a deletion of the region spanning the T9SS genes *gldN*

and *gldO*, was constructed to determine whether the T9SS is involved in secretion of RemA. Cells lacking *gldN* and *gldO* produced myc-tagged RemA (Figure 14) but failed to secrete it to the cell surface as determined by failure of latex spheres carrying antibodies against the myc-tag peptide to bind to the cells (Table 2). Complementation with pTB79, which carries *gldN*, restored surface exposure of myc-tagged RemA. The results suggest that the T9SS is required for secretion of RemA, in addition to its previously demonstrated roles in secretion of SprB and chitinase (33-35). SprB requires an additional protein, SprF, for secretion to the cell surface (31). SprF is thought to be an adapter to the T9SS that is specific for SprB, since SprF is not required for secretion of chitinase. Many of the *F. johnsoniae sprB* paralogs are adjacent to *sprF* paralogs, and the predicted SprF-like proteins may function in secretion of their cognate SprB-like proteins. *remA* does not have an *sprF*-like gene nearby. Cells of CJ2097 (*remA::myc-tag1 sprF*) bound and propelled spheres carrying antibodies against the myc-tag peptide, indicating that SprF is not required for secretion of RemA (Table 2).

Analysis of the *remA* paralogs *fjoh_0803*, *fjoh_0804*, *fjoh_0805*, and *fjoh_0806*. Four *remA* paralogs lie near *remA* on the *F. johnsoniae* genome (Figure 11). The products of *fjoh_0803*, *fjoh_0804*, *fjoh_0805*, and *fjoh_0806* exhibited 57%, 47%, 93%, and 64% identity respectively, to the C-terminal 500 amino acids of RemA, and exhibited more limited similarity over the rest of RemA. The region of RemA between 725 and 830 amino acids, which corresponds to the lectin domain, was not conserved in the four *remA* paralogs. To determine whether the *remA* paralogs function in gliding and phage sensitivity the region spanning *fjoh_0803-fjoh_0806* was deleted in wild type cells, in CJ1984 (Δ*remA*), and in CJ1985 (Δ*sprB* Δ*remA*). Deletion of *fjoh_0803-fjoh_0806*

from any of these strains had no effect on phage sensitivity, motility, or colony spreading; (Figure 13) and data not shown.

Involvement of RemA and cell-surface polysaccharides in cell-cell interactions. Wild type *F. johnsoniae* cells grown in EC medium formed small cell aggregates (Figure 16A). Cells of CJ1984 (Δ*remA*) were deficient in aggregate formation and complementation with *remA* on pRR39 restored the ability to form aggregates. The aggregates formed by the complemented strain were much larger than those formed by wild-type cells, suggesting that moderate overexpression of RemA from pRR39, which has a copy number of approximately 10, enhanced aggregation. Introduction of pRR39 into wild-type cells also enhanced aggregation. The control vector pCP23 did not cause cell aggregation indicating that *remA* was responsible for this phenomenon. The large cell aggregates formed for strains carrying pRR39 resulted in rapid settling of the cells from suspension, allowing macroscopic observation and quantitation of aggregation (Figure 16 B, C). The predicted lectin domain of RemA suggested the possibility that RemA bound to polysaccharides on the surface of neighboring cells. Addition of 5 mM D-galactose, L-rhamnose or D-lactose resulted in rapid dissolution of the aggregates, whereas addition of other sugars (D-glucose, D-mannose, D-fructose, D-ribose, D-sorbitol, D-sucrose, D-maltose and D-trehalose) at 5 to 100 mM did not (Figure 17 and data not shown). The ability to completely disperse aggregates by adding 5 mM galactose allowed us to rapidly estimate total biomass by measuring OD_{600} (Figure 16 C). Not surprisingly, the formation of large aggregates as a result of overexpression of RemA correlated with decreased total biomass (Figure 16 C), probably because of reduced availability of nutrients or O_2 in the dense aggregates. As mentioned earlier, RemA moves rapidly on the cell surface (Figure

15). Addition of galactose or rhamnose had no effect on the movement of RemA as observed using antibody-coated spheres or by immunofluorescence microscopy (data not shown).

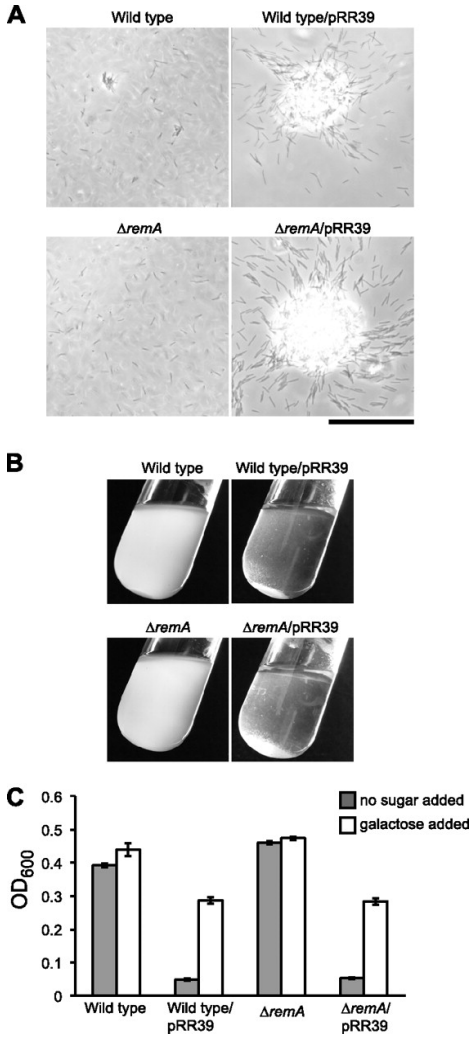

Figure 16. Effect of RemA on cell aggregation. Cells of CJ1827 (Wild type) and CJ1984 (Δ*remA*) containing either control plasmid pCP23 (images on the left in panels A and B), or *remA* expressing plasmid pRR39 (images on the right in panels A and B) were incubated in EC medium. (A) Observation of cells or cell clumps by phase contrast microscopy. Bar indicates 50 µm. (B) Macroscopic observation of cell clumps in culture tubes. (C) Turbidity (OD_{600}) of samples taken from the top of the culture tubes. Measurements were obtained from samples

taken directly from the tubes, and from samples taken after addition of 5 mM D-galactose and incubation for 5 min to cause cell dispersal.

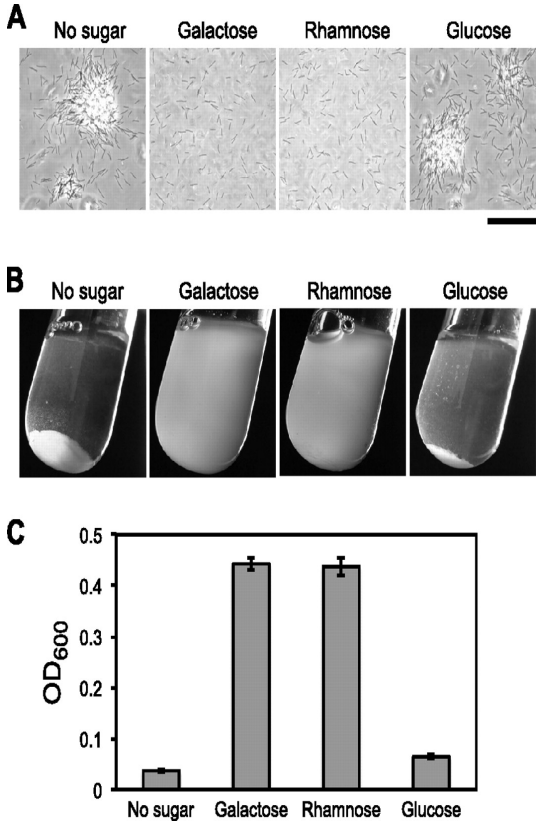

Figure 17. Effect of sugars on RemA mediated cell aggregation. Cells of CJ1827 (wild type) carrying pRR39 to overexpress RemA were transferred into test tubes containing various sugars at final concentrations of 5 mM. Cultures were incubated with gentle shaking for one hour at 23°C and examined for aggregation. (A) Observation of cells or cell clumps by phase contrast microscopy. Bar indicates 50 μm. (B) Macroscopic observation of cell clumps in culture tubes. C) Turbidity (OD_{600}) of samples taken from the top of the culture tubes.

remC, *wza*, and *wzc* were identified in the same genetic screen that resulted in the identification of *remA*, and the proteins encoded by these genes are predicted to be involved in polysaccharide synthesis and secretion. Secreted polysaccharides might interact with RemA and be involved in cell-cell or cell-substratum interactions. pRR39 was introduced into cells of CJ1584 [Δ(*sprC sprD sprB*)], CJ1598 [Δ(*sprC sprD sprB*)

wza::*HimarEm1*], CJ1602 [Δ(*sprC sprD sprB*) *wzc*::*HimarEm1*], and CJ1600 [Δ(*sprC sprD sprB*) *remC*::*HimarEm1*], in order to determine whether cells that overexpressed RemA but that were deficient in polysaccharide synthesis or secretion would form aggregates. Cell aggregates formed with CJ1584 carrying pRR39, but not with any of the strains with mutations in the predicted polysaccharide synthesis and secretion genes (Figure 18). This suggests that both RemA and secreted polysaccharides are required for aggregate formation. RemA may function as a cell-surface adhesin that interacts with polysaccharides synthesized and secreted by RemC, Wza, and Wzc. SprB, SprC, and SprD may also be involved in aggregate formation, since the aggregates formed by cells of CJ1584 [Δ(*sprC sprD sprB*)] carrying pRR39 were smaller than those formed by wild-type cells carrying the same plasmid (Figure 15A, 16A). However, although overexpression of RemA (from pRR39) resulted in cell aggregation, overexpression of SprB (from pSN60) did not (data not shown). Polysaccharide production and RemA expression do not need to occur in the same cell for aggregation to occur. Cells of CJ1984 (Δ*remA*), and of CJ1600 [Δ(*sprC sprD sprB*) *remC*::*HimarEm1*] carrying pRR39, neither of which formed aggregates in isolation, resulted in aggregate formation when they were mixed together (Figure 16). Similar results were obtained when cells of CJ1984 were mixed with cells of the *wza* mutant CJ1598 carrying pRR39.

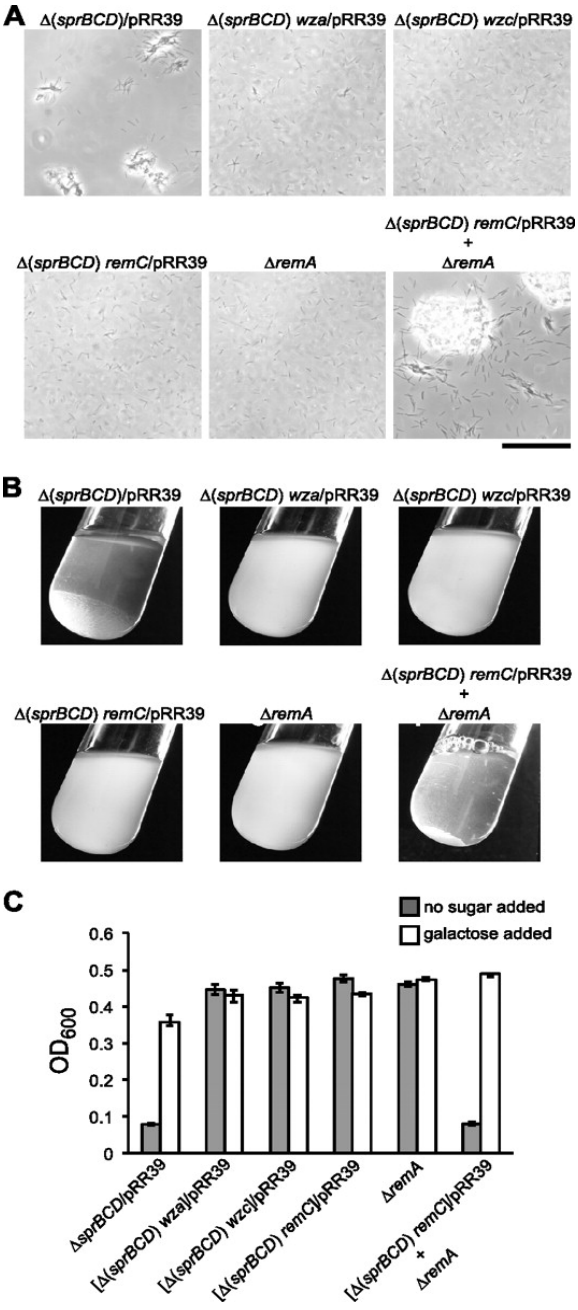

Figure 18. Effect of mutations in *remC*, *wza*, and *wzc* on cell aggregation. Cells of CJ1584 [Δ(*sprC sprD sprB*)], CJ1598 [Δ(*sprC sprD sprB*) *wza*::*HimarEm1*], CJ1602 [Δ(*sprC sprD sprB*) *wzc*::*HimarEm1*], CJ1600 [Δ(*sprC sprD sprB*) *remC*::*HimarEm1*], and CJ1984 (Δ*remA*), were incubated in EC medium. All strains carried pRR39 (to overexpress RemA) except for CJ1984 (D*remA*) which carried the control plasmid pCP23. To examine the ability of two non-aggregating strains to form aggregates when mixed together, 5 ml of CJ1600 [Δ(*sprC sprD sprB*) *remC*::*HimarEm1*] carrying pRR39, and 5 ml of CJ1984 (Δ*remA*) carrying pCP23 were mixed in a test tube and incubated for an additional 60 min. (A) Observation of cells or cell clumps by

phase contrast microscopy. Bar indicates 50 μm. (B) Macroscopic observation of cell clumps in culture tubes. (C) Turbidity (OD_{600}) of samples taken from the top of the culture tubes. Measurements were obtained from samples taken directly from the tubes, and from samples taken after addition of 5 mM D-galactose and incubation for 5 min to cause cell dispersal.

A fluorescent lectin was used to visualize secreted or cell-surface polysaccharides or oligosaccharides on cells of *F. johnsoniae*. Rhodamine-labeled *Ricinus communis* Agglutinin I (RCA_{120}), which binds galactose, labeled cell clumps and individual cells. The fluorescent lectin was propelled rapidly on the cell surface, see Movie S6 in the supplemental material of (36). This may indicate that some of the polysaccharide that was labeled with RCA_{120} also bound to RemA, so that the fluorescent lectin indirectly labeled RemA. Supporting this idea, strains lacking RemA failed to propel RCA_{120}. Cells of the *remC* mutant CJ1600 also failed to bind or propel RCA_{120}, suggesting that the putative glycosyltransferase RemC is involved in formation of the polysaccharide that is recognized by RCA_{120} ; see Movie S7 in the supplemental material of (36).

Discussion

Gliding motility of *F. johnsoniae* is thought to involve motors composed of Gld proteins anchored in the cell envelope that propel the adhesin SprB along the cell surface (12, 26, 34). Mutants lacking SprB exhibit motility defects, but they are still able to move, albeit weakly, on glass. This suggested the possibility that additional mobile adhesins might function to allow movement over some surfaces, and that SprB and these other adhesins may thus exhibit partial redundancy. Analysis of the *F. johnsoniae* genome revealed numerous potential *sprB* paralogs. A genetic approach was used to identify one *sprB* paralog, *remA*, which appears to encode a mobile cell-surface adhesin

that is partially redundant with SprB. Cells with mutations in *remA* exhibited motility defects that were only apparent when *sprB* was also defective. RemA and SprB are required for efficient infection by different *F. johnsoniae* bacteriophages, and may function as receptors for these phages. Both SprB and RemA appear to rely on the T9SS for secretion to the cell surface. Additional SprB paralogs may also function in gliding, and rely on the T9SS for secretion. This could explain why cells with mutations in the T9SS genes *gldK*, *gldL*, *gldM*, and *gldN*, exhibit complete resistance to bacteriophages, and complete loss of motility (2, 33).

Previous experiments suggested that SprB moves rapidly along the cell surface (26). Analysis of myc-tagged versions of RemA revealed that RemA behaves similarly. Spheres coated with antibodies against the myc-tag peptide bound specifically to cells expressing RemA-myc-tag-1, and the spheres were rapidly propelled along the length of the cell, around the pole, and back down the other side. Cells expressing myc-tagged RemA also propelled fluorescently labeled anti-myc antibodies. Spheres and fluorescent labeled antibodies moved at speeds of approximately 1 to 2 μm per second, which is similar to the speed at which cells glide on glass. Antibodies do not form permanent connections to their antigens, and it is possible for antibodies to tumble from one molecule of RemA to another. However, we do not expect the random tumbling of antibodies to be continuous and directional. The movements observed in this study were rapid, continuous, and directional, and indicate that RemA moves on the cell surface. The similar behaviors of SprB and RemA suggest that these cell-surface proteins both interact with the motility apparatus. The apparent partial redundancy between these

proteins may explain why cells lacking SprB retain some motility, and why cells lacking SprB and RemA have a greater motility defect.

The apparent rapid continuous movements of SprB and RemA over long distances is unprecedented for bacterial proteins. SprB and RemA appear to move from pole to pole (5 to 10 μm) in a few seconds, whereas other outer membrane or cell surface proteins that have been studied, such as *E. coli* LamB, travelled less than 0.3 μm from their starting point during 5 minutes (6). Some cytoplasmic proteins such as MinC, and cytoplasmic membrane proteins such as MinD, do migrate rapidly in *E. coli* cells (10, 29, 30). These proteins cycle from pole to pole and back again (a distance of about 6 μm) in 40 to 50 s, but even these dramatic movements are considerably slower than that observed for the *Flavobacterium* motility adhesins.

RemA has a region that is similar in sequence to galactose/rhamnose binding domains of SUEL-like lectins (38). Overexpression of RemA resulted in the formation of large aggregates of cells, and addition of galactose or rhamnose dispersed these aggregates. Cells of *remC*, *wza*, and *wzc* mutants, which are predicted to be defective for polysaccharide synthesis or secretion, failed to form large cell aggregates when RemA was overexpressed. Rhodamine-labeled lectin RCA_{120} interacted with wild-type cells, and with cells that overexpressed RemA. RCA_{120} was rapidly propelled on the cell surface, reminiscent of the movements observed for RemA. RCA_{120} failed to interact with cells lacking the polysaccharide synthesis and secretion proteins RemC, Wza, and Wzc, and RCA_{120} was not propelled on the surface of cells lacking RemA. The simplest explanation for these results is that the extracellular polysaccharides interact with both RemA and with RCA_{120}. Interaction of RemA with polysaccharides could facilitate

gliding of one cell over another cell, or could facilitate movement of cells over other polysaccharide-coated surfaces. By producing and secreting polysaccharides that interact with RemA or other cell surface motility proteins, cells may essentially produce their own 'road', and allow productive contact with a surface (such as perhaps glass) over which they might otherwise have difficulty moving. Cells could reuse such 'roads' resulting in the multicellular patterns that are characteristic of *F. johnsoniae* swarms and colonies. A similar strategy for interacting with surfaces, involving secreted polysaccharides and polysaccharide-binding-proteins, is used by the distantly related gliding bacterium, *Myxococcus xanthus*. Cells of *M. xanthus* move 50 times slower than those of *F. johnsoniae*, and they lack homologs for the *F. johnsoniae* motility proteins. *M. xanthus* uses two independent motility machineries, Type IV pili for 'S-motility' (41) and a separate motor system for 'A-motility' (25, 37, 42). Secreted polysaccharides have been proposed to function in both motility systems (18, 44). The Type IV pili interact with secreted polysaccharides containing glucosamine or N-acetylglucosamine (9, 16). Contact with a surface coated with polysaccharide results in pilus retraction and movement of the *M. xanthus* cell. Polysaccharides may also facilitate contact between proteins of the A-motility system and the substratum.

Our results support a model of *F. johnsoniae* motility in which gliding motors comprised of Gld proteins anchored in the cell envelope propel cell surface adhesins such as SprB and RemA (Figure 5, chapter 1). A similar model was proposed for the closely related bacterium '*Cytophaga*' sp. strain U67 in 1982, long before any of the components of the motility machinery had been identified (14). Some of the adhesins may interact directly with a surface, whereas others, such as RemA, may interact via secreted

polysaccharides. The polysaccharides may coat the surface, forming a 'road' over which cells travel. The action of the gliding 'motors' on the adhesins attached to the substratum result in cell movement. *F. johnsoniae* cells glide on agar, glass, Teflon, polystyrene, and presumably many other surfaces in nature. Genome analyses suggest that *F. johnsoniae* has the ability to make many different adhesins and polysaccharides (24), which may explain the ability of cells to crawl over these diverse surfaces.

SprB and RemA are mobile cell surface adhesins involved in *F. johnsoniae* gliding, but many mysteries remain regarding the motors that propel these adhesins, and the sensory transduction (chemotaxis) system that allows cells to control their movements. Most of the Gld and Spr proteins lack sequence similarity to proteins of known function, and typical components of bacterial chemotaxis systems are absent in *F. johnsoniae*, so it is likely that novel aspects of *Flavobacterium* motility await discovery. SprB and RemA provide convenient handles to examine the functioning of the gliding machinery in living cells.

Table 1. Strains and plasmids used in this study.

Strains	**Genotype and Description**[a]	**Source or reference**
UW101 (ATCC 17061)	Wild type	(22, 24)
CJ1584	Δ(*sprC sprD sprB*)	(31)
CJ1595	Δ(*sprC sprD sprB*) *remA*::*HimarEm1*; (Em^r)	This study
CJ1596	Δ(*sprC sprD sprB*) *remA*::*HimarEm1*; (Em^r)	This study
CJ1597	Δ(*sprC sprD sprB*) *remA*::*HimarEm1*; (Em^r)	This study
CJ1598	Δ(*sprC sprD sprB*) *wza*::*HimarEm1*; (Em^r)	This study
CJ1600	Δ(*sprC sprD sprB*) *remC*::*HimarEm1*; (Em^r)	This study
CJ1601	Δ(*sprC sprD sprB*) *remA*::*HimarEm1*; (Em^r)	This study
CJ1602	Δ(*sprC sprD sprB*) *wzc*::*HimarEm1*; (Em^r)	This study
CJ1603	Δ(*sprC sprD sprB*) *remB*::*HimarEm1*; (Em^r)	This study
CJ1827	*rpsL2*; (Sm^r) 'wild-type' strain used in construction of deletion mutants	(32)
CJ1922	*rpsL2* Δ*sprB*; (Sm^r)	(32)
CJ1984	*rpsL2* Δ*remA*; (Sm^r)	This study
CJ1985	*rpsL2* Δ*sprB* Δ*remA*; (Sm^r)	This study
CJ1986	*rpsL2* Δ(*fjoh_0803-fjoh_0806*); (Sm^r)	This study

CJ1987	*rpsL2* Δ*sprB* Δ(*fjoh_0803-fjoh_0806*); (Sm^r)	This study
CJ2072	*rpsL2* Δ*sprB remA::myc-tag-1*; (Sm^r)	This study
CJ2073	*rpsL2 remA::myc-tag-5*; (Sm^r)	This study
CJ2077	*rpsL2 remA::myc-tag-3*; (Sm^r)	This study
CJ2083	*rpsL2 remA::myc-tag-1*; (Sm^r)	This study
CJ2089	*rpsL2* Δ(*gldN gldO*) *remA::myc-tag-1*; (Sm^r)	This study
CJ2090	*rpsL2* Δ(*gldN gldO*); (Sm^r)	This study
CJ2097	*rpsL2 remA::myc-tag-1 sprF* ; (Sm^r Em^r)	This study
CJ2098	*rpsL2* Δ*remA* Δ(*fjoh_0803-fjoh_0806*); (Sm^r)	This study
CJ2100	*rpsL2* Δ*sprB* Δ*remA* Δ(*fjoh_0803-fjoh_0806*); (Sm^r)	This study
CJ2112	*rpsL2 remA::myc-tag-4*; (Sm^r)	This study
Plasmids		
pBC SK+	ColE1 ori; Cm^r	Stratagene
pMAL-c2	MalE fusion protein expression vector; Ap^r	New England Biolabs
pUC18	ColE1 ori; Ap^r	(40)
pCP23	*E. coli-F. johnsoniae* shuttle plasmid; Ap^r $(Tc)^r$	(1)
pCP29	*E. coli-F. johnsoniae* shuttle plasmid; Ap^r (Cf^r Em^r)	(13)
pLYL03	Plasmid carrying *ermF* gene; Ap^r (Em^r)	(15)
pHimarEm1	Plasmid carrying *HimarEm1*; Km^r (Em^r)	(2)

pMM332	Plasmid generated by self ligation of XbaI fragment spanning the site of insertion of *HimarEm1* in *remA* mutant CJ1597; Km^r (Em^r)	This study
pMM336	Plasmid generated by self ligation of XbaI fragment spanning the site of insertion of *HimarEm1* in *remA* mutant CJ1601; Km^r (Em^r)	This study
pNap3	Plasmid for construction of *gldNO* deletion strains; Ap^r (Em^r)	(33)
pRR36	3274 bp SphI-XbaI fragment of pMM336 spanning 3' end of *remA* inserted into pUC18; Ap^r	This study
pRR37	1592 bp HindIII-SphI fragment of pMM332 spanning 5' end of *remA* inserted into pRR36; Ap^r	This study
pRR38	4.9 kbp HindIII-XbaI fragment of pRR37 spanning *remA* inserted into pBC SK+; Cm^r	This study
pRR39	4.9 kbp KpnI-XbaI fragment of pRR38 spanning *remA* inserted into pCP23; Ap^r (Tc^r)	This study
pRR47	847 bp region within *sprF* amplified with primers 946 and 953, cloned into the XbaI and SphI sites of pLYL03. Used for construction of CJ2097; Ap^r (Em^r)	This study
pRR51	*rpsL*-containing suicide vector; Ap^r (Em^r)	(32)
pRR76	1.8 kbp region downstream of *remA* amplified with primers 760 and 1061, cloned into the SalI and PstI sites of pRR51; Ap^r (Em^r)	This study
pRR77	1.9 kbp region upstream of fjoh_0806 amplified with primers	This study

	1062 and 1063, cloned into the SalI and SphI sites of pRR51; Ap^r (Em^r)	
pRR78	Construct used to delete *remA*; 2.1 kbp region upstream of *remA* amplified with primers 1059 and 1060 and cloned into the BamHI and SalI sites of pRR76; Ap^r (Em^r)	This study
pRR79	Construct to delete *fjoh_0803* to *fjoh_0806*; 1.9 kbp region downstream of *fjoh_0803* amplified with primers 757 and 758 and cloned into the BamHI and SalI sites of pRR77; Ap^r (Em^r)	This study
pRR92	4.5 kbp fragment amplified using primers 761 and 1059 and containing myc-tag sequence (introduced using primers 1110 and 1112), inserted into pRR51. Used to construct *remA::*myc-tag-1 strains; Ap^r (Em^r)	This study
pRR93	4.4 kbp fragment amplified using primers 738 and 745 and containing myc-tag sequence (introduced using primers 1126 and 1128), inserted into pRR51. Used to construct *remA::*myc-tag-5 strains; Ap^r (Em^r)	This study
pRR95	4.4 kbp fragment amplified using primers 738 and 745 and containing myc-tag sequence (introduced using primers 1118 and 1120), inserted into pRR51. Used to construct *remA::*myc-tag-3 strains; Ap^r (Em^r)	This study
pRR96	4.4 kbp fragment amplified using primers 738 and 745 and containing myc-tag sequence (introduced using primers 1122	This study

	and 1124), inserted into pRR51. Used to construct *remA::*myc-tag-4 strains; Ap^r (Em^r)	
pSN60	pCP29 carrying *sprB*; Ap^r (Cf^r Em^r)	(26)
pSP18	1.96 kbp fragment encoding the 561 amino acid C-terminal fragment of the RemA protein, inserted between the BamH1 and Sal1 sites of pMAL-c2; Ap^r	This study
pTB79	pCP23 carrying *gldN*; Ap^r (Tc^r)	(2)

[a]Antibiotic resistance phenotypes: ampicillin, Ap^r; cefoxitin, Cf^r; chloramphenicol, Cm^r; erythromycin, Em^r; kanamycin, Km^r; streptomycin, Sm^r; tetracycline, Tc^r. Unless indicated otherwise, the antibiotic resistance phenotypes are those expressed in *E. coli*. The antibiotic resistance phenotypes given in parentheses are those expressed in *F. johnsoniae* but not in *E. coli*.

Table 2. Binding of Protein G-coated polystyrene spheres carrying antibodies against myc-tag peptide.

Strain	Description	Antibody added	Avg (SD) % of cells with spheres attached[a]
CJ1827	Wild type	No antibody	0.6 (0.5)
CJ1827	Wild type	Anti-myc	0.6 (1.1)
CJ2083	*remA::myc-tag-1*	No antibody	0.0 (0.0)
CJ2083	*remA::myc-tag-1*	Anti-myc	52.3 (3.2)
CJ2077	*remA::myc-tag-3*	Anti-myc	0.0 (0.0)
CJ2112	*remA::myc-tag-4*	Anti-myc	33.3 (3.1)
CJ2073	*remA::myc-tag-5*	Anti-myc	0.3 (0.5)
CJ2089	Δ(*gldN-gldO*) *remA::myc-tag-1*	Anti-myc	0.0 (0.0)
CJ2089 with pTB79 carrying *gldN*	Δ(*gldN-gldO*) *remA::myc-tag-1*/pTB79 (*gldN*)	Anti-myc	52.0 (3.0)
CJ2097	*remA::myc-tag-1 sprF*	Anti-myc	52.6 (4.0)

[a] Purified anti-Myc-tag antiserum and 0.5-μm-diameter protein G-coated polystyrene spheres were added to cells as described in Materials and Methods. Samples were introduced into a tunnel slide, incubated for 1 min at 25°C and examined using a phase-contrast microscope. Images were recorded for 30 s and 100 randomly selected cells

were examined for the presence of spheres that remained attached to the cells during this time. Numbers in parentheses are standard deviations (SD) calculated from three measurements.

Table 3. Primers used in this study.

Primers	Sequence and description
692	5' AAGGATTTCCTGCGATCGC 3'; used to confirm deletion of *gldN* and *gldO*
737	5' AGGCACCCCAGGCTTTACACT 3'; reverse primer in pLYL03, used to confirm disruption of *sprF*
738	5' GCGCAACAGGATCCCCTGGAATGCCAACTAATGG 3'; used in construction of pRR93 for *remA::myc-tag-5*, pRR95 for *remA::myc- tag-*3 and pRR96 for *remA::myc-tag-4*; BamHI site underlined
745	5' AATTGGGTCGACTTTTGGCACATCAGGAATGT 3'; used in construction of pSP18, pRR93 for *remA::myc-tag-5*, pRR95 for *remA::myc-tag*-3 and pRR96 for *remA::myc-tag-4*; SalI site underlined
757	5' ATCATCGGATCCATGCATGGGTGCTGCCTGGAG 3'; used in construction of pRR79 for fjoh_0803-0806 deletion, BamHI site unerlined
758	5' TCAAGTTGTCGACTTCCAATCCGGAAATCAGG 3'; used in construction of pRR79 for fjoh_0803-0806 deletion, SalI site underlined
760	5' TTTCACCTGCAGACATTTACAGCAAATCCTACTGG 3'; used in construction of pRR78 for remA deletion; PstI site underlined
761	5' TTTGTTCCGTCGACAGCAGAGAAACCAGTTGTATTGC 3'; used in construction of pRR92; SalI site underlined
762	5' CTGCTTACGGATCCGCTTGTTCTTCTGTATCTGCAG 3'; used in construction of pSP18; BamHI site underlined
778	5' CGGAACAATAAAGGGTGATTTGAC 3'; used to confirm deletion of *remA*
848	5’ AGGACGTTGCCGCTCTTAAACGTA 3’; used to confirm deletion of *sprB*
939	5’ ACAAGCCTCCTGCAATTCTCGAAG 3’; used to confirm deletion of *gldN* and *gld0*.
946	5’ GCTAGTCTAGAGCCAAGAGTTAAACCTACCGGTGT 3’; used to confirm disruption of *sprF*. XbaI site underlined.
953	5' GCTAGGCATGCATGCGTACCTGTATTGTAGGCTCC 3'; used to construct pRR47; SphI site underlined
964	5’ TGGTCGTTAAACCTAGGATCCGGT 3’; used to amplify and sequence

	the *rpsL* gene
1033	5’ GCTAGGTCGACATCGCTGATTTGACTGTTGGGCTG 3’; used in construction of pRR67; SalI site underlined
1059	5’ GCTAGGGATCCTACATCGGCTGCATTTGCAGAACC 3’; used in construction of pRR78 and pRR92; BamHI site underlined
1060	5’ GCTAGGTCGACGCCATTAGTTGGCATTCCAGG 3’; used in construction of pRR78 for *remA* deletion; SalI site underlined
1061	5’ GCTAGGTCGACGCCGATCAGGTGCTGCTTGTAAA 3’; used in construction of pRR78 for *remA* deletion; SalI site underlined
1062	5’ GCTAGGTCGACACTTGCAAGCTGCGCACTACCTAAA 3’; used in construction of pRR79 for fjoh_0803-0806 deletion; SalI site underlined
1063	5' GCTAGGCATGCTTGTGCTGGAGGAGGTGTGAAAGT3'; used in construction of pRR79 for fjoh_0803-0806 deletion, SphI site underlined
1068	5' GCCGCGTACAACATCTTTATCATGCG 3'; Primer used with primer 1060 for PCR to confirm fjoh_0803-0806 deletion
1118	5’GAGCAAAAATTAATTTCAGAGGAAGACTTAACAGCAACTTCTACAGTAG TTACAATCACT 3’; used in construction of pRR95 for *remA::myc-tag-3*; myc tag underlined
1120	5’TAAGTCTTCCTCTGAAATTAATTTTTGCTCATTGCACGTTCCACTTGTT GTTGC 3’; used in construction of pRR95 for *remA::myc-tag-3*; myc tag underlined
1122	5’GAGCAAAAATTAATTTCAGAGGAAGACTTAACTAGTCAATCAGTAGTT GAAAGTGCGCTT 3’; used in construction of pRR96 for *remA::myc-tag-4*; myc tag underlined
1124	5’TAAGTCTTCCTCTGAAATTAATTTTTGCTCTGCCGCGTGGCAGAAAGGA TTTAT 3’; used in construction of pRR96 for *remA::myc-tag-4*; myc tag underlined

References

1. **Agarwal, S., D. W. Hunnicutt, and M. J. McBride.** 1997. Cloning and characterization of the *Flavobacterium johnsoniae* (*Cytophaga johnsonae*) gliding motility gene, *gldA*. Proc. Natl. Acad. Sci. USA **94:**12139-12144.
2. **Braun, T. F., M. K. Khubbar, D. A. Saffarini, and M. J. McBride.** 2005. *Flavobacterium johnsoniae* gliding motility genes identified by *mariner* mutagenesis. J. Bacteriol. **187:**6943-6952.
3. **Braun, T. F., and M. J. McBride.** 2005. *Flavobacterium johnsoniae* GldJ is a lipoprotein that is required for gliding motility. J. Bacteriol. **187:**2628-2637.
4. **Chang, L. Y. E., J. L. Pate, and R. J. Betzig.** 1984. Isolation and characterization of nonspreading mutants of the gliding bacterium *Cytophaga johnsonae*. J. Bacteriol. **159:**26-35.
5. **Figurski, D. H., and D. R. Helinski.** 1979. Replication of an origin-containing derivative of plasmid RK2 dependent on a plasmid function provided in trans. Proc. Natl. Acad. Sci. USA **76:**1648-1652.
6. **Gibbs, K. A., D. D. Isaac, J. Xu, R. W. Hendrix, T. J. Silhavy, and J. A. Theriot.** 2004. Complex spatial distribution and dynamics of an abundant *Escherichia coli* outer membrane protein, LamB. Mol. Microbiol. **53:**1771-1783.
7. **Godchaux, W., III, L. Gorski, and E. R. Leadbetter.** 1990. Outer membrane polysaccharide deficiency in two nongliding mutants of *Cytophaga johnsonae*. J. Bacteriol. **172:**1250-1255.
8. **Godchaux, W., III, M. A. Lynes, and E. R. Leadbetter.** 1991. Defects in gliding motility in mutants of *Cytophaga johnsonae* lacking a high-molecular-weight cell surface polysaccharide. J. Bacteriol. **173:**7607-7614.
9. **Hu, W., Z. Yang, R. Lux, M. Zhao, J. Wang, X. He, and W. Shi.** 2012. Direct visualization of the interaction between pilin and exopolysaccharides of *Myxococcus xanthus* with eGFP-fused PilA protein. FEMS microbiology letters **326:**23-30.
10. **Hu, Z., and J. Lutkenhaus.** 1999. Topological regulation of cell division in *Escherichia coli* involves rapid pole to pole oscillation of the division inhibitor MinC under the control of MinD and MinE. Mol. Microbiol. **34:**82-90.
11. **Hunnicutt, D. W., and M. J. McBride.** 2000. Cloning and characterization of the *Flavobacterium johnsoniae* gliding motility genes, *gldB* and *gldC.* J. Bacteriol. **182:**911-918.
12. **Jarrell, K. F., and M. J. McBride.** 2008. The surprisingly diverse ways that prokaryotes move. Nat. Rev. Microbiol. **6:**466-476.
13. **Kempf, M. J., and M. J. McBride.** 2000. Transposon insertions in the *Flavobacterium johnsoniae ftsX* gene disrupt gliding motility and cell division. J. Bacteriol. **182:**1671-1679.
14. **Lapidus, I. R., and H. C. Berg.** 1982. Gliding motility of *Cytophaga* sp. strain U67. J. Bacteriol. **151:**384-398.

15. **Li, L.-Y., N. B. Shoemaker, and A. A. Salyers.** 1995. Location and characterization of the transfer region of a *Bacteroides* conjugative transposon and regulation of the transfer genes. J. Bacteriol. **177:**4992-4999.
16. **Li, Y., H. Sun, X. Ma, A. Lu, R. Lux, D. R. Zusman, and W. Shi.** 2003. Extracellular polysaccharides mediate pilus retraction during social motility of *Myxococcus xanthus*. Proc. Natl. Acad. Sci. USA **100:**5443-5448.
17. **Liu, J., M. J. McBride, and S. Subramaniam.** 2007. Cell-surface filaments of the gliding bacterium *Flavobacterium johnsoniae* revealed by cryo-electron tomography. J. Bacteriol. **189:**7503-7506.
18. **Lu, A., K. Cho, W. P. Black, X. Y. Duan, R. Lux, Z. Yang, H. B. Kaplan, D. R. Zusman, and W. Shi.** 2005. Exopolysaccharide biosynthesis genes required for social motility in *Myxococcus xanthus*. Mol. Microbiol. **55:**206-220.
19. **McBride, M. J.** 2001. Bacterial Gliding Motility: Multiple mechanisms for cell movement over surfaces. Annu. Rev. Microbiol. **55:**49-75.
20. **McBride, M. J.** 2004. Cytophaga-flavobacterium gliding motility. J. Mol. Microbiol. Biotechnol. **7:**63-71.
21. **McBride, M. J., and S. A. Baker.** 1996. Development of techniques to genetically manipulate members of the genera *Cytophaga*, *Flavobacterium*, *Flexibacter*, and *Sporocytophaga*. Appl. Environ. Microbiol. **62:**3017-3022.
22. **McBride, M. J., and T. F. Braun.** 2004. GldI is a lipoprotein that is required for *Flavobacterium johnsoniae* gliding motility and chitin utilization. J. Bacteriol. **186:**2295-2302.
23. **McBride, M. J., and M. J. Kempf.** 1996. Development of techniques for the genetic manipulation of the gliding bacterium *Cytophaga johnsonae*. J. Bacteriol **178:**583-590.
24. **McBride, M. J., G. Xie, E. C. Martens, A. Lapidus, B. Henrissat, R. G. Rhodes, E. Goltsman, W. Wang, J. Xu, D. W. Hunnicutt, A. M. Staroscik, T. R. Hoover, Y. Q. Cheng, and J. L. Stein.** 2009. Novel features of the polysaccharide-digesting gliding bacterium *Flavobacterium johnsoniae* as revealed by genome sequence analysis. Appl. Environ. Microbiol. **75:**6864-6875.
25. **Nan, B., J. Chen, J. C. Neu, R. M. Berry, G. Oster, and D. R. Zusman.** 2011. Myxobacteria gliding motility requires cytoskeleton rotation powered by proton motive force. Proceedings of the National Academy of Sciences of the United States of America **108:**2498-2503.
26. **Nelson, S. S., S. Bollampalli, and M. J. McBride.** 2008. SprB is a cell surface component of the *Flavobacterium johnsoniae* gliding motility machinery. J. Bacteriol. **190:**2851-2857.
27. **Nelson, S. S., P. P. Glocka, S. Agarwal, D. P. Grimm, and M. J. McBride.** 2007. *Flavobacterium johnsoniae* SprA is a cell-surface protein involved in gliding motility. J. Bacteriol. **189:**7145-7150.
28. **Pate, J. L., S. J. Petzold, and L.-Y. E. Chang.** 1979. Phages for the gliding bacterium *Cytophaga johnsonae* that infect only motile cells. Curr. Microbiol. **2:**257-262.

29. **Raskin, D. M., and P. A. de Boer.** 1999. MinDE-dependent pole-to-pole oscillation of division inhibitor MinC in *Escherichia coli*. J. Bacteriol. **181:**6419-6424.
30. **Raskin, D. M., and P. A. de Boer.** 1999. Rapid pole-to-pole oscillation of a protein required for directing division to the middle of *Escherichia coli*. Proc. Natl. Acad. Sci. USA **96:**4971-4976.
31. **Rhodes, R. G., S. S. Nelson, S. Pochiraju, and M. J. McBride.** 2011. *Flavobacterium johnsoniae sprB* is part of an operon spanning the additional gliding motility genes *sprC*, *sprD*, and *sprF*. J. Bacteriol. **193:**599-610.
32. **Rhodes, R. G., H. G. Pucker, and M. J. McBride.** 2011. Development and use of a gene deletion strategy for *Flavobacterium johnsoniae* to identify the redundant motility genes *remF*, *remG*, *remH*, and *remI*. J. Bacteriol. **193:**2418-2428.
33. **Rhodes, R. G., M. N. Samarasam, A. Shrivastava, J. M. van Baaren, S. Pochiraju, S. Bollampalli, and M. J. McBride.** 2010. F*lavobacterium johnsoniae gldN* and *gldO* are partially redundant genes required for gliding motility and surface localization of SprB. J. Bacteriol. **192:**1201-1211.
34. **Rhodes, R. G., M. N. Samarasam, E. J. Van Groll, and M. J. McBride.** 2011. Mutations in *Flavobacterium johnsoniae sprE* Result in Defects in Gliding Motility and Protein Secretion. Journal of bacteriology **193:**5322-5327.
35. **Sato, K., M. Naito, H. Yukitake, H. Hirakawa, M. Shoji, M. J. McBride, R. G. Rhodes, and K. Nakayama.** 2010. A protein secretion system linked to bacteroidete gliding motility and pathogenesis. Proc. Natl. Acad. Sci. USA **107:**276-281.
36. **Shrivastava, A., R. G. Rhodes, S. Pochiraju, D. Nakane, and M. J. McBride.** 2012. *Flavobacterium johnsoniae* RemA is a mobile cell-surface lectin involved in gliding. J. Bacteriol. **194:**3678-3688.
37. **Sun, M., M. Wartel, E. Cascales, J. W. Shaevitz, and T. Mignot.** 2011. Motor-driven intracellular transport powers bacterial gliding motility. Proc. Natl. Acad. Sci. USA **108:**7559-7564.
38. **Tateno, H.** 2010. SUEL-related lectins, a lectin family widely distributed throughout organisms. Biosci. Biotechnol. Biochem. **74:**1141-1144.
39. **Uenoyama, A., A. Kusumoto, and M. Miyata.** 2004. Identification of a 349-kilodalton protein (Gli349) responsible for cytadherence and glass binding during gliding of *Mycoplasma mobile*. J. Bacteriol. **186:**1537-1545.
40. **Vieria, J., and J. Messing.** 1982. The pUC plasmids, an M13mp7-derived system for insertion mutagenesis and sequencing with synthetic universal primers. Gene **19:**259-268.
41. **Wall, D., and D. Kaiser.** 1999. Type IV pili and cell motility. Mol. Microbiol. **32:**1-10.
42. **Wolgemuth, C., E. Hoiczyk, D. Kaiser, and G. Oster.** 2002. How myxobacteria glide. Current Biol. **12:**369-377.
43. **Wolkin, R. H., and J. L. Pate.** 1985. Selection for nonadherent or nonhydrophobic mutants co-selects for nonspreading mutants of *Cytophaga johnsonae* and other gliding bacteria. J. Gen. Microbiol. **131:**737-750.

44. **Yu, R., and D. Kaiser.** 2007. Gliding motility and polarized slime secretion. Mol. Microbiol. **63:**454-467.

Chapter 3. *Flavobacterium johnsoniae* GldK, GldL, GldM, and SprA are required for secretion of the cell-surface gliding motility adhesins SprB and RemA

Abstract

Flavobacterium johnsoniae cells move rapidly over surfaces by gliding motility. Gliding results from the movement of adhesins such as SprB and RemA along the cell surface. These adhesins are delivered to the cell surface by a *Bacteroidetes*-specific secretion system referred to as the Type IX secretion system (T9SS). GldN, SprE, SprF and SprT are involved in secretion by this system. Here we demonstrate that GldK, GldL, GldM, and SprA are each also involved in secretion. Nonpolar deletions of *gldK*, *gldL*, or *gldM* resulted in absence of gliding motility and in T9SS defects. The mutant cells produced SprB and RemA proteins but failed to secrete them to the cell surface. The mutants were resistant to phages that use SprB or RemA as receptors, and they failed to attach to glass, presumably because of the absence of cell surface adhesins. Deletion of *sprA* resulted in similar but slightly less dramatic phenotypes. *sprA* mutant cells failed to secrete SprB and RemA, but cells remained susceptible to some phages, and retained some limited ability to glide. The phenotype of the *sprA* mutant was similar to those previously described for *sprE* and *sprT* mutants. SprA, SprE, and SprT are needed for secretion of SprB and RemA, but may not be needed for secretion of some other proteins targeted to the T9SS. Genetic and molecular experiments demonstrate that *gldK*, *gldL*, *gldM*, and *gldN* form an operon, and suggest that the proteins encoded by these genes may interact to form part of the *F. johnsoniae* T9SS.

Introduction

Cells of *Flavobacterium johnsoniae* move rapidly over surfaces by gliding motility. *Flavobacterium* gliding motility does not involve flagella or pili, but instead relies on novel machinery that appears to be confined to members of the large and diverse phylum *Bacteroidetes* (12, 18). Genetic experiments identified Gld, Spr, and Rem proteins with roles in motility. A motor comprised of some of the Gld proteins is thought to propel cell surface adhesins, such as SprB and RemA. These adhesins interact with the substratum, or with polysaccharides that coat the substratum, and the action of the motor on the adhesins propels the cell (19, 35).

Some of the Gld and Spr proteins form a novel protein secretion system originally referred to as the Por protein secretion system (26, 27, 30). More recently this has been called the Type IX secretion system (T9SS) (18, 32), because the known components are not similar in sequence to proteins of Type I to Type VIII secretion systems (1, 6, 10). T9SSs are common in members of the phylum *Bacteroidetes*, but are apparently not found outside of that phylum (18). Proteins secreted by T9SSs have predicted N-terminal type 1 signal peptides and are thought to rely on the Sec system for export across the cytoplasmic membrane. They also have conserved C-terminal domains (CTDs) that appear to target them to the T9SS for secretion across the outer membrane (21, 33-36).

T9SSs have been studied in the nonmotile periodontal pathogen *Porphyromonas gingivalis*, and in *F. johnsoniae*. The *P. gingivalis* T9SS is involved in secretion of gingipain proteases and other virulence factors, and the *F. johnsoniae* T9SS is needed for secretion of the cell-surface motility adhesins SprB and RemA, and for secretion of a chitinase. In *F. johnsoniae*, GldN, SprE, SprF, and SprT (which are related to the *P.*

gingivalis T9SS proteins PorN, PorW, PorP, and PorT respectively) have been demonstrated to have roles in secretion (24, 26, 27, 30). GldK, GldL, GldM, and SprA were originally identified as proteins required for *F. johnsoniae* gliding motility (3, 20). Studies of *P. gingivalis* revealed that homologs to these proteins (PorK, PorL, PorM, and Sov respectively) are required for gingipain secretion (29, 30). Here we demonstrate that *F. johnsoniae* GldK, GldL, GldM, and SprA are each required for secretion of SprB and RemA, and for utilization of chitin. *gldK*, *gldL*, *gldM*, and *gldN* form an operon and the products of these genes each localize to the cell envelope where they may interact to form a complex involved in protein secretion.

Materials and Methods

Bacterial strains, plasmids, and growth conditions. *F. johnsoniae* ATCC 17061 strain UW101, was the wild-type strain used in this study. The streptomycin resistant *rpsL* mutant of UW101 (CJ1827) was used to construct strains with unmarked deletions (25). *F. johnsoniae* strains were grown in Casitone-yeast extract (CYE) medium (16) at 25^{o}C. To observe colony spreading, *F. johnsoniae* was grown at 25^{o}C on PY2 medium supplemented with 10 g of agar per L (2). Motility medium (MM) was used to observe movement of individual cells in wet mounts (14). Strains and plasmids used in this study are listed in Table 4, and primers used in this study are listed in Table 8. Sites of transposon insertions in *gldK*, *gldL*, *gldM*, and *gldN* are illustrated in Figure 19, as are the regions carried on plasmids used for complementation experiments. The plasmids used for complementation were all derived from pCP1 and have copy numbers of approximately 10 in *F. johnsoniae* (2, 13, 16). Antibiotics were used at the following

concentrations when needed: ampicillin, 100 μg/ml; cefoxitin, 100 μg/ml; chloramphenicol, 30 μg/ml; erythromycin, 100 μg/ml; streptomycin, 100 μg/ml; and tetracycline, 20 μg/ml.

Deletion of *gldK*, *gldL, gldM*, and *sprA*. Unmarked deletions were made as previously described (25). To make the *gldL* deletion a 2.4 kbp fragment downstream of *gldL* was amplified by PCR using primers 1199 (introducing a XbaI site) and 1200 (introducing a SalI site). The fragment was digested with XbaI and SalI and ligated into pRR51 that had been digested with the same enzymes, to generate pAB18. A 2.2 kbp fragment spanning the upstream region of *gldL* was amplified by PCR with primers 1197 (introducing a BamHI site) and 1198 (introducing an XbaI site). The fragment was digested with BamHI and XbaI and fused to the region downstream of *gldL* by ligation with pAB18 that had been digested with the same enzymes to generate the deletion construct pAB19. Plasmid pAB19 was introduced into the streptomycin resistant wild-type *F. johnsoniae* strain CJ1827 and the *remA*::*myc-tag-1* strain CJ2083 (35) by triparental conjugation, and *gldL* deletion mutants were isolated as previously described (25). Deletion of *gldL* was confirmed by PCR amplification using primers 690 and 707, which flank the *gldL* coding sequence. *gldK, gldM*, and *sprA* were deleted in wild-type CJ1827 and in the *remA*::*myc-tag-1* strain CJ2083 by the same approach using the primers listed in Table 8 and the plasmids listed in Table 4.

Transduction of *sprT* mutation into CJ2083 (*rpsL2 remA::myc-tag-1*). The *sprT* mutation in strain KDF001 was transduced into CJ2083 (*rpsL2 remA::myc-tag-1*) essentially as previously described (26), using phage fCj54 and selecting for erythromycin resistance.

Reverse transcriptase PCR (RT-PCR) to characterize the *gldK, gldL, gldM, gldN* operon. RNA was extracted from wild-type *F. johnsoniae* UW101 cells as described previously (24). Briefly, wild-type cells were grown in 25 ml of MM overnight at 25°C without shaking. Cells were harvested by centrifugation at 4,000 x g for 10 min. and the pellet was suspended in 450 ml of MM. RNAProtect (Qiagen, Valencia, CA) was added and pellet was collected as described previously (24). RNA was extracted and purified using the RNeasy minikit (Qiagen) according to the manufacturer's instructions except that RNasin (Promega Corp, Madison, WI) and RQ1 RNase-free DNase (Promega) were used as described previously (24). RNA concentrations (OD_{260}) and purity ($OD_{260/280}$) were determined by UV spectroscopy, and RNA integrity was verified by visualizing the intensity of the 16S and 23S rRNA bands on a 1% agarose gel.

RT PCR was used to determine the transcriptional organization of *gldK, gldL, gldM* and *gldN*. cDNA was generated using the SuperScript first-strand synthesis for RT-PCR kit (Invitrogen Corp., Carlsbad, CA) according to the manufacturer's instruction. RNA was reverse transcribed as described previously (24). Gene specific primer 695 was used for reverse transcription. For PCR, antisense primers used to generate the cDNA were used in various combinations with sense primers.

Expression of recombinant GldK, GldL, and GldM for antibody production. A 1308-bp fragment of *gldK* was amplified using Phusion DNA polymerase (New England Biolabs, Ipswich, MA) and primer 705 (introducing a Sal1 site) and primer 704 (introducing an EcoR1 site). The product was digested with EcoR1 and Sal1 and inserted into pET30a (Novagen, Madison, WI) that had been digested with the same enzymes, to generate pJVB4. A 607-bp fragment of *gldL* was amplified using primer 707 (introducing

a Sal1 site) and primer 706 (introducing an EcoR1 site) and the product was digested and inserted into pET30a as described above generating pJVB2. A 1311-bp fragment of *gldM* was amplified using primer 709 (introducing a Sal1 site) and primer 708. The PCR product was digested with SalI and EcoRI (which cuts within *gldM*) and inserted into pET30a as described above generating pJVB6. pJVB4, pJVB2, and pJVB6 encode proteins with amino terminal His-tag peptides fused to the C-terminal 434, 174, and 426 amino acids of GldK, GldL, and GldM respectively.

pJVB4, pJVB2, and pJVB6 were introduced into *E. coli* Rosetta2 (DE3) (Novagen), which produces seven rare tRNAs required for efficient expression of *F. johnsoniae* proteins in *E. coli* (19, 20). Expression was induced by addition of 1.0 mM IPTG (isopropyl-b-D-thiogalactopyranoside) and incubation for 3 h at 37^{o}C. Cells were collected by centrifugation, disrupted using a French pressure cell, and recombinant proteins were purified by Ni-affinity chromatography. Polyclonal antibodies against recombinant GldK, GldL, and GldM were produced, and affinity purified using the recombinant protein, by Proteintech Group, Inc. (Chicago, IL).

Detection and localization of GldK, GldL and GldM. Wild type and mutant cells of *F. johnsoniae* were grown to mid-log phase in CYE at 25°C. Cells were washed twice in distilled water by centrifugation at 4,000 x g, and were lysed by incubation for 5 min at 100^{o}C in SDS-PAGE loading buffer. Proteins (15 μg per lane) were separated by SDS–PAGE and Western blotting was performed as described previously (26). To determine protein localization, wild-type cells were grown to mid log phase in MM at 25°C with shaking. The cells were washed twice with distilled water, and EDTA-free Halt Protease Inhibitor Cocktail was added (Thermo fisher Scientific, Rockford, IL). The cells were

disrupted using a French Pressure cell and fractionated into soluble, inner membrane (Sarkosyl-soluble) and outer membrane (Sarkosyl-insoluble) fractions essentially as described previously (11). Proteins were separated by SDS-PAGE, equal amounts of each fraction based on the starting material were loaded per lane and Western blotting was performed as described previously (26).

Analysis of wild type and mutant cells for production and secretion of SprB and Myc-tagged RemA. Cells were grown to mid exponential phase in CYE medium at 25^{o}C. Production of SprB and Myc-tagged RemA was determined by Western blot analyses using antisera against SprB and RemA respectively, as previously described (26, 35). Secretion of SprB was examined essentially as previously described (27). Briefly, cells were grown overnight in MM medium at 25^{o}C. Purified anti-SprB (1 µl of a 1:10 dilution of a 300-mg/L stock), 0.5-µm-diameter Protein G-coated polystyrene spheres (1 µl of a 0.1% stock preparation; Spherotech Inc., Libertyville, IL), and bovine serum albumin (BSA) (1 µl of a 1% solution) were added to 7 µl of cells (approximately 5 x 10^{8} cells per ml) in MM. The cells were introduced into a tunnel slide and examined by phase-contrast microscopy at 25^{o}C. Samples were examined 2 min after spotting, and images were recorded for 30 s to determine the % of cells that had anti-SprB-coated spheres attached to them. Surface localized Myc-tagged RemA was detected similarly, except that antisera against the Myc Tag (EQKLISEEDL; AbCam, Cambridge, MA) was used instead of anti-SprB.

Microscopic observations of cell movement. Wild type and mutant cells were examined for movement over glass by phase-contrast microscopy. Cells were grown overnight in MM medium at 25^{o}C without shaking as previously described (14). Simple

tunnel slides were constructed using double stick tape, glass microscope slides, and glass cover slips, as previously described (35). Cells in MM were introduced into the tunnel slides, incubated for 5 min, and observed for motility using an Olympus BH2 phase-contrast microscope with a heated stage at 25°C. Images were recorded with a Photometrics CoolSNAP$_{cf}^2$ camera and analyzed using MetaMorph software (Molecular Devices, Downingtown, PA).

Measurements of bacteriophage sensitivity. The bacteriophages active against *F. johnsoniae* that were used in this study were ϕCj1, ϕCj13, ϕCj23, ϕCj28, ϕCj29, ϕCj42, ϕCj48 and ϕCj54 (4, 23, 39). Sensitivity to bacteriophages was determined essentially as previously described by spotting 5 ml of phage lysates (10^9 plaque forming units/ml) onto lawns of cells in CYE overlay agar (11). The plates were incubated for 24 h at 25°C to observe lysis.

Measurement of chitin utilization. The ability of *F. johnsoniae* to utilize chitin was assayed as described previously (26). *F. johnsoniae* cells were grown overnight in MM media without shaking at 25°C. 2 µl of cells were spotted on MYA-chitin containing appropriate antibiotics and plates were incubated for 2.5 days.

Microscopic observations of cell attachment. Wild-type and mutant cells of *F. johnsoniae* were examined for attachment to glass using a Petroff-Hausser counting chamber, as previously described with slight modifications (26). Cells were grown overnight in MM medium without shaking at 25°C. The culture was diluted with an equal volume of fresh MM and incubated at 25°C without shaking until a cell density equivalent to OD_{600} of 0.4 was reached. Cells (2.5 µl) were added to a Petroff-Hausser counting chamber, covered with glass coverslip, and allowed to incubate for 2 minutes at

25°C. The number of cells attached to 9 randomly selected 0.03-mm^2 regions of the glass coverslip was determined.

Results

***gldK, gldL, gldM* and *gldN* form an operon.** Previous results indicated that *gldL*, *gldM*, and *gldN* are co-transcribed (3). The situation regarding *gldK*, which lies upstream of *gldL*, was less clear. It was suggested that *gldK* was transcribed separately, but the *gldK* transcript was not detected by Northern blot analysis, leaving the operon structure uncertain. Complementation analyses used to determine operon structure were also inconclusive, because moderate overexpression of *gldK* and *gldL* together in wild-type cells resulted in a dramatic decrease in growth and in motility, complicating analysis of polar effects of mutations (3). In order to understand the importance of GldK, GldL, and GldM to gliding motility and protein secretion, we revisited the transcriptional organization of these genes.

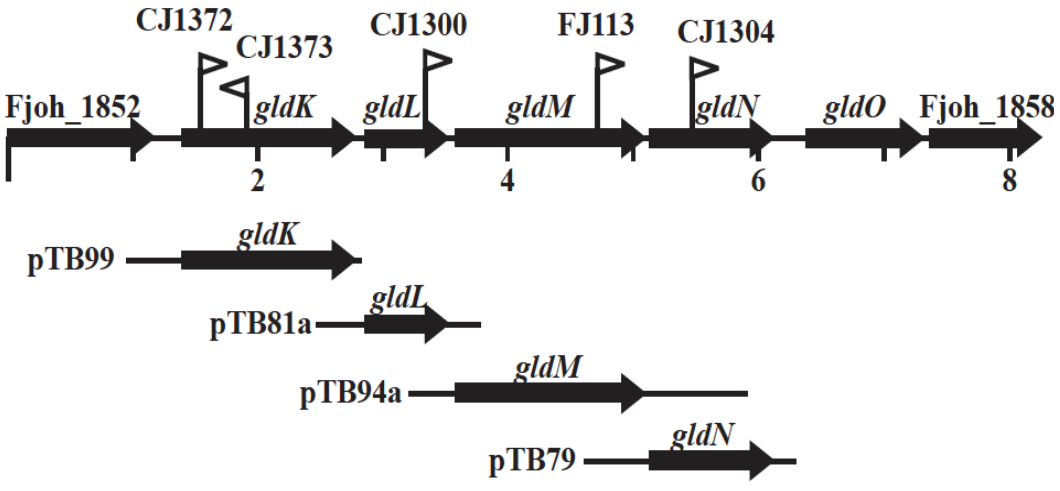

Figure 19. Map of the *gldKLMN* region. Numbers below the map refer to kilobase pairs of sequence. The sites of *HimarEm* insertions are indicated by triangles. Orientations of *HimarEm* insertions are indicated by the direction in which the triangles are pointing, with triangles pointing to the right having IR2 on the right side. The regions of DNA carried by plasmids used in this study are indicated beneath the map

To begin to address the transcriptional organization we examined the ability of pTB99, which carries *gldK*, to complement various *gldK* mutants. Two of the mutants (UW102-57 and UW102-141) had single base substitutions in *gldK*, whereas the other two (CJ1372 and CJ1373) had *HimarEm* transposon insertions in *gldK*. The sites of the mutations in UW102-57 and UW102-141 were determined by amplification and sequencing. UW102-57 had an "A" to "T" substitution at position 1054 numbered from the "A" of the *gldK* start codon, and UW102-141 had a "G" to "A" substitution at position 1158 as previously reported (3). The substitutions converted the codons for R_{352} and W_{386} respectively to stop codons. pTB99 restored motility to UW102-57 and UW102-141, but failed to restore motility to either of the *gldK HimarEm* mutants (Figure 20). These results suggested that the base substitution mutations resulted in nonpolar mutations, whereas the *HimarEm* insertions may have exhibited polar effects on downstream genes.

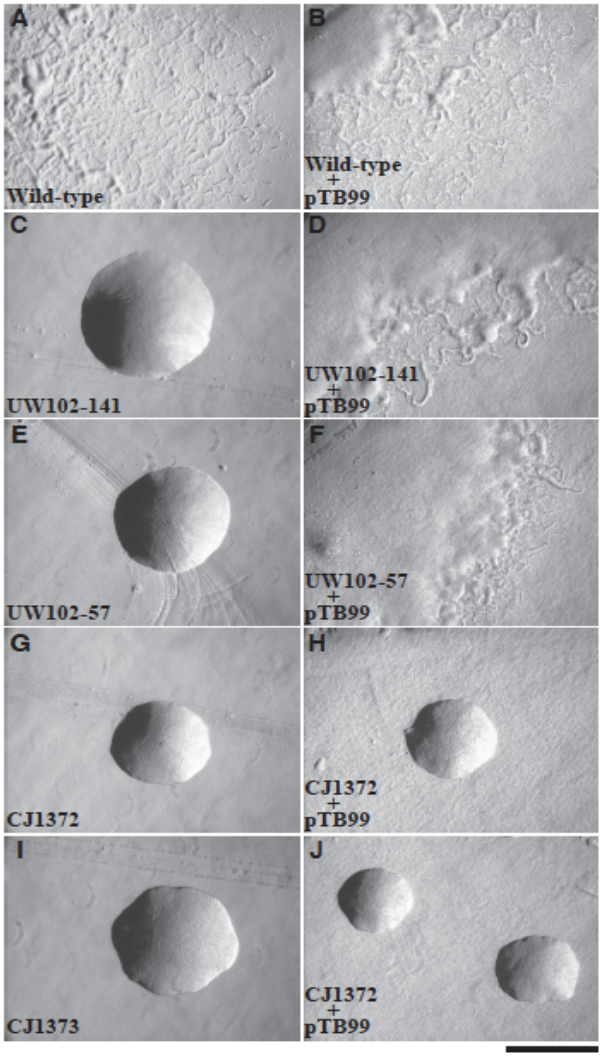

Figure 20. Photomicrographs of *F. johnsoniae* colonies. Colonies were incubated at 25°C on PY2 agar for 36 h. Photomicrographs were taken with a Photometrics Cool-SNAP$_{cf}^{2}$ camera mounted on an Olympus IMT-2 phase-contrast microscope. (A) Wild-type *F. johnsoniae* UW101. (B) *F. johnsoniae* UW101 with pTB99 which carries *gldK*. (C) *gldK* point mutant UW102-141. (D) UW102-141 complemented with pTB99. (E) *gldK* point mutant UW102-57. (F) UW102-57 complemented with pTB99. (G) *gldK Himar* mutant CJ1372. (H) CJ1372 with pTB99. (I) *gldK Himar* mutant CJ1373. (J) CJ1373 with pTB99. Bar indicates 1 mm, and applies to all panels.

To explore the issue of polarity more directly we examined the levels of GldK, GldL, GldM, and GldN proteins in *HimarEm* induced GldK mutants. GldK, GldL, and GldM were overexpressed in *E. coli* and antisera were raised against each protein. These proteins were each detected in cells of wild-type *F. johnsoniae*, but they were absent from appropriate *gld* deletion mutants (Figure 21). Western blot analysis revealed that strains CJ1372 and CJ1373, which have transposon insertions in *gldK*, not only lacked GldK protein but also had little if any GldL, GldM, and GldN proteins (Figure 21 and data not shown). Similarly, strains with transposon insertions in *gldL* produced little GldM or GldN, and strains with transposon insertions in *gldM* were deficient in GldN (data not shown). The results provide additional evidence of polarity of the *gldK* mutations, and suggest that *gldK*, *gldL*, *gldM* and *gldN* may be cotranscribed.

We recently developed a method to generate in-frame deletions of *F. johnsoniae* genes (25). Using this method, strains with deletions of *gldK*, *gldL*, and *gldM* were generated. In contrast to the transposon mutants described above, CJ2122 (Δ*gldK*), produced GldL, GldM, and GldN, indicating that the mutation was nonpolar, and that GldK protein was not required for production of GldL, GldM, and GldN (Figure 21). The *gldK* deletion mutant produced wild-type levels of GldL and GldM (Figure 21, panels B and C), but produced reduced levels of GldN (Figure 21 D). Complementation of the *gldK* deletion mutant with pTB99, which carries *gldK*, restored GldK and GldN to wild type levels. Restoration of GldN levels by expression of GldK argues against a polar effect of the *gldK* deletion mutation on expression of *gldN*. Analysis of CJ2157, (Δ*gldL*) and CJ2262 (Δ*gldM*) gave similar results. CJ2157 failed to produce GldL protein, but produced GldM and GldN, and CJ2262 failed to produce GldM protein but produced

GldN (Figure 21 C, D). The strains with deletions in *gldL* and *gldM* were similar to *gldK* deletions in that they had low levels of GldN protein. One possible explanation for these results is that GldK, GldL, GldM, and GldN may form a complex, and GldN may be unstable in the absence of any of its partners. This may also explain the low levels of GldL observed in CJ2262 (Δ*gldM*) (Figure 21 B) and the reduced levels of GldK protein in strains with mutations in *gldL*, *gldM*, and *gldN* (Figure 21 A).

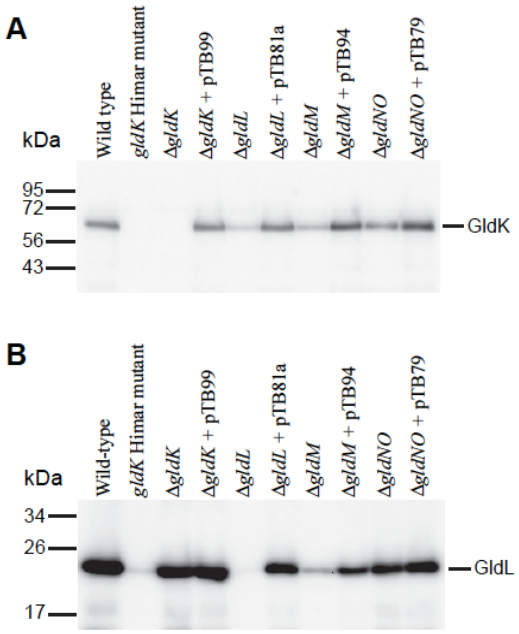

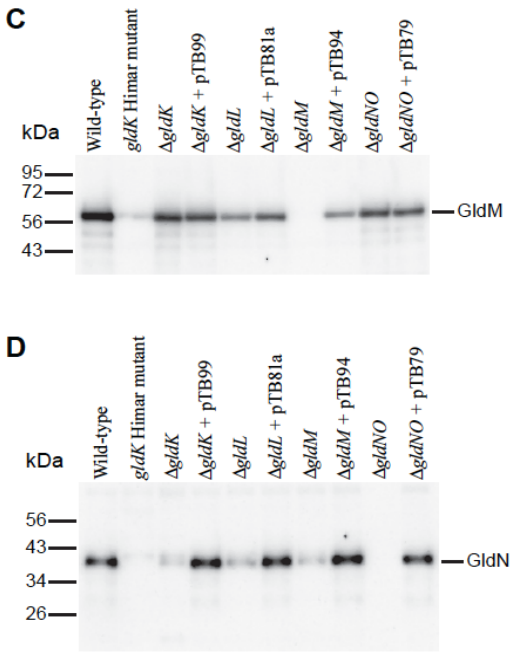

Figure 21. Western blot immunodetection of GldK (Panel A), GldL (Panel B), GldM (Panel C), and GldN (Panel D) in whole-cell extracts of wild-type, mutant, and complemented strains of *F. johnsoniae*. The wild-type strain was CJ1827 (*rpsL2*), the *gldK Himar* mutant was CJ1372, and the strains with deletions in *gldK*, *gldL*, *gldM* and *gldNO* were CJ2122, CJ2157, CJ2262, and CJ2090 respectively. pTB99, pTB81a, pTB94, and pTB79 express GldK, GldL, GldM, and GldN respectively, and thus complement the indicated mutants. 15 micrograms of protein was loaded in each lane.

The results presented above suggest that *gldK*, *gldL*, *gldM*, and *gldN* form an operon. RT PCR analysis confirmed the presence of a transcript spanning *gldK*, *gldL*, *gldM*, and *gldN* (Figure 22). A predicted *Flavobacterium* consensus promoter sequence (TANNTTTG) was identified 97 bp upstream of the *gldK* start codon, and 5' RACE analysis identified the start site of transcription 5 bp downstream of the final 'G' of this promoter sequence (3). An inverted repeat (AAAAAACTCTTACTACCTTTGTAGT AAGAGTTTTTT) that may function as a transcription terminator, was present 22 bp downstream of the *gldN* stop codon. Genetic and molecular evidence previously

demonstrated that *gldO,* which lies downstream of the *gldKLMN* operon and which is partially redundant with *gldN,* is transcribed independently. Transposon insertions in *gldN* were not polar on *gldO*, and the *gldN* mutants produced GldO protein (26).

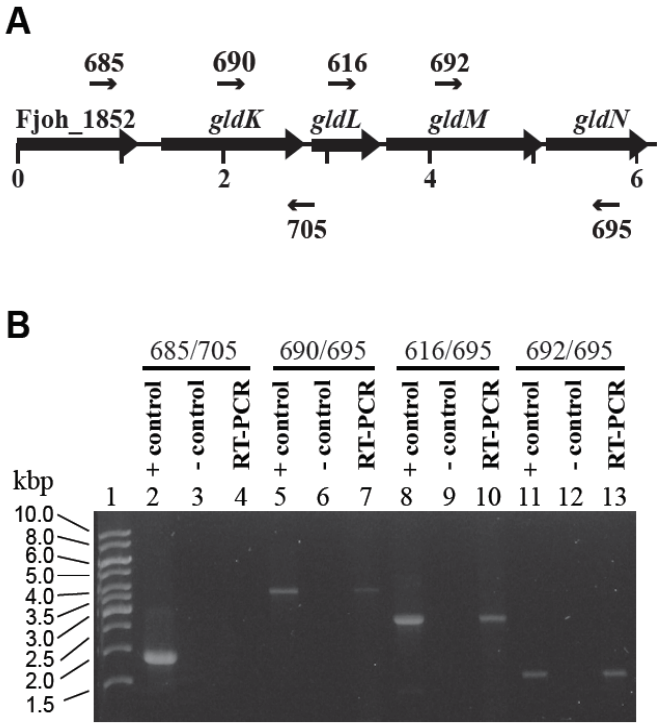

Figure 22. RT-PCR analysis of the *gldKLMN* operon. (A) Map of the *gldKMLN* operon with primers used for RT-PCR (numbered arrows). (B) RT-PCR of wild-type *F. johnsoniae* UW101 RNA. Reverse transcription was carried out with primer 695, which is complementary to a sequence internal to *gldN*. PCR was conducted using the primer pairs shown. For each primer pair three reaction mixtures were loaded onto the gel: a positive control PCR using *F. johnsoniae* chromosomal DNA as template (lanes 2, 5, 8, 11), a no-RT control reaction mixture (lanes 3, 6, 9, 12), and a RT-PCR mixture (lanes 4, 7, 10, 13). Lane 1, 1-kb DNA ladder as a size standard. Lane 2-4, primer pair 685:705. Lane 5-7, primer pair 690:695. Lane 8-10, primer pair 616:695. Lane 11-13, primer pair 692:695.

GldK, GldL, and GldM are each required for gliding. As previously reported, transposon insertions in *gldK*, *gldL*, and *gldM* result in complete loss of motility (3). Given the concerns regarding polarity of these mutations we analyzed the phenotypes of the in-frame deletions to determine the roles of the individual proteins. Cells with deletion mutations in *gldK*, *gldL*, or *gldM* were completely nonmotile. They formed nonspreading colonies on agar media (Figure 23) and exhibited no cell movements in wet mounts on glass (Movies S1, S2, and S3 in the supplemental material of Shrivastava et al. in review). In each case complementation with the appropriate gene restored motility. Cells of the deletion mutants were also examined by time-lapse microscopy for possible slow or intermittent movements on glass or agar using methods previously described (18), but no movements were observed. The results indicate that GldK, GldL, and GldM are each essential for gliding motility. Previous experiments demonstrated that the presence of GldN, or its paralog GldO, is also required for gliding (26).

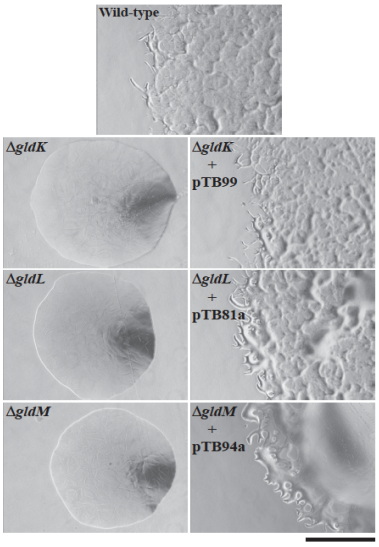

Figure 23. *gldK, gldL* and *gldM* are each required for formation of spreading colonies. Colonies were grown for 36 h at 25°C on PY2 agar medium. Photomicrographs were taken with a

Photometrics Cool-SNAP$_{cf}^2$ camera mounted on an Olympus IMT-2 phase-contrast microscope. The wild-type strain was CJ1827. CJ1827, CJ2122 (Δ*gldK*), CJ2157 (Δ*gldL*), and CJ2262 (Δ*gldM*) carried control vector pCP23, so that all strains were resistant to tetracycline and could be grown on identical media. pTB99, pTB81a, and pTB94a, express GldK, GldL, and GldM respectively. Bar indicates 0.5 mm and applies to all panels.

GldK, GldL, and GldM are each required for secretion of the cell-surface motility adhesins, SprB and RemA. Components of the *F. johnsoniae* T9SS such as GldN, SprE, SprF, and SprT are required for surface localization of SprB (26, 27, 30). GldN has also previously been shown to be required for secretion of the mobile cell-surface motility adhesin RemA (26, 35). Here we examined the roles of GldK, GldL, and GldM in secretion of SprB and of recombinant RemA which carried a myc-tag to allow easy detection. Cells with deletion mutations in *gldK*, *gldL*, or *gldM* produced SprB and myc-tagged RemA proteins as determined by Western blot analyses (Figure 24), but they failed to secrete these proteins to the cell surface (Tables 5 and 6). Anti-SprB-coated polystyrene spheres attached readily to wild-type cells but failed to attach to cells of an *sprB* deletion mutant or to cells that carried deletions for *gldK*, *gldL*, or *gldM* (Table 5). Complementation with plasmid expressing the appropriate gene in each case restored SprB to the cell surface. Similarly, Anti-Myc-coated polystyrene spheres attached readily to CJ2083, which expresses myc-tagged RemA, but they failed to attach to cells with mutations in *gldK*, *gldL*, or *gldM* (Table 6).

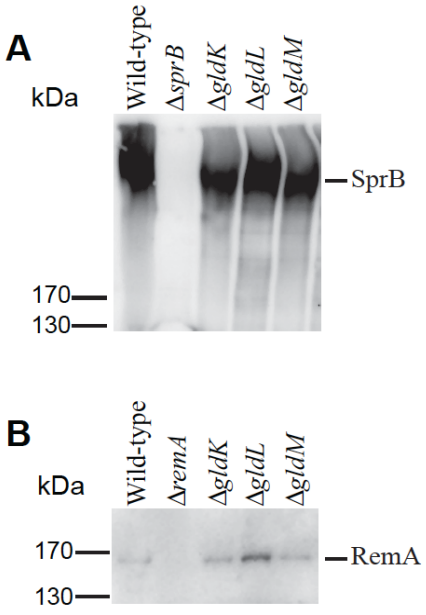

Figure 24. Immunodetection of SprB and RemA in cells of wild-type and mutant *F. johnsoniae* strains. (A) Cell extracts (15 μg of protein) of wild type (CJ1827), Δ*sprB* (CJ1922), Δ*gldK* (CJ2122), Δ*gldL* (CJ2157), and Δ*gldM* (CJ2262) were examined by Western blotting using antiserum against SprB. (B) Cell extracts (15 mg of protein) of wild type (CJ2083), Δ*remA* (CJ1984), Δ*gldK* (CJ2140), Δ*gldL* (CJ2281), and Δ*gldM* (CJ2263) were examined by Western blotting using antiserum against RemA. All strains in panel B except Δ*remA* (CJ1984) were derived from CJ2083 and thus expressed the myc-tagged version of RemA.

Cells of *gldK*, *gldL*, and *gldM* mutants were also resistant to infection by bacteriophages that infect wild-type cells (Figure 25). SprB is thought to be a receptor for phages ϕCj1, ϕCj13, ϕCj23 and ϕCj29 (19), and RemA appears to be a receptor for phages ϕCj42, ϕCj48 and ϕCj54 (35), so it is not surprising that mutants with defects in secretion of SprB, RemA, and perhaps additional cell surface motility proteins, exhibit phage resistance.

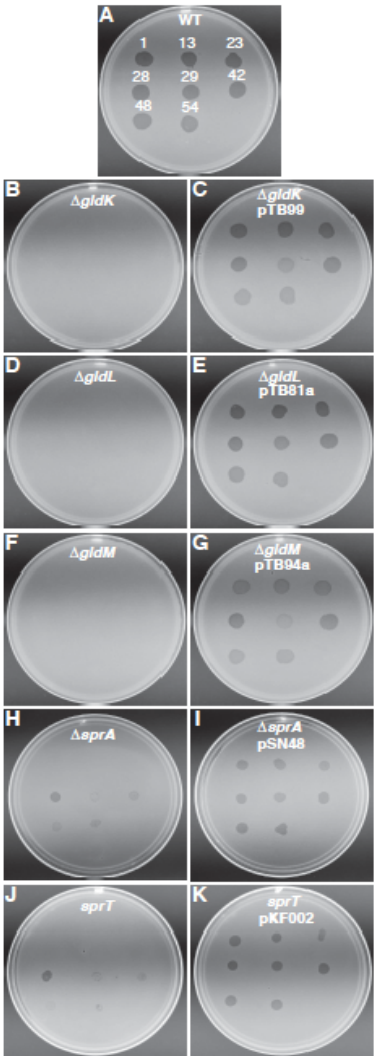

Figure 25. Effect of mutations on susceptibility to phages. Bacteriophages (5 ml of lysates containing approximately 10^9 PFU/ml) were spotted onto lawns of cells in CYE overlay agar. The plates were incubated at 25°C for 24 h to observe lysis. Bacteriophages were spotted in the following order from left to right, as indicated also by the numbers in panel A: top row, ϕCj1, ϕCj13, and ϕCj23; middle row ϕCj28, ϕCj29, and ϕCj42; bottom row, ϕCj48 and ϕCj54. (A) Wild type *F. johnsoniae* CJ1827. (B) CJ2122 (Δ*gldK*). (C) CJ2122 complemented with pTB99 which carries *gldK*. (D) CJ2157 (Δ*gldL*). (E) CJ2157 complemented with pTB81a which carries *gldL*. (F) CJ2262 (Δ*gldM*). (G) CJ2262 complemented with pTB94a which carries *gldM*. (H) CJ2302 (Δ*sprA*). (I) CJ2302 complemented with pSN48 which carries *sprA*. (J) KDF001 (*sprT*). (K) KDF001 complemented with pKF002 which carries *sprT*.

Cells of the deletion mutants were also deficient in attachment to glass (Table 7) as has previously been observed for other motility mutants of *F. johnsoniae* (20). This may be the result of the absence of motility adhesins such as SprB and RemA on the cell surface. However, lack of SprB and RemA on the cell surface cannot explain the entire attachment defect. Cells of an *sprB* mutant or of a *remA* mutant attached to glass almost as well as wild-type cells and cells lacking both genes were only partially deficient in attachment to glass (Table 7). In contrast, cells with mutations in *gldK*, *gldL*, or *gldM* were completely deficient in attachment to glass. This suggests that cell-surface adhesins in addition to SprB and RemA are secreted by the T9SS. Proteins secreted by T9SSs typically have conserved CTDs identified by the TIGRFAMs, TIGR04131 and TIGR04183. Analysis of the *F. johnsoniae* genome revealed fifty-two proteins with these T9SS CTD's (Table 9). Some of these may be the additional cell-surface adhesins that contribute to the ability of wild-type cells to attach to glass.

GldK, GldL, and GldM are each required for chitin utilization. *F. johnsoniae* was originally identified as a chitin digesting bacterium (37). It produces a variety of proteins involved in chitin utilization, including at least one extracellular chitinase that we refer to as ChiA, encoded by Fjoh_4555. Mutations in the T9SS genes *gldN, sprE*, and *sprT* result in defects in chitin utilization, and defects in secretion of ChiA (26, 27, 30). Cells with deletion mutations in *gldK*, *gldL*, and *gldM* were examined for chitin utilization (Figure 26). Deletion of any of these genes resulted in inability to digest colloidal chitin, indicating that GldK, GldL and GldM are each required for chitin digestion and suggesting that they may be required for secretion of ChiA.

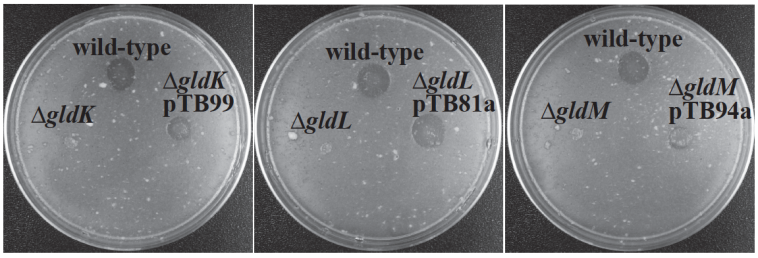

Figure 26. *gldK, gldL* and *gldM* are each required for chitin utilization. Approximately 4 x 10^7 cells of *F. johnsoniae* were spotted on MYA-chitin medium containing tetracycline and incubated at 25°C for 60 h. (A) 1, wild-type *F. johnsoniae* CJ1827; 2, CJ2122 (Δ*gldK*); 3 CJ2122 complemented with pTB99 which carries *gldK*. (B) 1, wild-type *F. johnsoniae* CJ1827; 2, CJ2157 (Δ*gldL*); 3)CJ2157 complemented with pTB81a which carries *gldL*. (C) 1, wild-type *F. johnsoniae* CJ1827; 2, CJ2262 (Δ*gldM*); 3, CJ2262 complemented with pTB94a which carries *gldM*. CJ1827, CJ2122, CJ2157, and CJ2262 carried control vector pCP23, so that all strains were resistant to tetracycline.

Localization of GldK, GldL, and GldM. GldK, GldL and GldM were each present primarily in the insoluble (membrane) fraction of cell extracts (Figure 27). GldK is a predicted outer membrane (OM) lipoprotein, and GldL and GldM have hydrophobic alpha helical segments that are predicted to anchor them to the cytoplasmic membrane (CM) (3). The mild detergent Sarkosyl solubilizes the *F. johnsoniae* CM while leaving the OM intact (11). Sarkosyl solubilization was used to examine protein localization. GldL and GldM were enriched in the Sarkosyl soluble (CM) fraction as predicted, whereas GldK was present in both the Sarkosyl soluble (CM) and Sarkosyl insoluble (OM) fractions. While integral OM proteins of *F. johnsoniae* are in general not solubilized by Sarkosyl, lipoproteins, such as GldK, might have a more tenuous connection to the outer membrane and thus might be partially solubilized by this treatment. The absence of GldL and GldM in the Sarkosyl insoluble fraction suggests that the cytoplasmic membrane was solubilized by the detergent, and the enrichment of GldK

in this fraction suggests that GldK may be primarily associated with the OM.

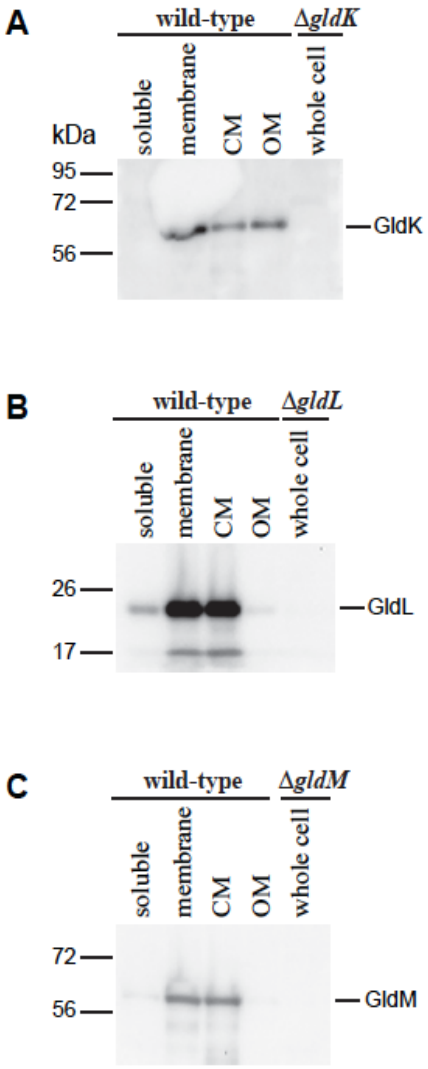

Figure 27. Cell fractionation and immunodetection of GldK, GldL and GldM. Cell fractions of wild type *F. johnsoniae* CJ1827 cells (Lanes 1-4) and extracts of *gld* mutants (lanes 5 were examined for GldK (panel A), GldL (panel B), and GldM (panel C) by Western blot analyses. Lanes 1, soluble fraction of cell extract (cytoplasmic and periplasmic proteins). Lanes 2, insoluble fraction of cell extract (primarily membrane proteins). Lanes 3, Sarkosyl soluble fraction of membranes (CM; primarily cytoplasmic membrane proteins). Lanes 4, Sarkosyl insoluble fraction of membranes (OM; primarily outer membrane proteins). Lanes 5, cell extracts of *gldK*, *gldL*, or *gldM* mutants to demonstrate specificity of the antisera used in each panel.

SprA is required for secretion of SprB and RemA, and for utilization of chitin. SprA is an outer membrane protein that is involved in gliding motility (20). SprA is similar in sequence to the *P. gingivalis* T9SS protein Sov (20, 29). The similarity between SprA and Sov suggested that SprA may have a role in secretion. *sprA* deletion mutants were constructed and examined for secretion of SprB and RemA. The mutants produced SprB and RemA proteins (Figure 28) but failed to secrete them to the cell surface (Table 5, Table 6), suggesting that SprA has a role in secretion. Previous results using transposon-induced *sprA* mutants suggested that SprA was not completely essential for chitin utilization (20). The *sprA* mutants were severely but incompletely deficient in chitin utilization. Since the mutants analyzed would have produced truncated SprA protein that might have been partially functional we revisited this phenotype with the deletion mutant. The *sprA* deletion mutant CJ2302 failed to utilize chitin, suggesting a more severe defect in chitinase secretion than was observed for the transposon-induced mutant (Figure 29).

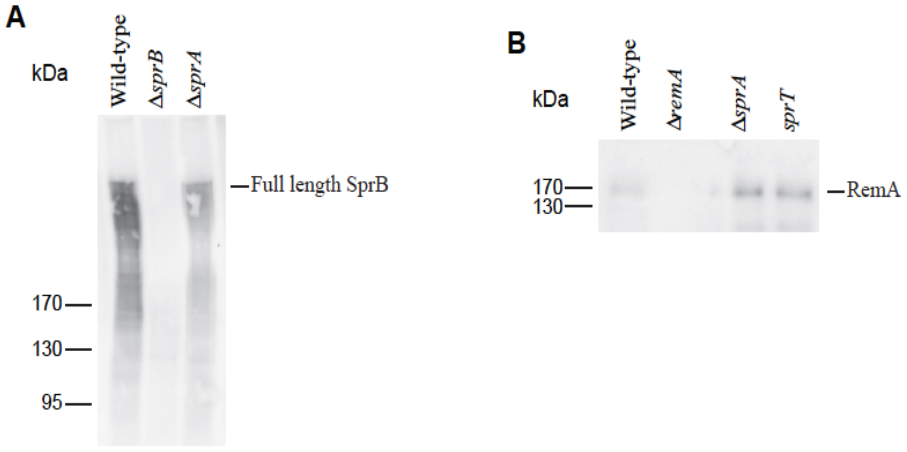

Figure 28. Immunodetection of SprB and RemA in cells of wild-type and mutant *F. johnsoniae* strains. (A) Cell extracts (15 µg of protein) of wild type (CJ1827), Δ*sprB* (CJ1922), and Δ*sprA* (CJ2302),were examined by Western blotting using antiserum against SprB. (B) Cell extracts (15

µg of protein) of wild type (CJ2083), Δ*remA* (CJ1984), Δ*sprA* (CJ2317), and *sprT* disruption mutant (CJ2327), were examined by Western blotting using antiserum against RemA. All strains in panel B except Δ*remA* (CJ1984) were derived from CJ2083 and thus expressed the myc-tagged version of RemA.

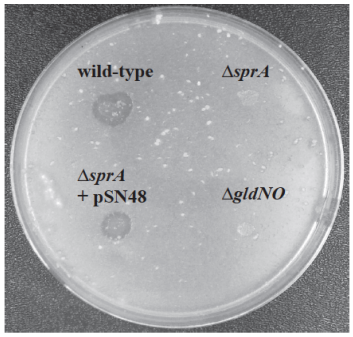

Figure 29. Effect of deletion of *sprA* on ability to utilize chitin. Approximately 4 x 10^7 cells of wild-type *F. johnsoniae* CJ1827, sprA mutant CJ2302, CJ2302 complemented with pSN48 which carries *sprA*, and *gldNO* mutant CJ2090, were spotted on MYA-chitin medium and incubated for 2 d at 25°C.

SprT and SprE have previously been shown to be required for secretion of SprB and for chitin utilization (27, 30). Like SprA, SprT is also required for secretion of RemA (Table 6, and see Figure 28). The involvement of SprE in RemA secretion is less certain, but the resistance of *sprE* mutants to phages ϕCj42, ϕCj48, and ϕCj54, that are thought to use RemA as a receptor, suggests a role for SprE in RemA secretion also (27, 35). Cells with mutations in *sprA*, *sprE*, and *sprT* were each deficient in attachment to glass (Table 7), presumably as a result of failure to secrete SprB, RemA, and other adhesins to the cell surface.

SprA, SprE, and SprT may be less central than GldK, GldL, GldM, and GldN to protein secretion and to gliding motility. Cells with mutations in *sprA*, *sprE*, and *sprT* differ from those of the *gldK*, *gldL*, *gldM*, and *gldNO* deletion mutants in two respects. First, cells of the *gld* mutants are completely nonmotile, whereas cells of *sprA*, *sprE*, and *sprT* mutants are severely deficient in motility, but exhibit weak gliding movements on wet glass surfaces (20, 27, 30). This phenotype was verified for the newly constructed *sprA* deletion mutant (Movie S4 in the supplemental material of Shrivastava et al. in review). Second, cells of the *gld* mutants were completely resistant to infection by all bacteriophages tested, whereas cells or *sprA*, *sprE*, and *sprT* mutants exhibited resistance to some but not all bacteriophages. They exhibited increased resistance to ϕCj1, ϕCj13, ϕCj23 and ϕCj29, as do *sprB* mutants (19, 24), and they were partially resistant to ϕCj42, ϕCj48, and ϕCj54, as are *remA* mutants (35), but they remained susceptible to ϕCj28 (Figure 25). Resistance of *gldK*, *gldL*, *gldM*, and *gldNO* mutants to phages such as ϕCj28 that infect cells of CJ1985 (Δ*sprB* Δ*remA*) (35) supports the idea suggested above that the T9SS secretes cell-surface proteins in addition to SprB and RemA. The sensitivity of *sprA*, *sprE*, and *sprT* mutants to phages such as ϕCj28 suggests that although SprA, SprE, and SprT are needed for secretion of some proteins by the T9SS, they may be less central to the function of this secretion system than are GldK, GldL, GldM, and GldN/O. The similar phenotypes of *sprA*, *sprE*, and *sprT* mutants also suggest the possibility that the proteins encoded by these genes may function together to support T9SS function.

Discussion

gldK, *gldL*, *gldM*, and *gldN* were originally discovered as genes required for *F. johnsoniae* gliding motility (3). Later, orthologs of these genes (*porK*, *porL*, *porM*, and *porN* respectively) were demonstrated to be required for secretion of *P. gingivalis* gingipains (30). The *P. gingivalis* secretion system was referred to as the Por secretion system (30), or more recently as the T9SS (18, 32). In *F. johnsoniae*, *gldN* and/or its paralog *gldO* were shown to be essential for secretion of the motility adhesins SprB and RemA (26, 35). The results presented here demonstrate that *F. johnsoniae gldK*, *gldL*, and *gldM* are cotranscribed with *gldN*, and that the products of each of these genes are required for secretion of SprB and RemA. The outer membrane motility protein SprA, an ortholog of the *P. gingivalis* T9SS protein Sov, is also shown to be required for secretion of SprB and RemA. The results suggest that GldK, GldL, GldM, GldN and SprA are each components of the *F. johnsoniae* T9SS. Other components of this system, previously shown to be involved in secretion in *F. johnsoniae*, include SprE, SprF, and SprT (24, 27, 30), which are similar in sequence to the *P. gingivalis* T9SS proteins PorW, PorP, and PorT respectively (30, 31). The demonstration that the *F. johnsoniae* orthologs of the *P. gingivalis* T9SS proteins have roles in protein secretion provides independent confirmation of the function of these proteins. Similar proteins are found in many members of the large and diverse phylum *Bacteroidetes*, suggesting that T9SSs are common in this phylum (18).

The phenotypes of the *F. johnsoniae* mutants suggest that GldK, GldL, GldM and GldN are essential for T9SS function, and that SprA, SprE and SprT are essential for secretion of many, but perhaps not all, proteins targeted to this system. Cells lacking

GldK, GldL, GldM, or GldN and its paralog GldO, failed to secrete SprB and RemA and were completely deficient in gliding motility and in attachment to glass. They were also deficient in chitin utilization. The defect in chitin utilization is likely the result of failure to secrete the chitinase encoded by Fjoh_4555, as previously reported for an *sprT* mutant (30). SprB and RemA appear to function as receptors for some but not all *F. johnsoniae* phages. Cells lacking GldK, GldL, GldM, or GldN and GldO were resistant to all phages tested, suggesting that some other proteins secreted by the T9SS also serve as phage receptors. In contrast, cells with mutations in *sprA*, *sprE*, and *sprT* exhibited partial phage resistance. They were resistant to phages ϕCj1, ϕCj13, ϕCj23 and ϕCj29 (indicating the absence of SprB on the cell surface) and were partially resistant to ϕCj42, ϕCj48, and ϕCj54 (suggesting the absence of RemA on the cell surface). They remained fully susceptible to ϕCj28. These results support the suggestion that GldK, GldL, GldM, and GldN (or GldO) are essential components of the T9SS whereas SprA, SprE, and SprT are required for secretion of SprB and RemA but not for secretion of some other cell surface phage receptors secreted by the T9SS.

GldK, GldL, GldM and GldN may form a complex. Orthologs of *gldK*, *gldL*, *gldM*, and *gldN* are present in many members of the phylum *Bacteroidetes*, and they appear to be invariably clustered together on the genome in this order suggesting that, as in *F. johnsoniae*, they may be transcribed as a unit. Of twenty-seven sequenced genomes analyzed that had each of these genes (18), twenty-six had *gldK*, *gldL*, *gldM*, and *gldN* organized as in *F. johnsoniae*, and the twenty-seventh, (*Chitinophaga pinensis*), had the same organization except that a 201 bp open reading frame of unknown function was

present between *gldK* and *gldL*. Unlike the highly conserved gene order, the sequences of the individual proteins have diverged substantially (Figures 30-33). This argues against recent horizontal gene transfer as an explanation for the conserved gene order. Phylogenetic trees based on GldK, GldL, GldM, and GldN sequences closely match phylogenetic trees based on 16S rRNAs (Figures 34-38) suggesting that the T9SS genes have primarily been passed vertically. The genetic organization of *gldK*, *gldL*, *gldM*, and *gldN* has probably been conserved because it is important for function. For example, the products of conserved gene clusters often interact (5). GldK, GldL, GldM, and GldN may interact to form a T9SS complex, and coordinated expression may be required for efficient assembly of this complex.

Several experimental observations support the suggestion that GldK, GldL, GldM, and GldN interact. First, as indicated above, cells with nonpolar mutations in *gldL*, *gldM*, and *gldN* had decreased levels of GldK protein. Similarly, cells with mutations in *gldM* had decreased levels of GldL protein, and cells with nonpolar mutations in *gldK*, *gldL*, and *gldM* had decreased levels of GldN protein (Figure 21). These results suggest the possibility of instability of the proteins in the absence of their partners. Second, moderate overexpression (less than 10-fold) of *gldK* and *gldL* together, but not individually, in wild-type cells resulted in adverse affects on growth and motility, suggesting interaction between the encoded proteins (3). Third, a *gldK* mutant was identified that could be partially suppressed by moderate overexpression of *gldL* (3). Finally, the *P. gingivalis* T9SS proteins PorK, PorL, PorM, and PorN, (orthologs of *F. johnsoniae* GldK, GldL, GldM, and GldN respectively) migrate as a large complex in blue native PAGE (30).

Comparative analysis of GldK, GldL, GldM, and GldN proteins. GldK, GldL, GldM, and GldN are novel proteins, and their exact functions in secretion and motility are not known. Analysis of genome sequences revealed orthologs to the genes encoding each of these proteins in many members of the phylum *Bacteroidetes*, but not in bacteria belonging to other phyla (18). GldK is the most highly conserved of the four proteins. Fifty-six residues are completely conserved among the twenty-six sequences examined (Figure 30). Each of the proteins has an N-terminal type 2 signal peptide followed immediately by a cysteine, characteristic of bacterial lipoproteins. GldK is similar to sulfatase-modifying enzymes such as human formylglycine-generating enzyme FGE. FGE activates sulfatases by catalyzing the conversion of the active-site cysteine to formylglycine. GldK is not thought to have this activity however, since it lacks the active site cysteine residues corresponding to C336 and C341 of FGE (7). The conserved regions of GldK may be important for protein folding, and/or for protein-protein interactions, but further studies will be needed to determine the exact functions of these regions. GldL and GldM localize to the cytoplasmic membrane, and sequence analyses suggest that they each have hydrophobic alpha helical membrane-spanning regions. The N-terminal region of GldL is highly conserved and has two predicted membrane-spanning helices (Figure 31). The second transmembrane helix has a glutamate residue that is conserved in all twenty-six sequences. The high conservation of this charged residue within a hydrophobic stretch is unusual, and suggests the possibility that it may have an important function. For example it may be involved in harvesting cellular energy to power secretion, although other explanations are possible. The remainder of the GldL protein is predicted to be soluble. Several regions of strong conservation are scattered

across this soluble region of the protein, including a pocket of high identity near the C-terminus. GldM has a single predicted transmembrane helix. This region lies near the N-terminus and is very highly conserved (Figure 32). The high levels of conservation in the transmembrane regions of GldL and GldM suggest that these have functions in secretion and/or motility beyond simple membrane anchoring. GldN is the least conserved of the four proteins (Figure 33), with only two residues (N_{77} and N_{265}; numbered based on *F. johnsoniae* GldN) present in each sequence. GldN appears to have a cleavable type 1 signal peptide, but there is little else to assist in prediction of function. The presence of GldN, or the nearly identical GldO, is essential for motility and for secretion of SprB, RemA, and chitinase (26, 35). Future studies will be needed to elucidate their roles in these processes.

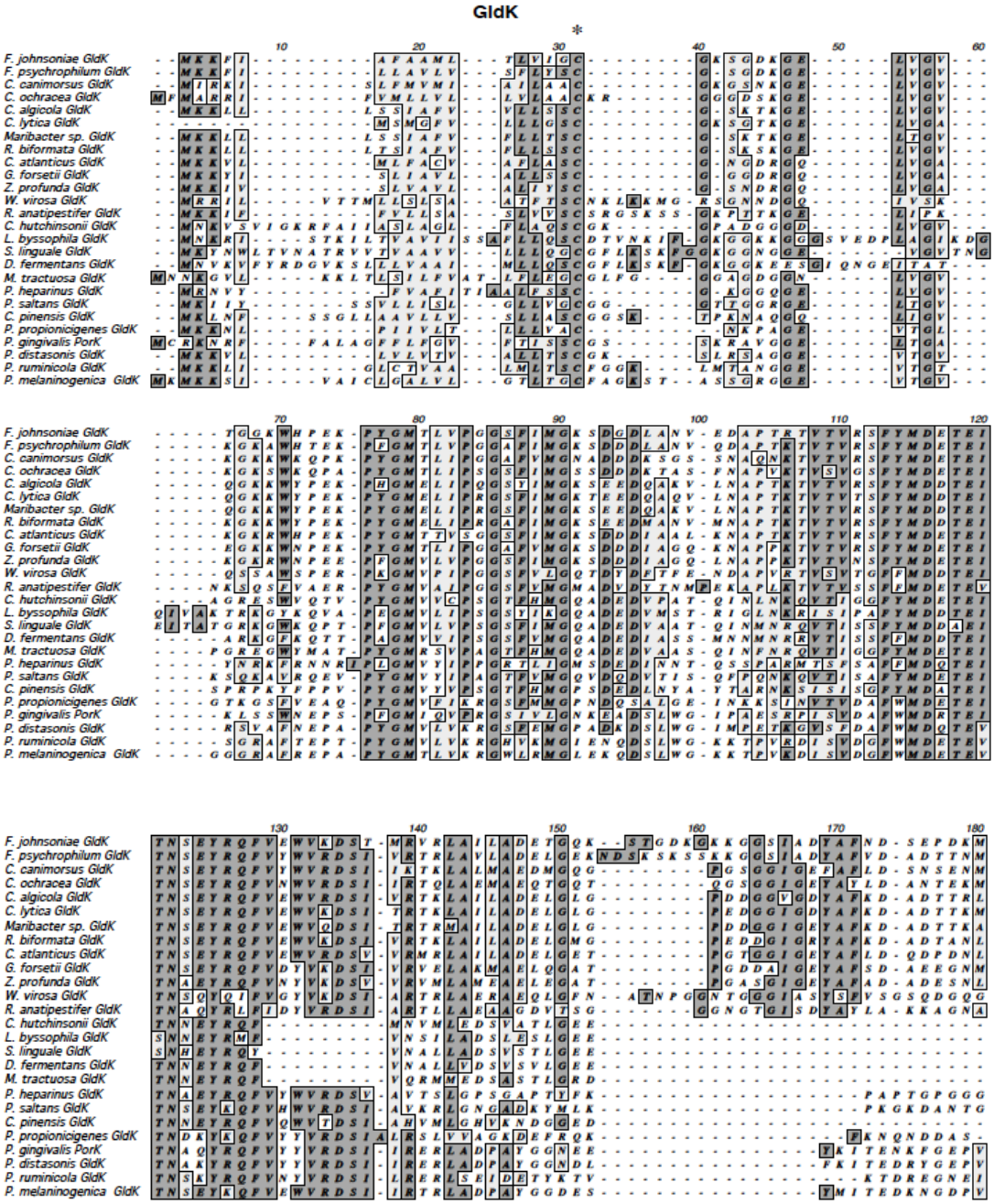
GldK
F. johnsoniae GldK
F. psychrophilum GldK
C. canimorsus GldK
C. ochracea GldK
C. algicola GldK
C. lytica GldK
Maribacter sp. GldK
R. biformata GldK
C. atlanticus GldK
G. forsetii GldK
Z. profunda GldK
W. virosa GldK
R. anatipestifer GldK
C. hutchinsonii GldK
L. byssophila GldK
S. linguale GldK
D. fermentans GldK
M. tractuosa GldK
P. heparinus GldK
P. saltans GldK
C. pinensis GldK
P. propionicigenes GldK
P. gingivalis PorK
P. distasonis GldK
P. ruminicola GldK
P. melaninogenica GldK

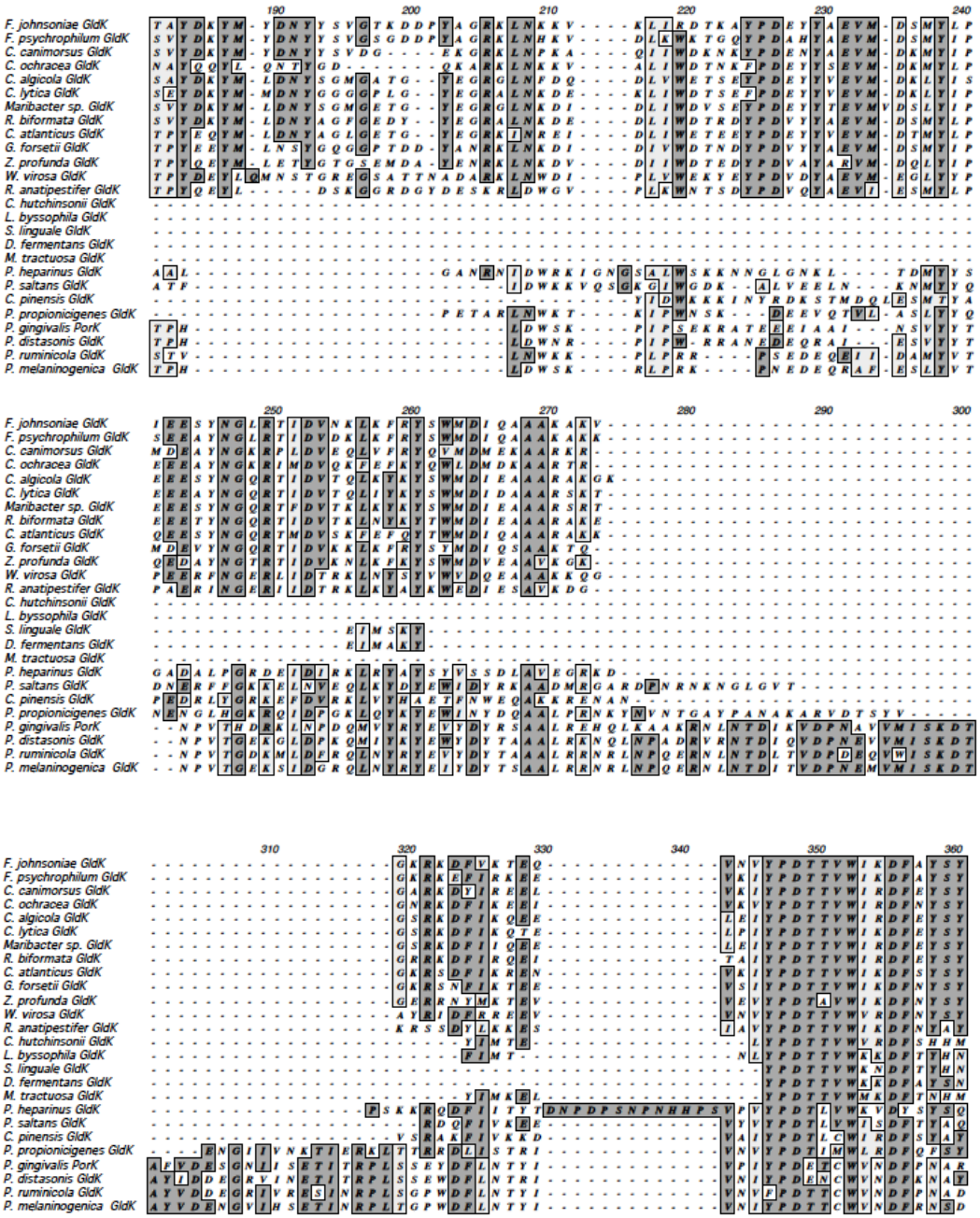

Figure 30. Alignment of GldK using MUSCLE. Dark shading indicates identical amino acids and light shading indicates similar amino acids. '*' indicates conserved N-terminal cysteine of the mature lipoprotein.

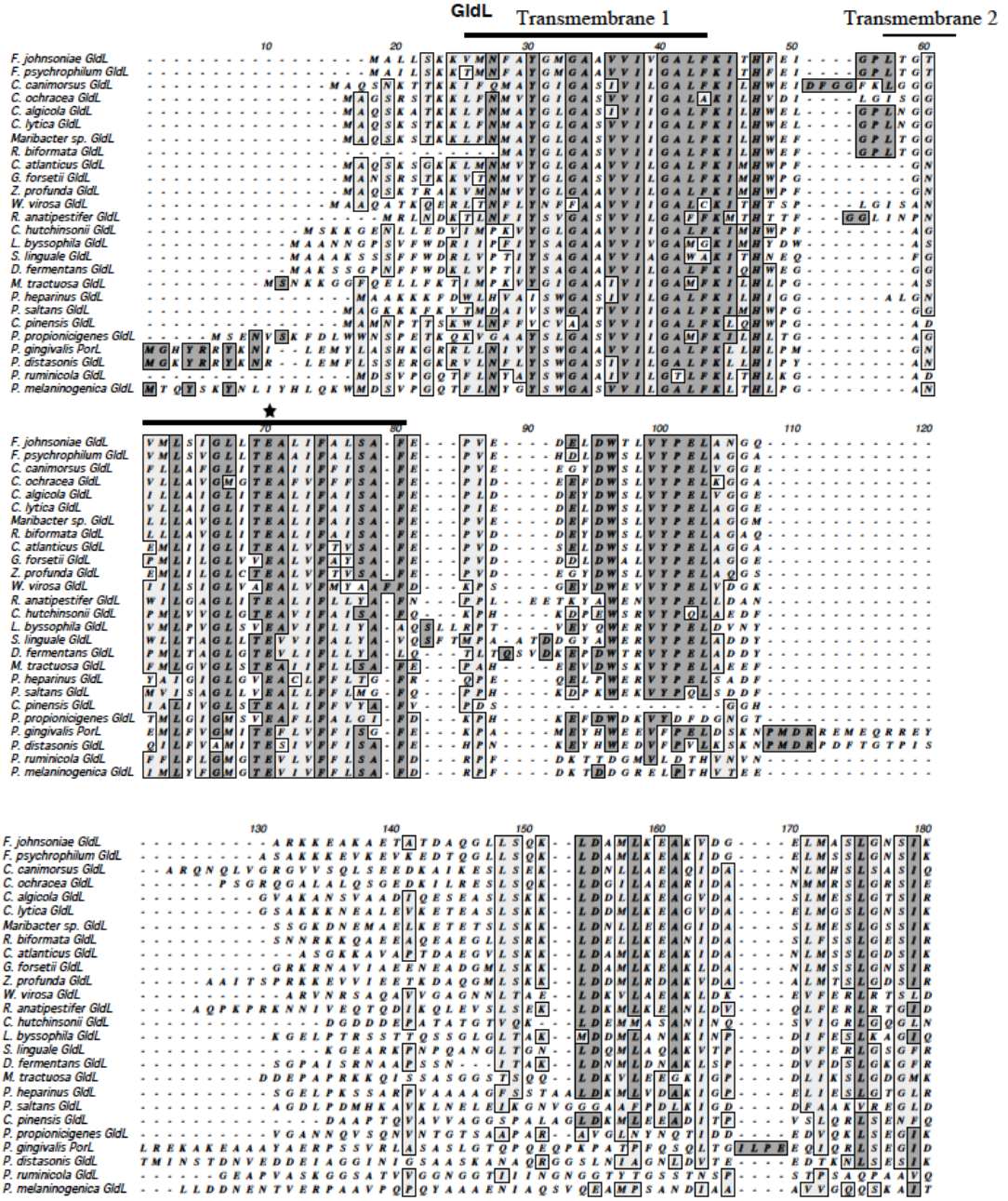
GldL
Transmembrane 1
Transmembrane 2
F. johnsoniae GldL
F. psychrophilum GldL
C. canimorsus GldL
C. ochracea GldL
C. algicola GldL
C. lytica GldL
Maribacter sp. GldL
R. biformata GldL
C. atlanticus GldL
G. forsetii GldL
Z. profunda GldL
W. virosa GldL
R. anatipestifer GldL
C. hutchinsonii GldL
L. byssophila GldL
S. linguale GldL
D. fermentans GldL
M. tractuosa GldL
P. heparinus GldL
P. saltans GldL
C. pinensis GldL
P. propionicigenes GldL
P. gingivalis PorL
P. distasonis GldL
P. ruminicola GldL
P. melaninogenica GldL

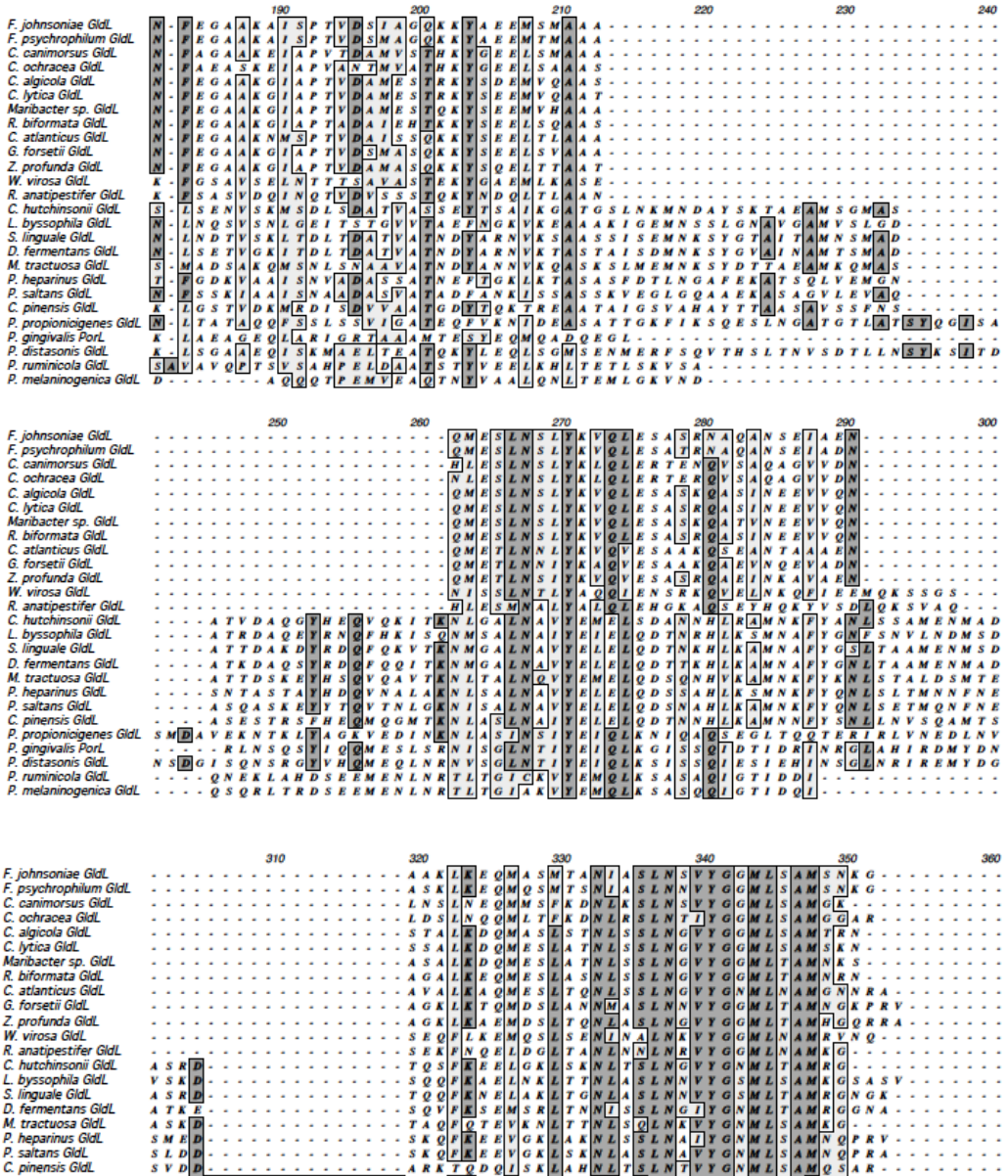
190
200
210
220
230
240
250
260
270
280
290
300
310
320
330
340
350
360
F. johnsoniae GldL
F. psychrophilum GldL
C. canimorsus GldL
C. ochracea GldL
C. algicola GldL
C. lytica GldL
Maribacter sp. GldL
R. biformata GldL
C. atlanticus GldL
G. forsetii GldL
Z. profunda GldL
W. virosa GldL
R. anatipestifer GldL
C. hutchinsonii GldL
L. byssophila GldL
S. linguale GldL
D. fermentans GldL
M. tractuosa GldL
P. heparinus GldL
P. saltans GldL
C. pinensis GldL
P. propionicigenes GldL
P. gingivalis PorL
P. distasonis GldL
P. ruminicola GldL
P. melaninogenica GldL

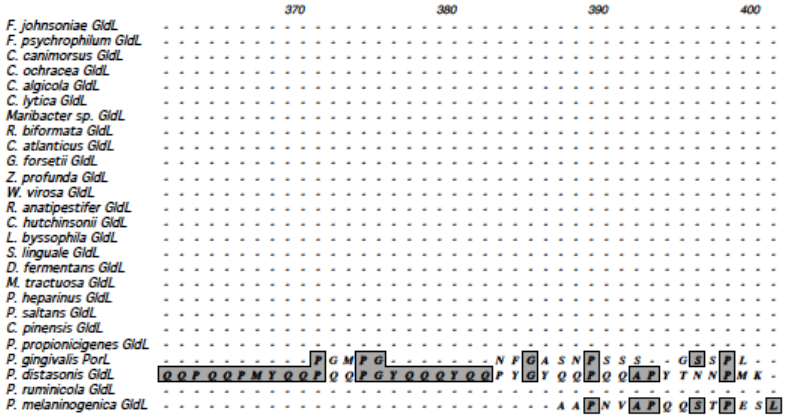

Figure 31. Alignment of GldL using MUSCLE. Dark shading indicates identical amino acids and light shading indicates similar amino acids. Transmembrane regions 1 and 2 are indicated. Star indicates conserved glutamate within transmembrane region 2.

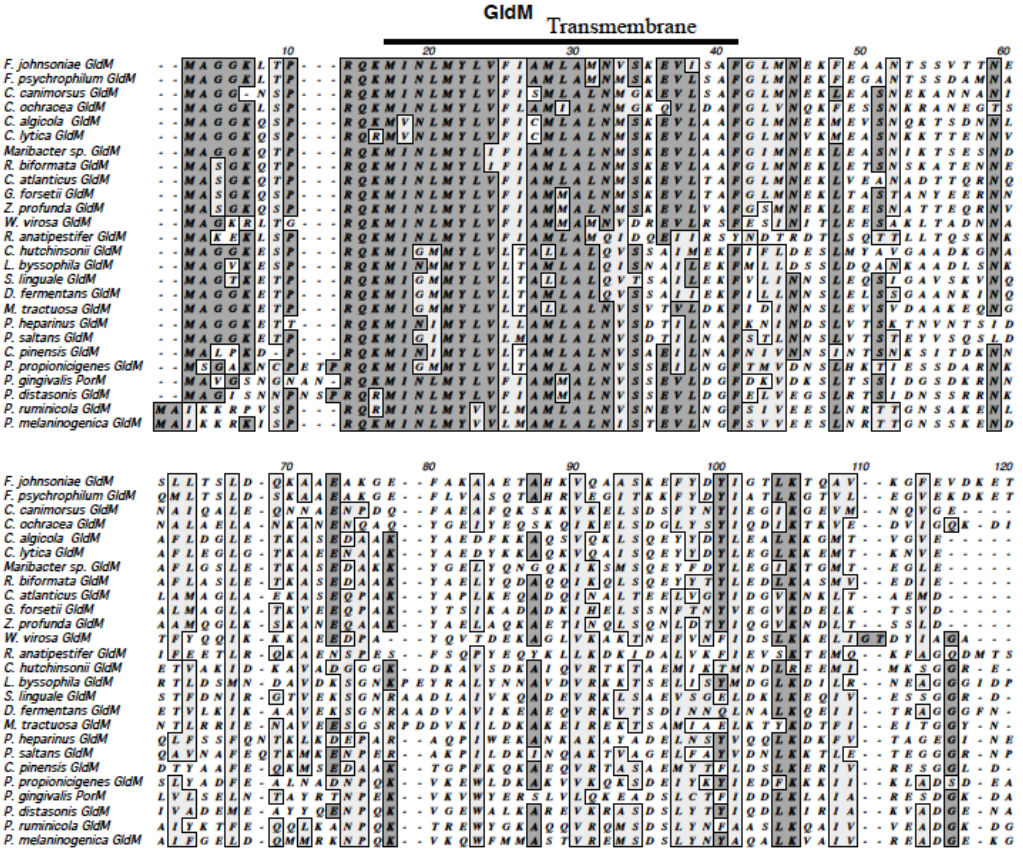

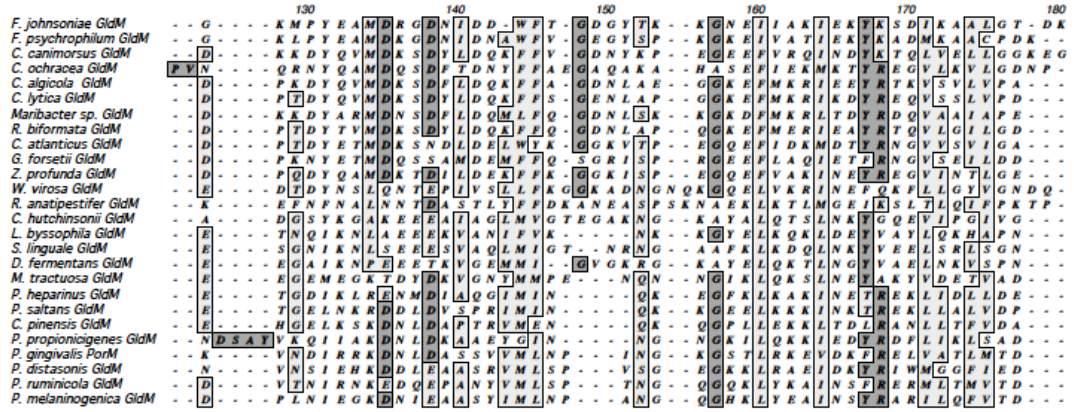
130
140
150
160
170
180
F. johnsoniae GldM
F. psychrophilum GldM
C. canimorsus GldM
C. ochracea GldM
C. algicola GldM
C. lytica GldM
Maribacter sp. GldM
R. biformata GldM
C. atlanticus GldM
G. forsetii GldM
Z. profunda GldM
W. virosa GldM
R. anatipestifer GldM
C. hutchinsonii GldM
L. byssophila GldM
S. linguale GldM
D. fermentans GldM
M. tractuosa GldM
P. heparinus GldM
P. saltans GldM
C. pinensis GldM
P. propionicigenes GldM
P. gingivalis PorM
P. distasonis GldM
P. ruminicola GldM
P. melaninogenica GldM

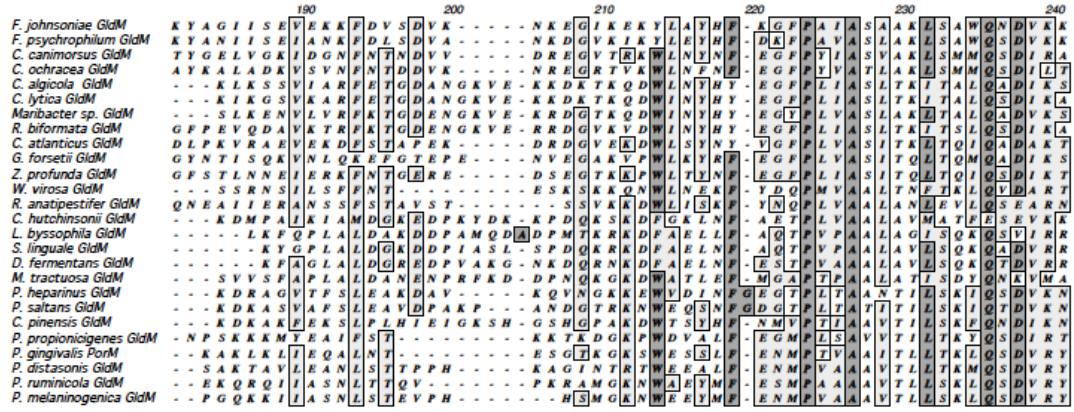
190
200
210
220
230
240
F. johnsoniae GldM
F. psychrophilum GldM
C. canimorsus GldM
C. ochracea GldM
C. algicola GldM
C. lytica GldM
Maribacter sp. GldM
R. biformata GldM
C. atlanticus GldM
G. forsetii GldM
Z. profunda GldM
W. virosa GldM
R. anatipestifer GldM
C. hutchinsonii GldM
L. byssophila GldM
S. linguale GldM
D. fermentans GldM
M. tractuosa GldM
P. heparinus GldM
P. saltans GldM
C. pinensis GldM
P. propionicigenes GldM
P. gingivalis PorM
P. distasonis GldM
P. ruminicola GldM
P. melaninogenica GldM

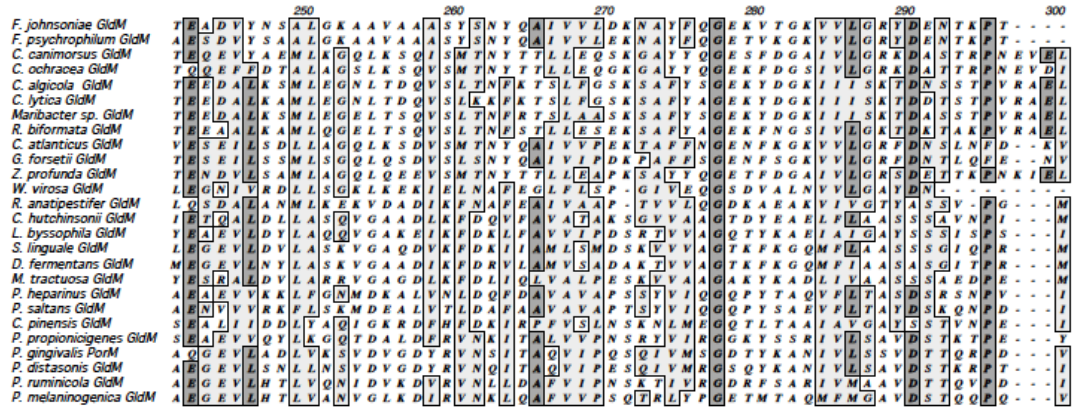
250
260
270
280
290
300
F. johnsoniae GldM
F. psychrophilum GldM
C. canimorsus GldM
C. ochracea GldM
C. algicola GldM
C. lytica GldM
Maribacter sp. GldM
R. biformata GldM
C. atlanticus GldM
G. forsetii GldM
Z. profunda GldM
W. virosa GldM
R. anatipestifer GldM
C. hutchinsonii GldM
L. byssophila GldM
S. linguale GldM
D. fermentans GldM
M. tractuosa GldM
P. heparinus GldM
P. saltans GldM
C. pinensis GldM
P. propionicigenes GldM
P. gingivalis PorM
P. distasonis GldM
P. ruminicola GldM
P. melaninogenica GldM

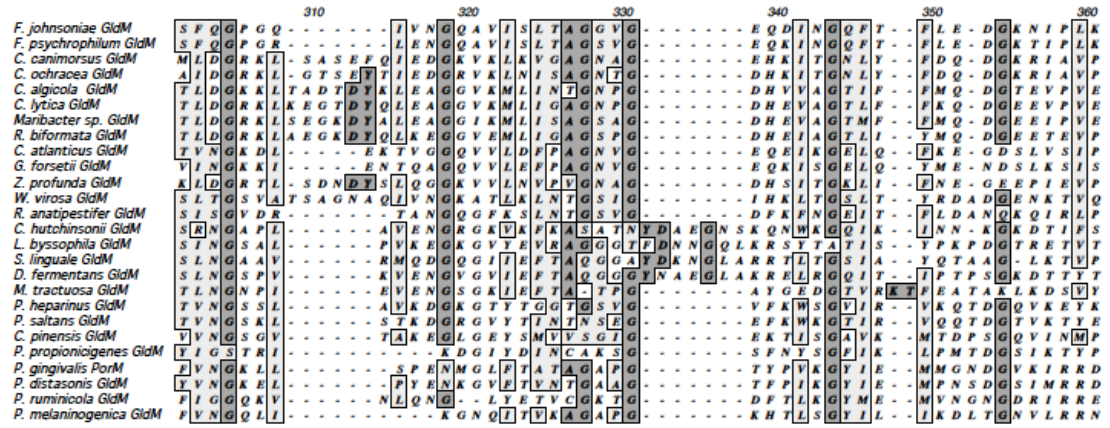
310
320
330
340
350
360
F. johnsoniae GldM
F. psychrophilum GldM
C. canimorsus GldM
C. ochracea GldM
C. algicola GldM
C. lytica GldM
Maribacter sp. GldM
R. biformata GldM
C. atlanticus GldM
G. forsetii GldM
Z. profunda GldM
W. virosa GldM
R. anatipestifer GldM
C. hutchinsonii GldM
L. byssophila GldM
S. linguale GldM
D. fermentans GldM
M. tractuosa GldM
P. heparinus GldM
P. saltans GldM
C. pinensis GldM
P. propionicigenes GldM
P. gingivalis PorM
P. distasonis GldM
P. ruminicola GldM
P. melaninogenica GldM

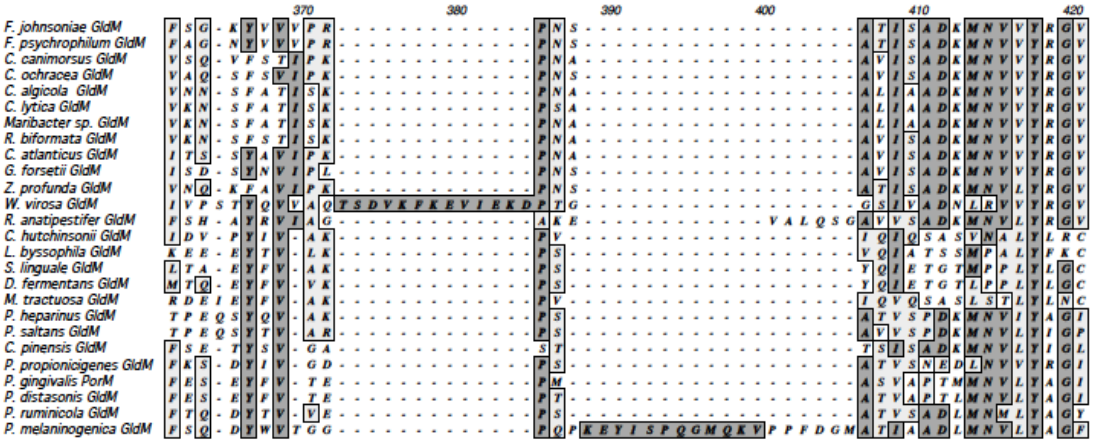
370
380
390
400
410
420
F. johnsoniae GldM
F. psychrophilum GldM
C. canimorsus GldM
C. ochracea GldM
C. algicola GldM
C. lytica GldM
Maribacter sp. GldM
R. biformata GldM
C. atlanticus GldM
G. forsetii GldM
Z. profunda GldM
W. virosa GldM
R. anatipestifer GldM
C. hutchinsonii GldM
L. byssophila GldM
S. linguale GldM
D. fermentans GldM
M. tractuosa GldM
P. heparinus GldM
P. saltans GldM
C. pinensis GldM
P. propionicigenes GldM
P. gingivalis PorM
P. distasonis GldM
P. ruminicola GldM
P. melaninogenica GldM

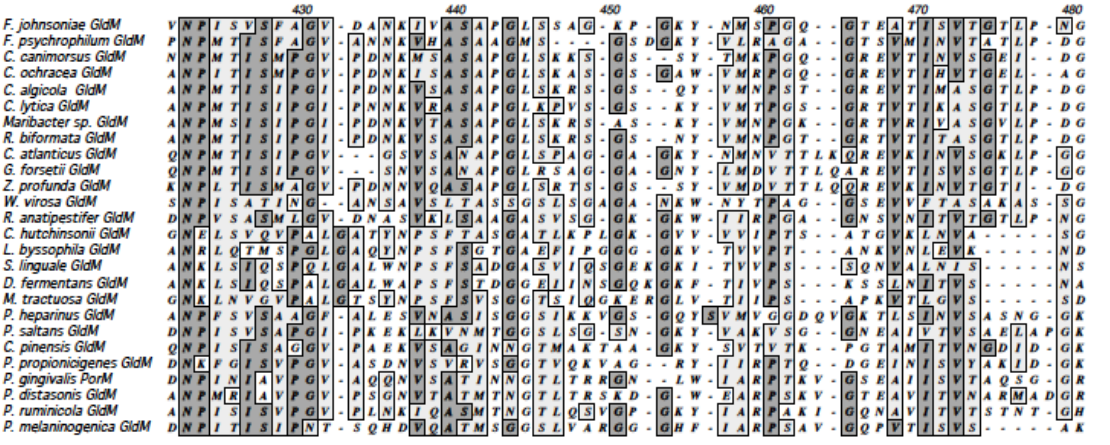
430
440
450
460
470
480
F. johnsoniae GldM
F. psychrophilum GldM
C. canimorsus GldM
C. ochracea GldM
C. algicola GldM
C. lytica GldM
Maribacter sp. GldM
R. biformata GldM
C. atlanticus GldM
G. forsetii GldM
Z. profunda GldM
W. virosa GldM
R. anatipestifer GldM
C. hutchinsonii GldM
L. byssophila GldM
S. linguale GldM
D. fermentans GldM
M. tractuosa GldM
P. heparinus GldM
P. saltans GldM
C. pinensis GldM
P. propionicigenes GldM
P. gingivalis PorM
P. distasonis GldM
P. ruminicola GldM
P. melaninogenica GldM

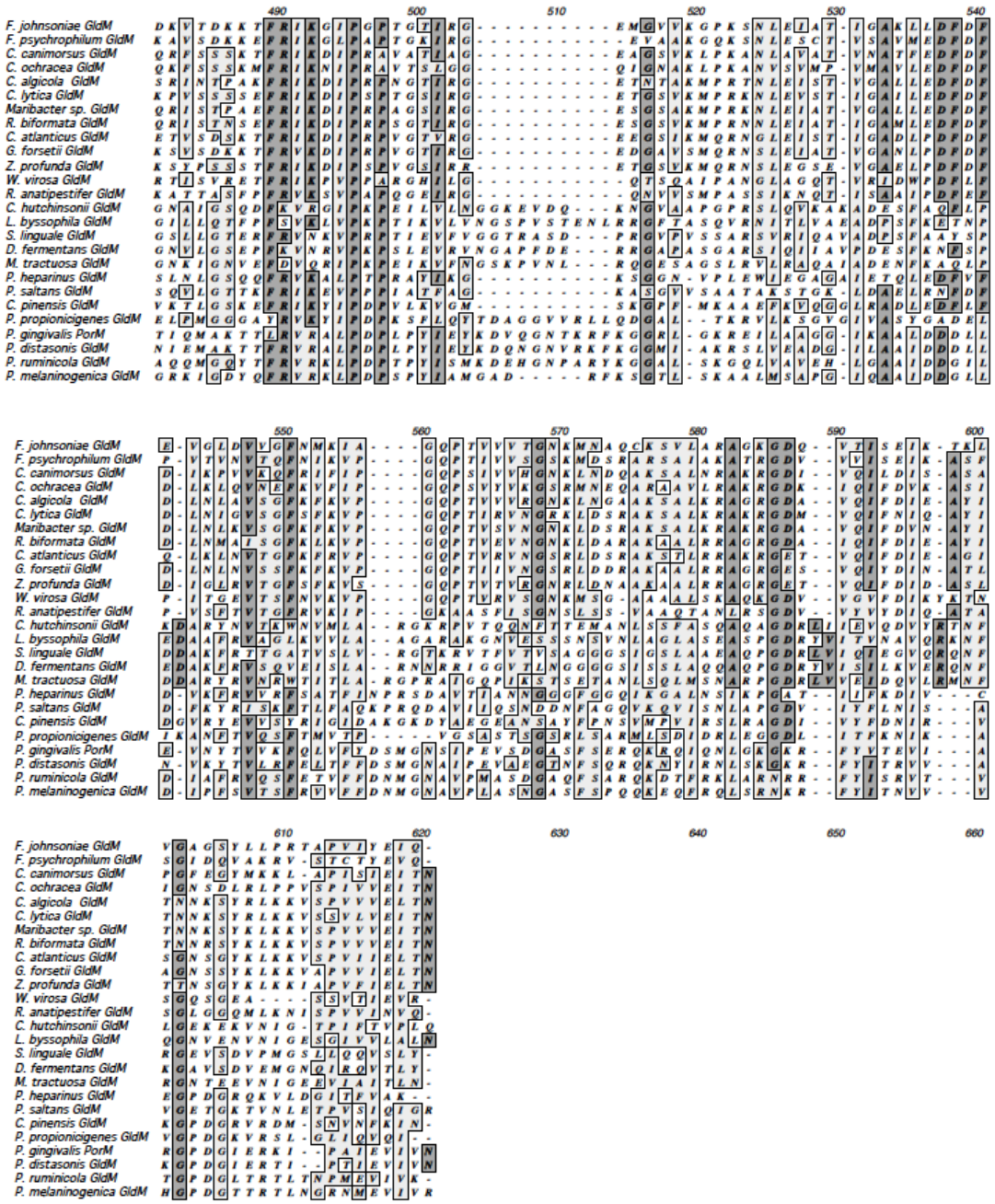

Figure 32. Alignment of GldM using MUSCLE. Dark shading indicates identical amino acids and light shading indicates similar amino acids. Transmembrane region is indicated.

GldN

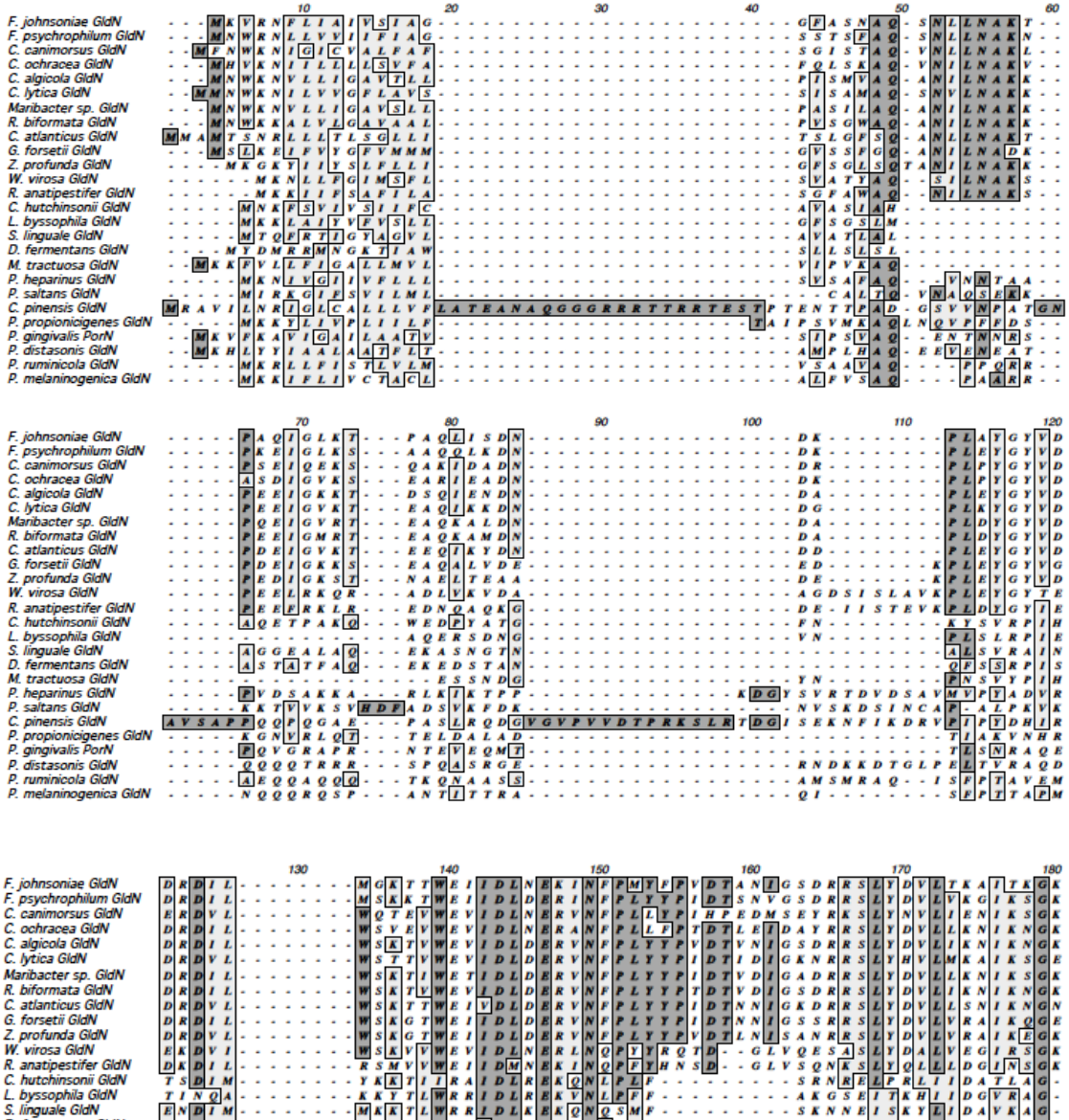
F. johnsoniae GldN
F. psychrophilum GldN
C. canimorsus GldN
C. ochracea GldN
C. algicola GldN
C. lytica GldN
Maribacter sp. GldN
R. biformata GldN
C. atlanticus GldN
G. forsetii GldN
Z. profunda GldN
W. virosa GldN
R. anatipestifer GldN
C. hutchinsonii GldN
L. byssophila GldN
S. linguale GldN
D. fermentans GldN
M. tractuosa GldN
P. heparinus GldN
P. saltans GldN
C. pinensis GldN
P. propionicigenes GldN
P. gingivalis PorN
P. distasonis GldN
P. ruminicola GldN
P. melaninogenica GldN

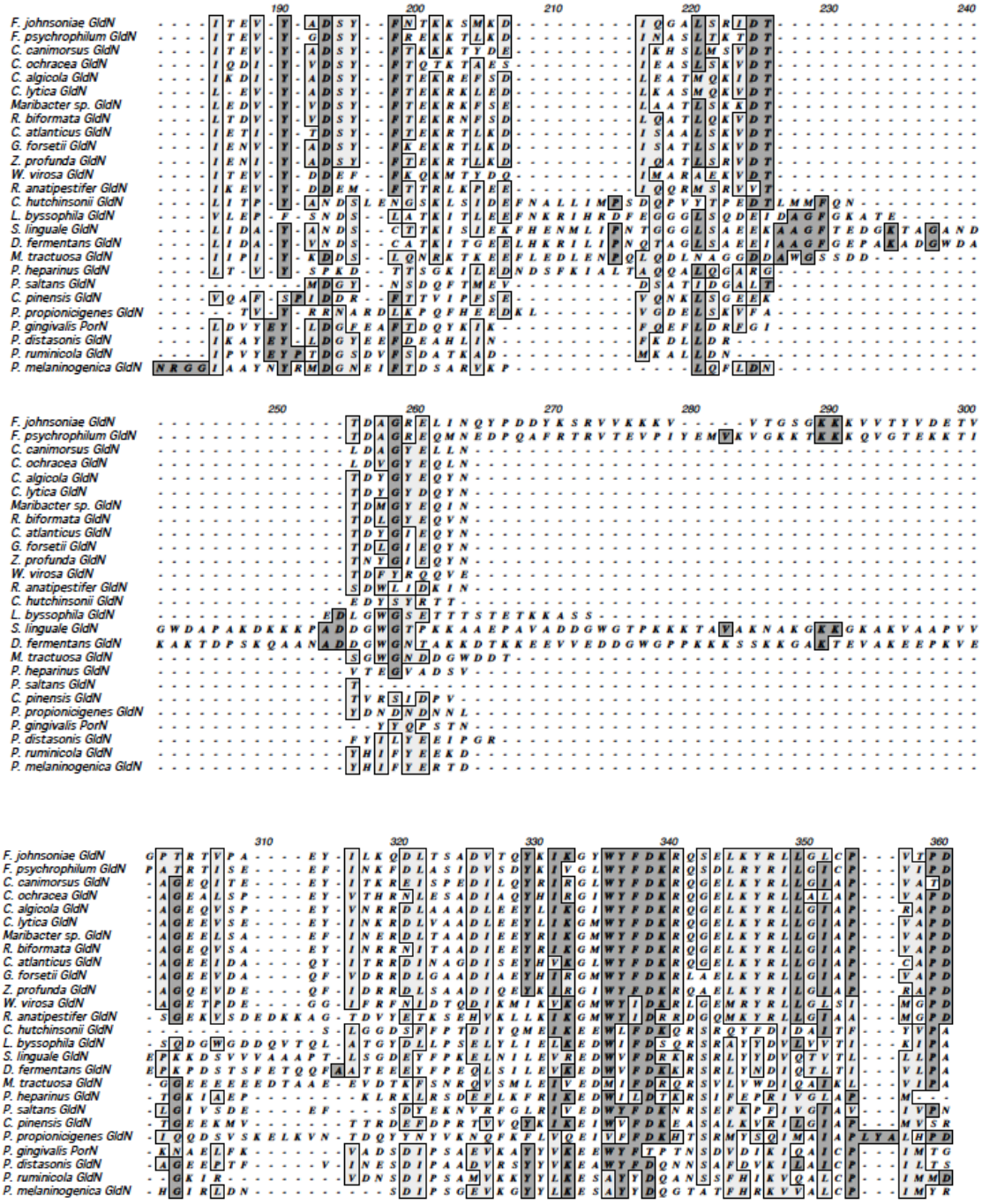
F. johnsoniae GldN
F. psychrophilum GldN
C. canimorsus GldN
C. ochracea GldN
C. algicola GldN
C. lytica GldN
Maribacter sp. GldN
R. biformata GldN
C. atlanticus GldN
G. forsetii GldN
Z. profunda GldN
W. virosa GldN
R. anatipestifer GldN
C. hutchinsonii GldN
L. byssophila GldN
S. linguale GldN
D. fermentans GldN
M. tractuosa GldN
P. heparinus GldN
P. saltans GldN
C. pinensis GldN
P. propionicigenes GldN
P. gingivalis PorN
P. distasonis GldN
P. ruminicola GldN
P. melaninogenica GldN

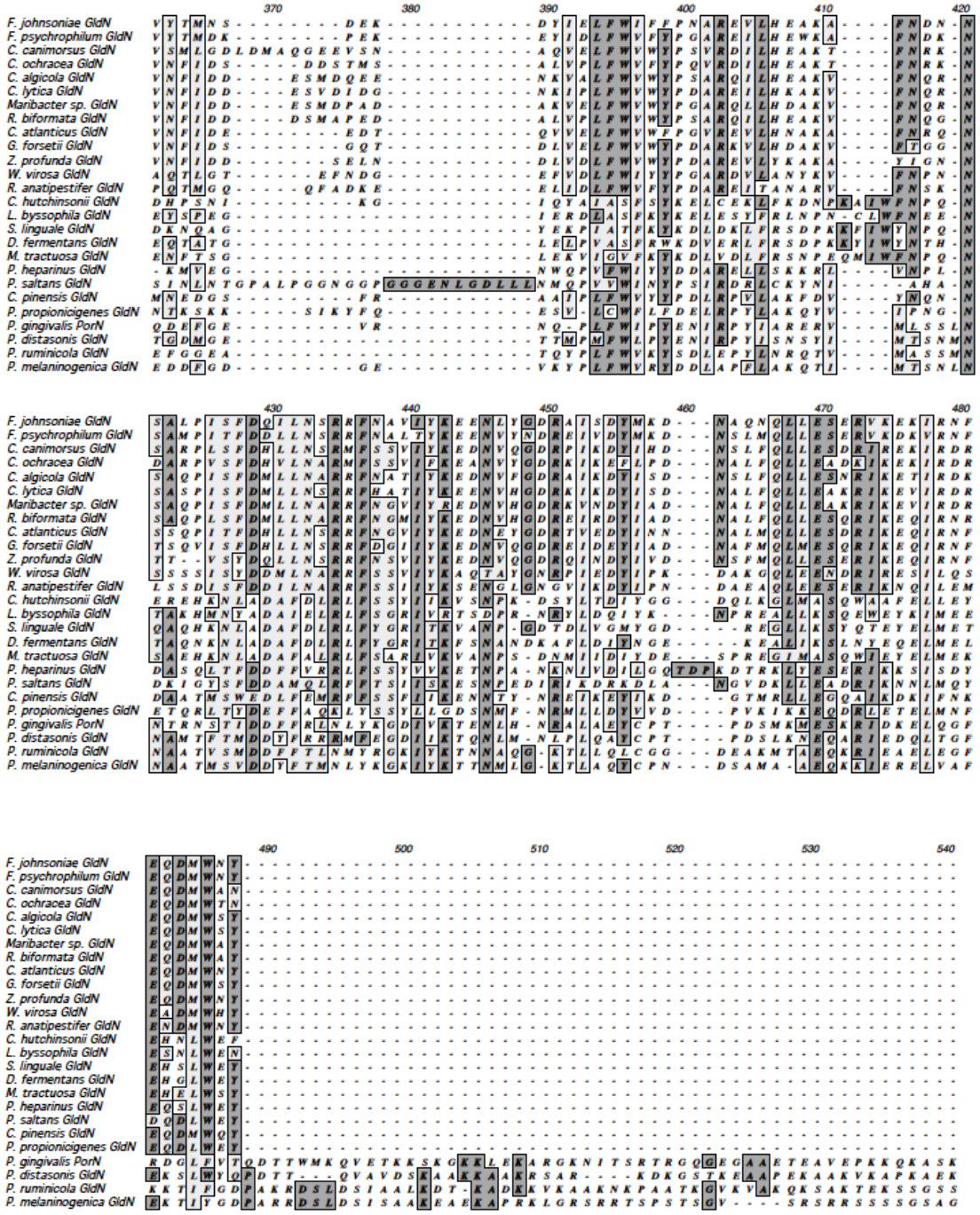
370
380
390
400
410
420
F. johnsoniae GldN
F. psychrophilum GldN
C. canimorsus GldN
C. ochracea GldN
C. algicola GldN
C. lytica GldN
Maribacter sp. GldN
R. biformata GldN
C. atlanticus GldN
G. forsetii GldN
Z. profunda GldN
W. virosa GldN
R. anatipestifer GldN
C. hutchinsonii GldN
L. byssophila GldN
S. linguale GldN
D. fermentans GldN
M. tractuosa GldN
P. heparinus GldN
P. saltans GldN
C. pinensis GldN
P. propionicigenes GldN
P. gingivalis PorN
P. distasonis GldN
P. ruminicola GldN
P. melaninogenica GldN
430
440
450
460
470
480
490
500
510
520
530
540

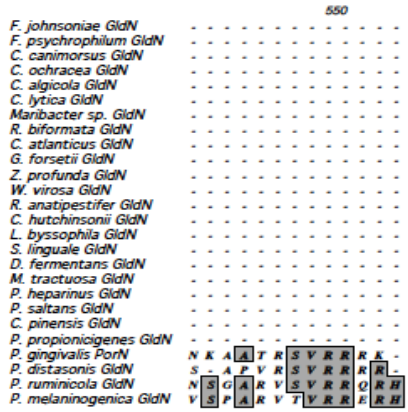

Figure 33. Alignment of GldN using MUSCLE. Dark shading indicates identical amino acids and light shading indicates similar amino acids.

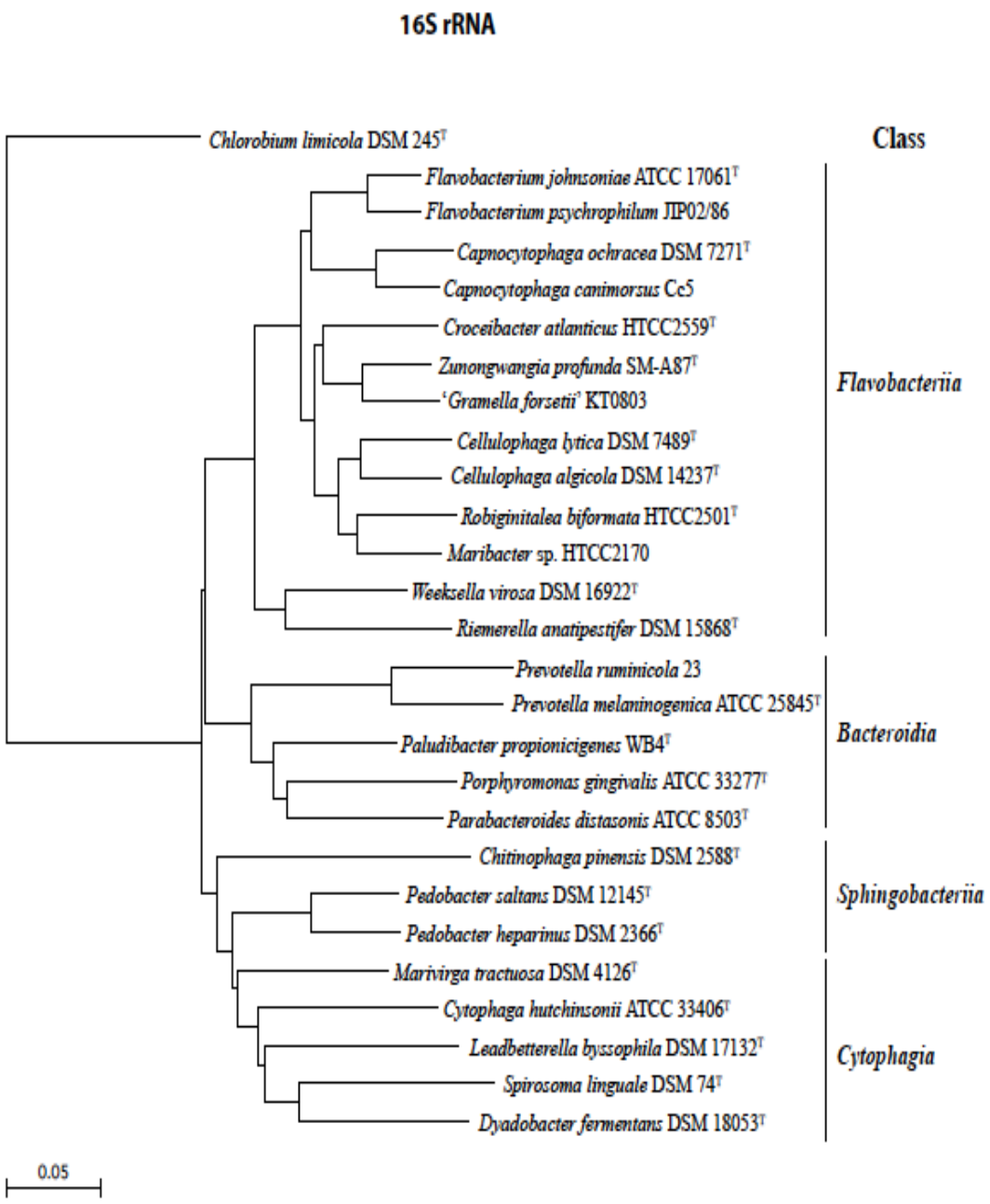

Figure 34. Phylogenetic tree of members of the phylum *Bacteroidetes* based on 16s rRNA sequences. Sequences were aligned by CLUSTALW and the phylogenetic tree was generated using the Neighbor Joining method with *Chlorobium Dimicola* DSM 245 as an outgroup.

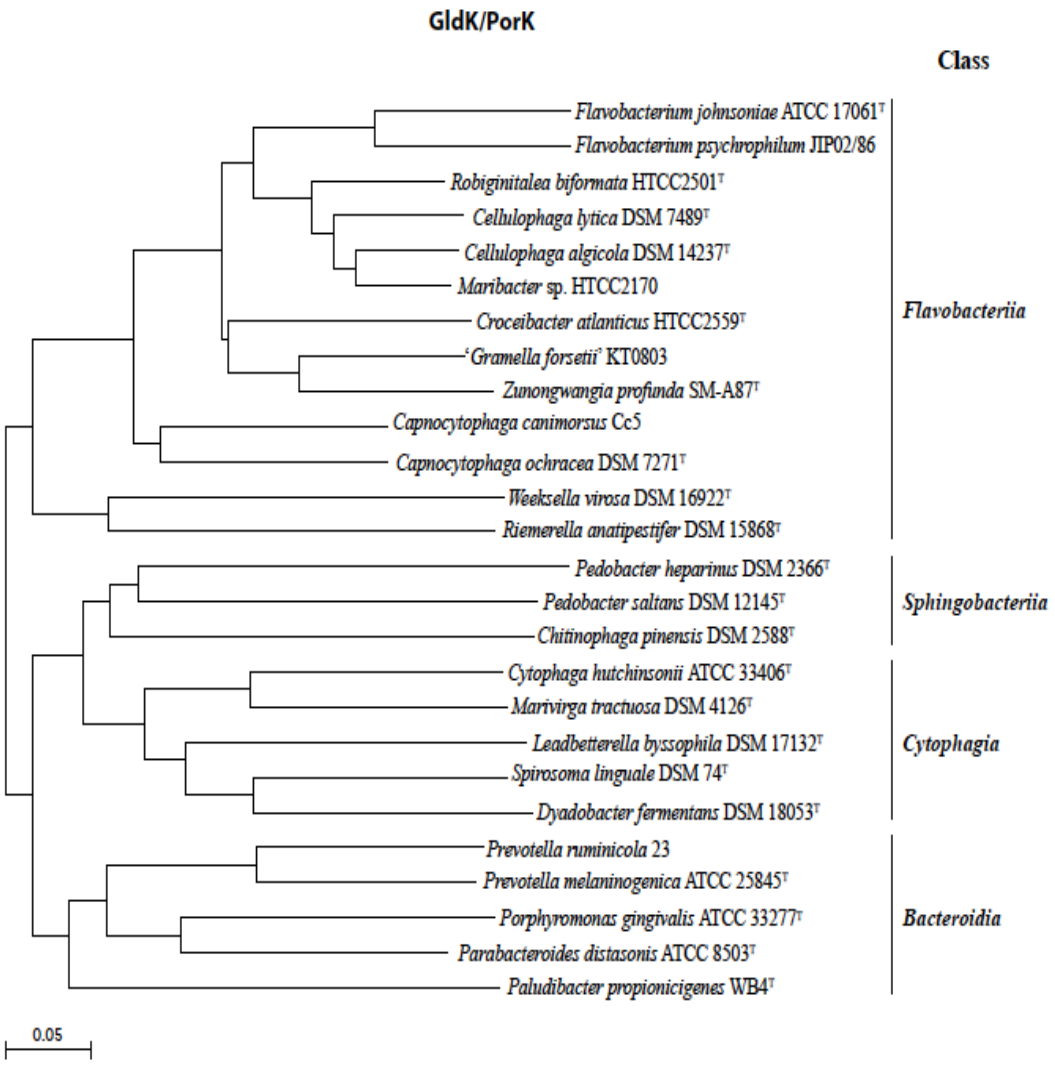

Figure 35. Phylogenetic tree based on GldK protein sequences. Sequences were aligned by MUSCLE and the phylogenetic tree was generated using the Neighbor Joining method. Since orthologs of GldK are not found outside the phylum *Bacteroidetes* there was no obvious outgroup so midpoint rooting was used.

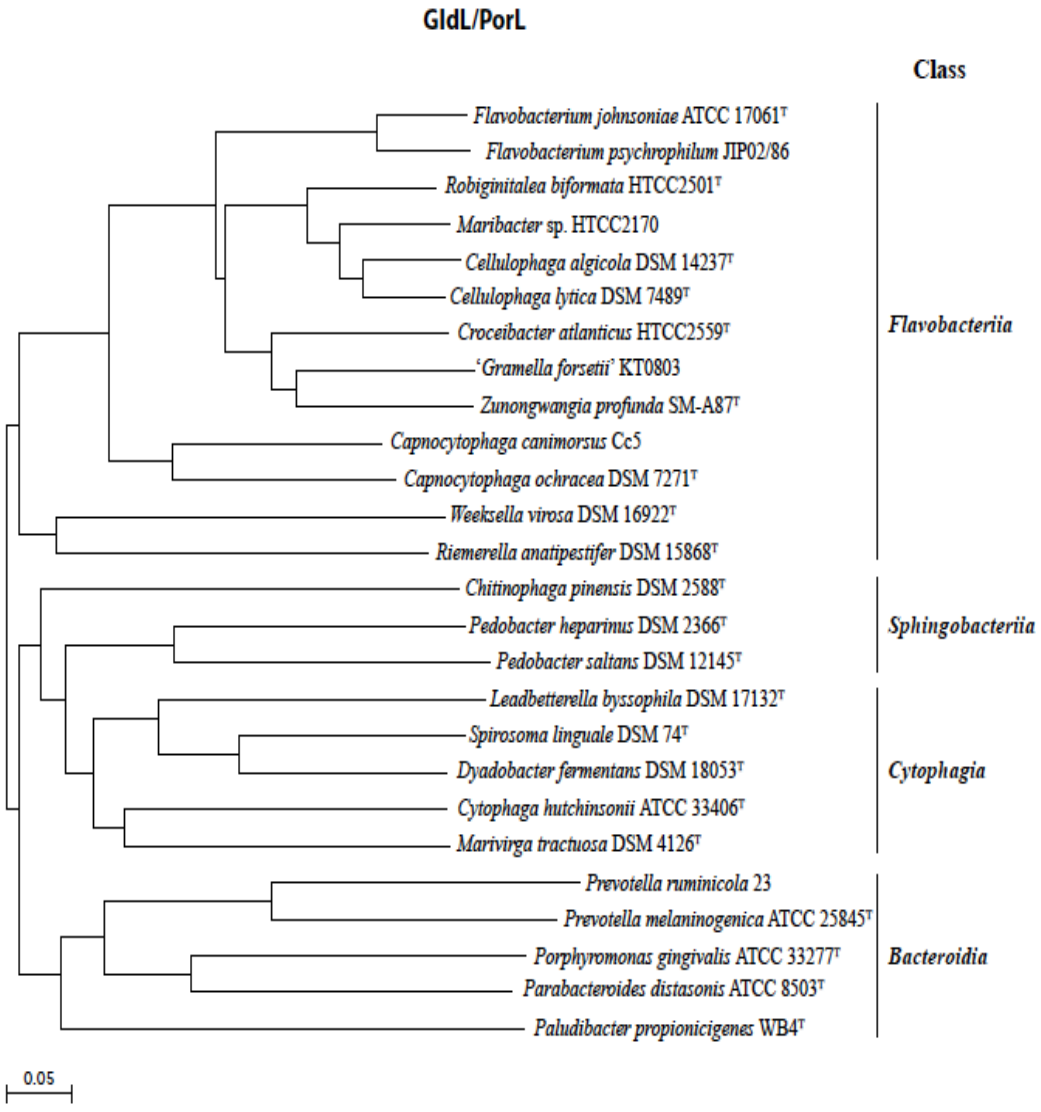

Figure 36. Phylogenetic tree based on GldL protein sequences. Sequences were aligned by MUSCLE and the phylogenetic tree was generated using the Neighbor Joining method. Since orthologs of GldK are not found outside the phylum *Bacteroidetes* there was no obvious outgroup so midpoint rooting was used.

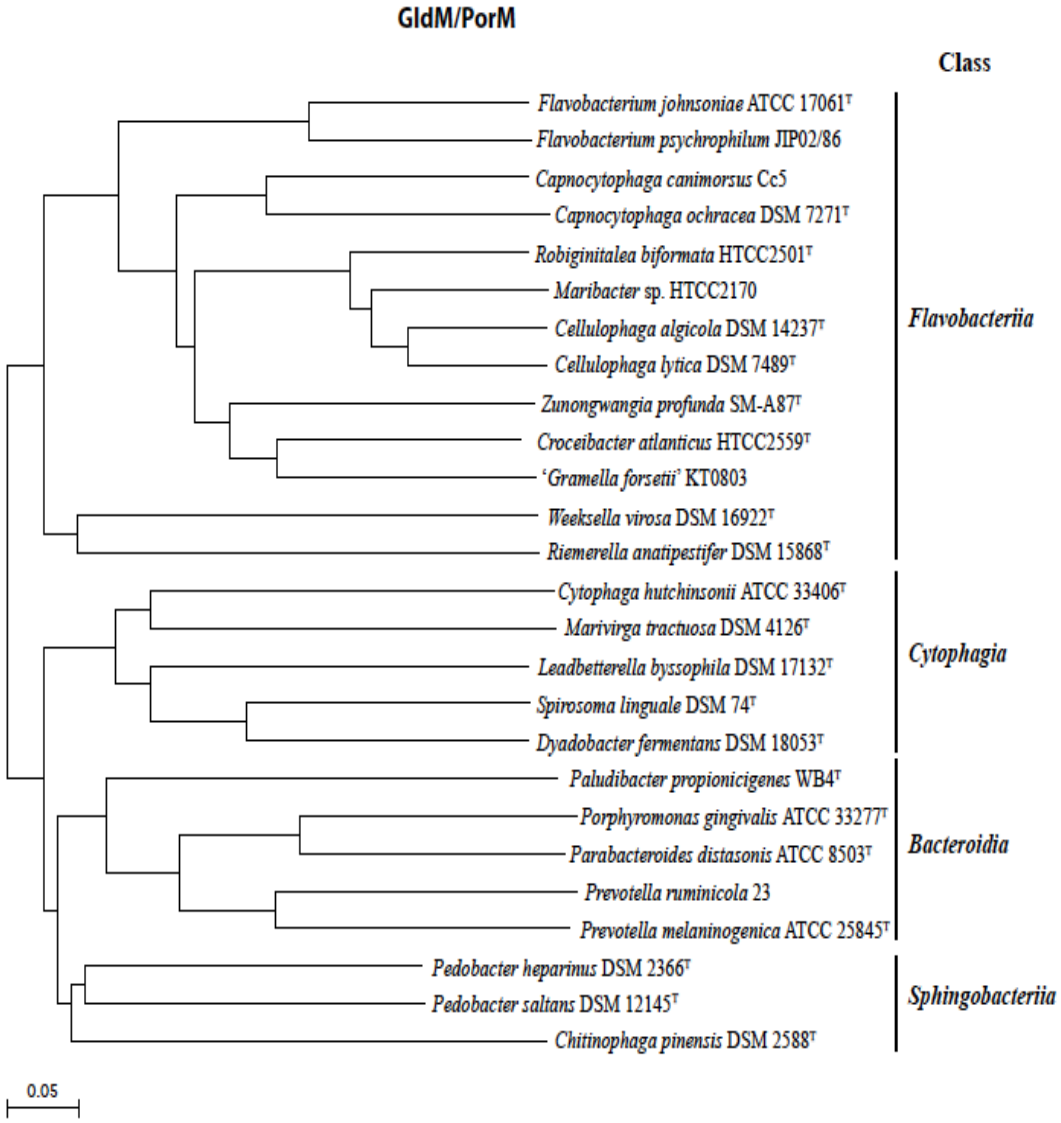

Figure 37. Phylogenetic tree based on GldM protein sequences. Sequences were aligned by MUSCLE and the phylogenetic tree was generated using the Neighbor Joining method. Since orthologs of GldK are not found outside the phylum *Bacteroidetes* there was no obvious outgroup so midpoint rooting was used.

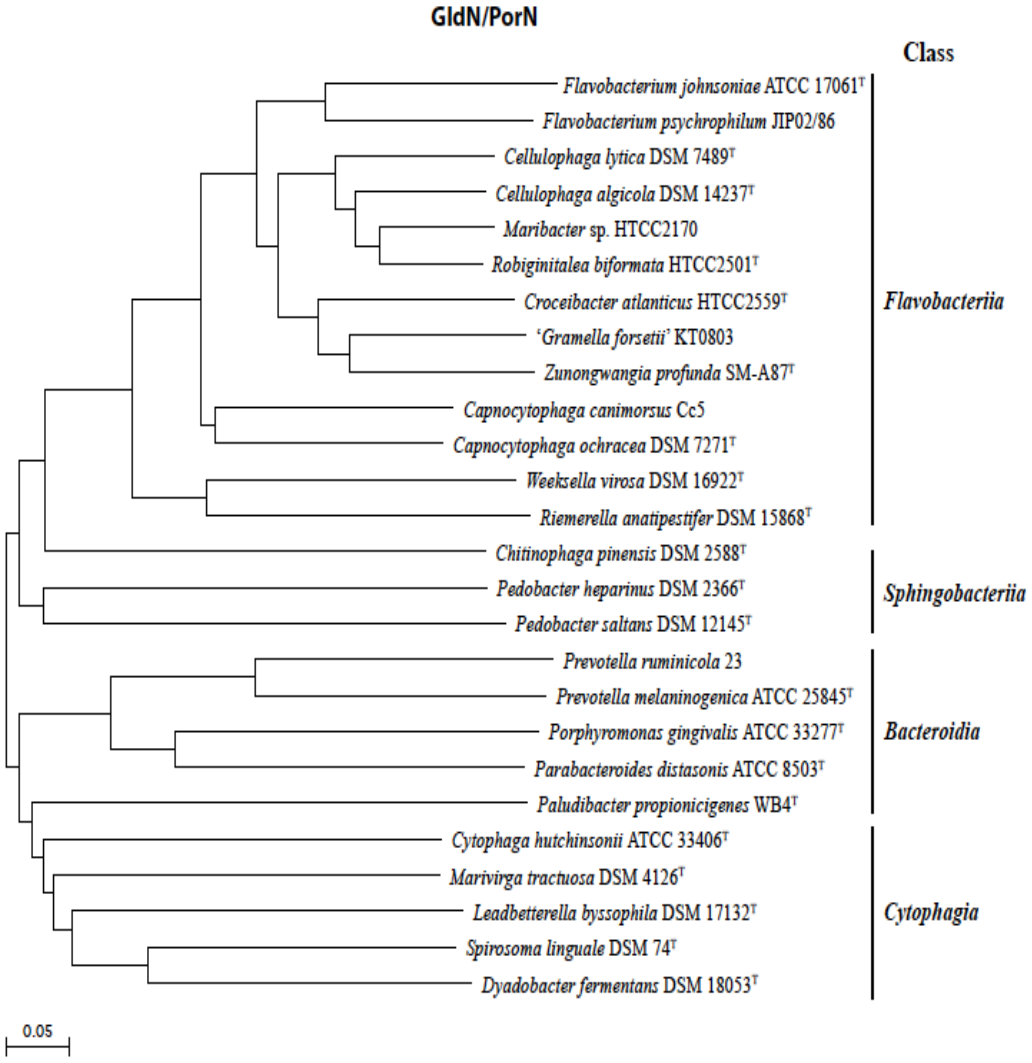

Figure 38. Phylogenetic tree based on GldN protein sequences. Sequences were aligned by MUSCLE and the phylogenetic tree was generated using the Neighbor Joining method. Since orthologs of GldK are not found outside the phylum *Bacteroidetes* there was no obvious outgroup so midpoint rooting was used.

The results presented indicate that GldK, GldL, GldM, and SprA are each required for secretion of SprB, RemA and chitinase. These proteins presumably function with other previously known components of the *F. johnsoniae* T9SS, including GldN, SprE, and SprT, that are also required for secretion of the same proteins. The predicted outer membrane protein SprF, which exhibits similarity to *P. gingivalis* T9SS protein PorP, is also required for secretion of SprB, but is not needed for secretion of RemA or for chitin utilization (24, 35). Unlike *P. gingivalis*, *F. johnsoniae* has many *sprF*-like (*porP*-like) genes that may encode semi-redundant proteins involved in secretion of different proteins. A model depicting our current understanding of the *F. johnsoniae* T9SS is illustrated in Figure 39. As shown in this diagram, GldL and GldM are the only known cytoplasmic membrane components of the *F. johnsoniae* T9SS. As such, they have potential roles in harvesting cellular energy to power secretion, as suggested above, but further experiments will be needed to determine their exact functions.

GldK, GldL, and GldM are required not only for secretion, but also for gliding motility. The motility defects of cells lacking these proteins may be explained by their inability to deliver motility adhesins, such as SprB and RemA, to the cell surface. However GldK, GldL, and GldM may also have more direct roles in cell movement. Although the cell-surface adhesins involved in motility are known, the motor for cell movement has not yet been identified. Gliding of *F. johnsoniae* and related bacteria is known to require the proton gradient across the cytoplasmic membrane (8, 9, 22, 28), and proteins that span this membrane must be involved in converting this into cell movement.

Twelve Gld proteins required for gliding of *F. johnsoniae* have been identified (3), and only four of these (GldF, GldG, GldL, and GldM) are thought to span the cytoplasmic membrane. GldF and GldG do not appear to be central components of the gliding machinery because some relatives of *F. johnsoniae* lack these proteins and yet exhibit rapid gliding motility (18). This leaves GldL and GldM as candidates for the motor proteins that harvest cellular energy and propel SprB and RemA, resulting in cell movement. Alternatively, some other unidentified cytoplasmic membrane proteins may perform these motor functions. Further study is needed to determine whether GldL and GldM have roles in gliding beyond secretion of SprB and RemA, and to determine the exact functions of each of the T9SS proteins in protein secretion.

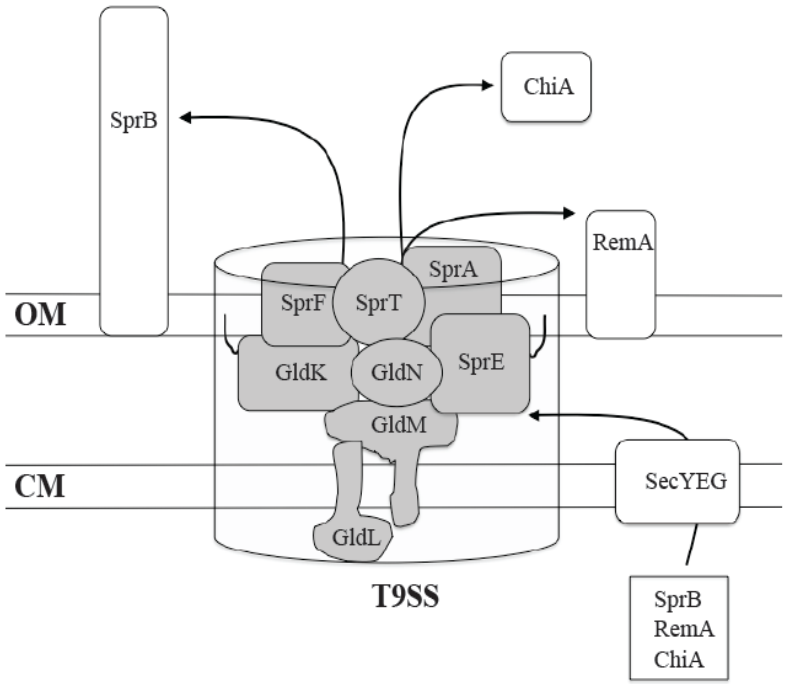

Figure 39. Model of the *F. johnsoniae* T9SS. GldK, GldL, GldM, and GldN form the core components that are required for secretion. GldO, (not shown) is nearly identical to GldN and is partially redundant with it. The outer membrane proteins SprA and SprT, and the lipoprotein

SprE are thought to be required for secretion of SprB, RemA, and ChiA, but they may not be required for secretion of all proteins targeted to the T9SS. SprF is needed for secretion of SprB, but not for secretion of RemA and ChiA. *F. johnsoniae* has many paralogs of *sprF*, that may encode proteins involved in secretion of proteins other than SprB. Predicted outer membrane proteins PorU and PorV (not shown) may also have roles in secretion of some proteins by the T9SS. Proteins targeted to the T9SS all have predicted type 1 signal peptides, and are predicted to be exported across the cytoplasmic membrane by the Sec system before being secreted across the outer membrane by the T9SS. Black lines indicate lipid tails on lipoproteins. Proteins are not drawn to scale and stoichiometry of components is not known.

Table 4. Strains and plasmids used in this study.

***F. johnsoniae* Strains**	**Genotype and Description[a]**	**Source or reference**
UW101 (ATCC 17061)	Wild type	(15, 17)
UW102-57	spontaneous *gldK* mutant	(3, 4)
UW102-141	spontaneous *gldK* mutant	(3, 4)
CJ1372	*gldK*::*HimarEm1*; (Em^r)	(3)
CJ1373	*gldK*::*HimarEm1*; (Em^r)	(3)
CJ1827	*rpsL2*; (Sm^r) 'wild-type' strain used in construction of deletion mutants	(25)
CJ1922	*rpsL2* Δ*sprB*; (Sm^r)	(25)
CJ1984	*rpsL2* Δ*remA*; (Sm^r)	(35)
CJ1985	*rpsL2* Δ*sprB* Δ*remA*; (Sm^r)	(35)
CJ2083	*rpsL2 remA::myc-tag-1*; (Sm^r)	(35)
CJ2090	*rpsL2* Δ(*gldN gldO*); (Sm^r)	(35)
CJ2122	*rpsL2* Δ*gldK*; (Sm^r)	This study
CJ2140	*rpsL2* Δ*gldK* in *remA::myc-tag-1* background; (Sm^r)	This study

CJ2157	*rpsL2* Δ*gldL*; (Sm^r)	This study
CJ2262	*rpsL2* Δ*gldM*; (Sm^r)	This study
CJ2263	*rpsL2* Δ*gldM* in *remA::myc-tag-1* background; (Sm^r)	This study
CJ2281	*rpsL2* Δ*gldL* in *remA::myc-tag-1* background; (Sm^r)	This study
CJ2089	*rpsL2* Δ(*gldN gldO*) *remA::myc-tag-1*; (Sm^r)	This study
CJ2302	*rpsL2* Δ*sprA*; (Sm^r)	This study
CJ2317	*rpsL2* Δ*sprA* in *remA::myc-tag-1* background; (Sm^r)	This study
CJ2327	*sprT* disruption in *remA::myc-tag-1* background; (Em^r, Sm^r)	This study
KDF001	*sprT* mutant	(30)
FJ149	*sprE* mutant	(27)
Plasmids		
pBC SK+	ColE1 ori; Cm^r	Stratagene
pMAL-c2	MalE fusion protein expression vector; Ap^r	New England Biolabs

pUC18	ColE1 ori; Ap^r	(38)
pCP23	*E. coli-F. johnsoniae* shuttle plasmid; Ap^r $(Tc)^r$	(2)
pCP29	*E. coli-F. johnsoniae* shuttle plasmid; Ap^r (Cf^r Em^r)	(13)
pRR51	*rpsL*-containing suicide vector; Ap^r (Em^r)	(25)
pAB18	2.4 kbp region downstream of *gldL* was amplified with primers 1199 and 1200 and cloned into XbaI-SalI site of pRR51.	This study
pAB19	Construct used to delete *gldL*; 2.2 kbp region upstream of *gldL* amplified with primer pair 1197-1198 cloned into BamHI-XbaI site of pAB18.	This study
pAB30	Construct used to delete *sprA;* 2.5 kbp upstream and 2.5 kbp downstream of *sprA* was amplified by primer pair 1333-1334 and 1335-1336 respectively and cloned into BamHI-SalI site of pRR51.	This study
pJJ01	Construct used to delete *gldK*. 1.8 kbp upstream and 1.9 kbp downstream of *gldK* was amplified by primer pair 1209-1210 and 1211-1212 respectively and cloned into BamHI-SphI site of pRR51.	This study
pJJ02	Construct used to delete *gldM*. 2.6 kbp upstream and 2.4 kbp downstream of *gldM* was amplified by primer pair 1237-1214 and 1215-1238 respectively and cloned into BamHI-SphI site of pRR51.	This study
pTB99	pCP23 carrying *gldK*; Ap^r (Tc^r)	(3)

pTB81a	pCP23 carrying *gldL*; Ap^r (Tc^r)	(3)
pTB94a	pCP23 carrying *gldM*; Ap^r (Tc^r)	(3)
pTB79	pCP23 carrying *gldN*; Ap^r (Tc^r)	(3)
pKF002	pCP23 carrying *sprT*; Ap^r (Tc^r)	(30)
pSN48	pCP23 carrying *sprA*; Ap^r (Tc^r)	(20)

[a]Antibiotic resistance phenotypes: ampicillin, Ap^r; cefoxitin, Cf^r; chloramphenicol, Cm^r; erythromycin, Em^r; streptomycin, Sm^r; tetracycline, Tc^r. Unless indicated otherwise, the antibiotic resistance phenotypes are those expressed in *E. coli*. The antibiotic resistance phenotypes given in parentheses are those expressed in *F. johnsoniae* but not in *E. coli*.

Table 5. Binding of Protein G-coated polystyrene spheres carrying anti-SprB antibodies.

Strain	Description	Antibody added	Avg (SD) % of cells with spheres attached[a]
CJ1827/pCP23	Wild type with control plasmid pCP23	No antibody	0.0 (0.0)
CJ1827/pCP23	Wild type with control plasmid pCP23	Anti-SprB	53.7 (3.1)
CJ1922/pCP23	Δ*sprB* with control plasmid pCP23	Anti-SprB	1.0 (1.0)

CJ2122/pCP23	Δ*gldK* with control plasmid pCP23	Anti-SprB	0.3 (0.6)
CJ2122/pTB99	Δ*gldK* with pTB99 carrying *gldK*	Anti-SprB	54 (2.0)
CJ2157/pCP23	Δ*gldL* with control plasmid pCP23	Anti-SprB	0.3 (0.6)
CJ2157/pTB81a	Δ*gldL* with pTB81a carrying *gldL*	Anti-SprB	54.3 (3.5)
CJ2262/pCP23	Δ*gldM* with control plasmid pCP23	Anti-SprB	0.0 (0.0)
CJ2262/pTB94a	Δ*gldM* with pTB94a carrying *gldM*	Anti-SprB	56.0 (2.0)
CJ2302/pCP23	Δ*sprA* with control plasmid pCP23	Anti-SprB	0.3 (0.6)
CJ2302/pSN48	Δ*sprA* with pSN48 carrying *sprA*	Anti-SprB	51.3 (4.0)

[a]Purified anti-SprB antiserum and 0.5-μm-diameter protein G-coated polystyrene spheres were added to cells as described in Materials and Methods. Samples were introduced into a tunnel slide, incubated for 1 min at 25^{o}C and examined using a phase-contrast microscope. Images were recorded for 30 s and 100 randomly selected cells were examined for the presence of spheres that remained attached to the cells during this time. Numbers in parentheses are standard deviations (SD) calculated from three measurements.

Table 6. Binding of Protein G-coated polystyrene spheres carrying antibodies against myc-tag peptide.

Strain	Description	Antibody added	Avg (SD) % of cells with spheres attached[a]
CJ1827	Wild type	Anti-myc	0.0 (0.0)
CJ1984	Δ*remA*	Anti-myc	0.0 (0.0)
CJ2083	*remA::myc-tag-1*	No antibody	0.0 (0.0)
CJ2083	*remA::myc-tag-1*	Anti-myc	54.0 (4.0)
CJ2140/pCP23	Δ*gldK, remA::myc-tag-1* with control plasmid pCP23	Anti-myc	1.0 (0.0)
CJ2140/pTB99	Δ*gldK, remA::myc-tag-1* with pTB99 carrying *gldK*	Anti-myc	57.0 (1.0)
CJ2281/pCP23	Δ*gldL, remA::myc-tag-1* with control plasmid pCP23	Anti-myc	1.0 (1.0)
CJ2281/pTB81a	Δ*gldL, remA::myc-tag-1* with pTB81a carrying *gldL*	Anti-myc	52.7 (2.1)
CJ2263/pCP23	Δ*gldM, remA::myc-tag-1* with control plasmid pCP23	Anti-myc	1.0 (1.0)
CJ2263/pTB94a	Δ*gldM, remA::myc-tag-1* with pTB94a carrying *gldM*	Anti-myc	53.0 (1.7)
CJ2317	Δ*sprA, remA::myc-tag-1*	Anti-myc	0.6 (0.5)

CJ2317/pSN48	Δ*sprA, remA::myc-tag-1* with pSN48 carrying *sprA*	Anti-myc	55.3 (2.5)
CJ2327	*sprT, remA::myc-tag-1*	Anti-myc	0.0 (0.0)
CJ2327/pKF002	*sprT, remA::myc-tag-1* with pKKF002 carrying *sprT*	Anti-myc	64.6 (2.0)

[a]Purified anti-Myc-tag antiserum and 0.5-μm-diameter protein G-coated polystyrene spheres were added to cells as described in Materials and Methods. Samples were introduced into a tunnel slide, incubated for 1 min at 25^{o}C and examined using a phase-contrast microscope. Images were recorded for 30 s and 100 randomly selected cells were examined for the presence of spheres that remained attached to the cells during this time. Numbers in parentheses are standard deviations (SD) calculated from three measurements.

Table 7. Effect of deletion of *gldK*, *gldL*, *gldM*, and *sprA* on attachment of cells to glass coverslips.

Strain	Description	Avg no. of cells attached to 0.03-mm^2 region of glass coverslip[a]
CJ1827/pCP23	Wild type with control vector pCP23	69.1 (4.9)
CJ2122/pCP23	Δ*gldK* with control vector pCP23	0.3 (0.5)
CJ2122/pTB99	Δ*gldK* with pTB99 carrying *gldK*	67.7 (8.6)
CJ2157/pCP23	Δ*gldL* with control vector pCP23	0.3 (0.5)
CJ2157/TB81a	Δ*gldL* with pTB81a carrying *gldL*	60.7 (6.8)
CJ2262/pCP23	Δ*gldM* with control vector pCP23	0.6 (1.0)
CJ2262/pTB94a	Δ*gldM* with pTB94a carrying *gldM*	24.1 (2.5)
CJ2302/pCP23	Δ*sprA* with control vector pCP23	0.1 (0.3)
CJ2302/pSN48	Δ*sprA* with pSN48 carrying *sprA*	64.2(8.5)
KDF001	*sprT* mutant	1.4 (1.3)
KDF001/pKF002	*sprT* mutant with pKF002 carrying *sprT*	53 (5.4)
FJ149	*sprE* mutant	2.6 (1.2)
CJ1922/pCP23	Δ*sprB* with control vector pCP23	66.6 (11.3)
CJ1984/pCP23	Δ*remA* with control vector pCP23	54.8 (7.3)
CJ1985/pCP23	Δ*sprB* Δ*remA* with control vector pCP23	22.6 (4.1)

[a]Approximately 10^6 cells in 2.5 ml of MM medium were introduced into a Petroff-Hausser counting chamber and incubated for 2 min at 25°C. Samples were observed using an Olympus

BH-2 phase-contrast microscope, and cells attached to a 0.03-mm^2 region of the cover glass were counted. Numbers in parentheses are standard deviations calculated from 9 measurements.

Table 8. Primers used in this study

Primers	**Sequence and Description**
685	5’ TCCGCTGGAAGAAGAGGAAC 3’; used for RT PCR. Binds upstream of *gldK*. Also used to check *gldK* deletion.
690	5’ GATGAGTATTATGCTGAAGTAATGG 3’; used for RT PCR. Binds in *gldK* region. Also used to check *gldL* deletion.
616	5’ CAGTTGAGGATGAATTAGATTGG 3’; used for RT PCR. Binds in *gldL* region. Also used to check *gldM* deletion.
692	5’ AAGGATTTCCTGCGATCGC 3’; used for RT PCR. Binds in *gldM* region.
695	5’ TTAAGATATACTCAGCAGGAACCG 3’; used for RT PCR. Binds in *gldN* region.
704	5’ TTGGTGAATTCGGAGGGAAATGGCATCCTG 3’; used in construction of pJVB4. EcoRI site underlined.
705	5’ TATACACGTCGACATTATTATTTTCTTCCGCC 3’; used in construction of pJVB4. Also used for RT PCR. SalI site underlined.
706	5’ AGGGACAGAATTCCTTTCTATCGGTCTTTTGACTGAGG 3’; used in construction of pJVB2. EcoRI site underlined.
707	5’ CTTCTGTGTCGACGTTAATTTTCCTCCTGCC 3’; used in construction of pJVB2. Also used to check *gldK* and *gldL* deletions. SalI site underlined.
708	5’ CAGCTCACAAAGTTCAGGCTGC 3’; used in construction of pJVB6.
709	5’ AGTTTTAGTCGACTTATTATTGTATTTCGTAAATTACC 3’; used in construction of pJVB6. SalI site underlined.
733	TAGAAGGTCGACCTCCAGCGATAGAAACAATAGC; used to check *gldM* deletion. Binds downstream of *gldM.*

1197	5' GCTAGGGATCCGGCTGAGCCTGTATTTCGAG 3'; used in construction of pAB19 for *gldL* deletion. BamHI site underlined.
1198	5' GCTAGTCTAGACATAACTTTTTTACTTAATAATGCCAT 3'; used to construct pAB19 for *gldL* deletion. XbaI site underlined.
1199	5' GCTAGTCTAGAGGTATGCTTTCTGCAATGAGTAAC 3'; used in construction of pAB19 for *gldL* deletion. XbaI site underlined.
1200	5' GCTAGGTCGACAGTACTTCACGTGCATTTGGG 3'; used in construction of pAB19 for *gldL* deletion. SalI site underlined.
1333	5’ GCTAGGGATCCCACGACGATCAGCACGGA3’; used in construction of pAB30 for *sprA* deletion. BamHI site underlined. Also used to check *sprA* deletion.
1334	5' GCTAGTCTAGATGACCGCAAAACGTTACCACA 3'; used in construction of pAB30 for *sprA* deletion. XbaI site underlined.
1335	5' GCTAGTCTAGAGTTATTTCGACGTCATTCCCG 3'; used in construction of pAB30 for *sprA* deletion. XbaI site underlined.
1336	5' GCTAGGTCGACCTCCCTGAATCTGCACCATGT 3'; used in construction of pAB30 for *sprA* deletion. SalI site underlined. Also used to check *sprA* deletion.
1209	5’ GCTAGGGATCCGCCAATTGCTGTTTACAAAGGAG 3’; used in construction of pJJ01 for *gldK* deletion. BamHI site underlined.
1210	5’ GCTAGGTCGACACCTGACTTACCACAGCCGAT 3’; used in construction of pJJ01 for *gldK* deletion. SalI site underlined.
1211	5’GCTAGGTCGACATGGGAACTCAAGTAACAGGAGGC 3’; used in construction of pJJ01 for *gldK* deletion. SalI site underlined.
1212	5’ GCTAGGCATGCTGTAGCCTCAGTACCTTGACCTGG 3’; used in construction of pJJ01 for *gldK* deletion. SphI site underlined.
1237	5’ GCTAGGGATCCTCCGCTGGAAGAAGAGGAAC 3’; used in construction of pJJ02 for *gldM* deletion. BamHI site underlined.
1214	5’GCTAGGTCGACCTGTCTAGGGGTTAATTTTCCTCC 3’; used in construction of pJJ02 for *gldM* deletion. SalI site underlined.

1215	5’ GCTAGGTCGACCCAAGAACTGCTCCGGTAATTTAC 3’; used in construction of pJJ02 for *gldM* deletion. SalI site underlined.
1238	5’ GCTAGGCATGCACAAGCCTCCTGCAATTCTCGAAG 3’; used in construction of pJJ02 for *gldM* deletion. SphI site underlined.

Table 9. *F. johnsoniae* genes predicted to encode proteins secreted by the T9SS.

Locus tag	Gene name	TIGRFAM family[1]	Predicted function
Fjoh_0074		TIGR04183	endonuclease/exonuclease/phosphatase family (pfam03372)
Fjoh_0547		TIGR04183	
Fjoh_0549		TIGR04183	cell adhesion related domain (pfam07705)
Fjoh_0707		TIGR04183	
Fjoh_0798		TIGR04183	peptidase (pfam13574)
Fjoh_0808	*remA*	TIGR04183	gliding motility adhesin
Fjoh_0848		TIGR04183	tetratricopeptide repeat protein (pfam13371; pfam13414)
Fjoh_0886		TIGR04183	peptidase (pfam01447; pfam02868)
Fjoh_0979	*sprB*	TIGR04131	gliding motility adhesin
Fjoh_1022		TIGR04183	glycosyl hydrolase (pfam01270)
Fjoh_1123		TIGR04131	
Fjoh_1188		TIGR04183	
Fjoh_1189		TIGR04183	lectin/glucanase/pectate lyase (pfam13385; pfam13573)
Fjoh_1208		TIGR04183	a amylase (pfam00128)
Fjoh_1231		TIGR04183	pectate lyase (pfam00544)
Fjoh_1269		TIGR04183	pectate lyase (pfam13573)
Fjoh_1408		TIGR04183	a amylase (pfam00128)
Fjoh_1645		TIGR04131	Hyalin repeat, adhesion (pfam02494)
Fjoh_1720		TIGR04131	lectin (IPR016186; IPR016187; IPR001304)
Fjoh_1905		TIGR04183	glycosyl hydrolase/lectin (pfam02055; pfam14200)
Fjoh_1985		TIGR04131	Hyalin repeat, adhesion (pfam02494)
Fjoh_2150		TIGR04183	
Fjoh_2273		TIGR04131	
Fjoh_2336		TIGR04183	
Fjoh_2338		TIGR04183	
Fjoh_2339		TIGR04183	
Fjoh_2389		TIGR04183	peptidase (pfam00082)
Fjoh_2456		TIGR04183	

Fjoh_2666		TIGR04183	
Fjoh_3203		TIGR04183	bacterial Ig-like domain (pfam02368)
Fjoh_3246		TIGR04183	
Fjoh_3296		TIGR04183	
Fjoh_3324		TIGR04183	glucose/sorbosone dehydrogenase/ carbohydrate binding (pfam07995; pfam03422)
Fjoh_3421		TIGR04183	
Fjoh_3478		TIGR04131	
Fjoh_3731		TIGR04183	
Fjoh_3777		TIGR04183	
Fjoh_3855		TIGR04183	
Fjoh_3952		TIGR04131	
Fjoh_3971		TIGR04131	
Fjoh_4051		TIGR04183	pectate lyase (pfam13573)
Fjoh_4174		TIGR04183	lectin/carbohydrate binding (pfam14200; pfam03422)
Fjoh_4175		TIGR04183	glycosyl hydrolase/carbohydrate binding (pfam00704; pfam03422)
Fjoh_4176		TIGR04183	lectin/carbohydrate binding (pfam14200; pfam03422)
Fjoh_4177		TIGR04183	glycosyl hydrolase (pfam00722)
Fjoh_4242		TIGR04183	peptidase (pfam00082)
Fjoh_4436		TIGR04183	
Fjoh_4538		TIGR04131	
Fjoh_4721		TIGR04183	endonuclease (pfam04231)
Fjoh_4723		TIGR04183	endonuclease (pfam04231)
Fjoh_4750		TIGR04131	pectate lyase (pfam13573)
Fjoh_4934		TIGR04131	
Fjoh_4948		TIGR04183	

[1]-TIGR04131 is described as ‘gliding motility-associated C-terminal domain’, and TIGR04183 is described as ‘Por secretion system C-terminal sorting domain’ on the J.Craig Venter Institute TIGR website.

(http://www.jcvi.org/cgi-bin/tigrfams/index.cgi)

References

1. **Abdallah, A. M., N. C. Gey van Pittius, P. A. Champion, J. Cox, J. Luirink, C. M. Vandenbroucke-Grauls, B. J. Appelmelk, and W. Bitter.** 2001. Type VII secretion--mycobacteria show the way. Nat. Rev. Microbiol. **5:**883-891.
2. **Agarwal, S., D. W. Hunnicutt, and M. J. McBride.** 1997. Cloning and characterization of the *Flavobacterium johnsoniae* (*Cytophaga johnsonae*) gliding motility gene, *gldA*. Proc. Natl. Acad. Sci. USA **94:**12139-12144.
3. **Braun, T. F., M. K. Khubbar, D. A. Saffarini, and M. J. McBride.** 2005. *Flavobacterium johnsoniae* gliding motility genes identified by *mariner* mutagenesis. J. Bacteriol. **187:**6943-6952.
4. **Chang, L. Y. E., J. L. Pate, and R. J. Betzig.** 1984. Isolation and characterization of nonspreading mutants of the gliding bacterium *Cytophaga johnsonae*. J. Bacteriol. **159:**26-35.
5. **Dandekar, T., B. Snel, M. Huynen, and P. Bork.** 1998. Conservation of gene order: a fingerprint of proteins that physically interact. Trends Biochem Sci **23:**324-328.
6. **Desvaux, M., M. Hebraud, R. Talon, and I. R. Henderson.** 2009. Secretion and subcellular localizations of bacterial proteins: a semantic awareness issue. Trends in microbiology **17:**139-145.
7. **Dierks, T., A. Dickmanns, A. Preusser-Kunze, B. Schmidt, M. Mariappan, K. von Figura, R. Ficner, and M. G. Rudolph.** 2005. Molecular basis for multiple sulfatase deficiency and mechanism for formylglycine generation of the human formylglycine-generating enzyme. Cell **121:**541-552.
8. **Duxbury, T., B. A. Humphrey, and K. C. Marshall.** 1980. Continuous observations of bacterial gliding motility in a dialysis microchamber: the effects of inhibitors. Arch. Microbiol. **124:**169-175.
9. **Dzink-Fox, J. L., E. R. Leadbetter, and W. Godchaux, III.** 1997. Acetate acts as a protonophore and differentially affects bead movement and cell migration of the gliding bacterium *Cytophaga johnsonae* (*Flavobacterium johnsoniae*). Microbiology **143:**3693-3701.
10. **Economou, A., P. J. Christie, R. C. Fernandez, T. Palmer, G. V. Plano, and A. P. Pugsley.** 2006. Secretion by numbers: protein traffic in prokaryotes Mol. Microbiol. **62:**308-319.
11. **Hunnicutt, D. W., and M. J. McBride.** 2000. Cloning and characterization of the *Flavobacterium johnsoniae* gliding motility genes, *gldB* and *gldC*. J. Bacteriol. **182:**911-918.
12. **Jarrell, K. F., and M. J. McBride.** 2008. The surprisingly diverse ways that prokaryotes move. Nat. Rev. Microbiol. **6:**466-476.
13. **Kempf, M. J., and M. J. McBride.** 2000. Transposon insertions in the *Flavobacterium johnsoniae ftsX* gene disrupt gliding motility and cell division. J. Bacteriol. **182:**1671-1679.

14. **Liu, J., M. J. McBride, and S. Subramaniam.** 2007. Cell-surface filaments of the gliding bacterium *Flavobacterium johnsoniae* revealed by cryo-electron tomography. J. Bacteriol. **189:**7503-7506.
15. **McBride, M. J., and T. F. Braun.** 2004. GldI is a lipoprotein that is required for *Flavobacterium johnsoniae* gliding motility and chitin utilization. J. Bacteriol. **186:**2295-2302.
16. **McBride, M. J., and M. J. Kempf.** 1996. Development of techniques for the genetic manipulation of the gliding bacterium *Cytophaga johnsonae*. J. Bacteriol **178:**583-590.
17. **McBride, M. J., G. Xie, E. C. Martens, A. Lapidus, B. Henrissat, R. G. Rhodes, E. Goltsman, W. Wang, J. Xu, D. W. Hunnicutt, A. M. Staroscik, T. R. Hoover, Y. Q. Cheng, and J. L. Stein.** 2009. Novel features of the polysaccharide-digesting gliding bacterium *Flavobacterium johnsoniae* as revealed by genome sequence analysis. Appl. Environ. Microbiol. **75:**6864-6875.
18. **McBride, M. J., and Y. Zhu.** 2013. Gliding motility and Por secretion system genes are widespread among members of the phylum *Bacteroidetes*. J. Bacteriol. **195:**270-278.
19. **Nelson, S. S., S. Bollampalli, and M. J. McBride.** 2008. SprB is a cell surface component of the *Flavobacterium johnsoniae* gliding motility machinery. J. Bacteriol. **190:**2851-2857.
20. **Nelson, S. S., P. P. Glocka, S. Agarwal, D. P. Grimm, and M. J. McBride.** 2007. *Flavobacterium johnsoniae* SprA is a cell-surface protein involved in gliding motility. J. Bacteriol. **189:**7145-7150.
21. **Nguyen, K. A., J. Travis, and J. Potempa.** 2007. Does the importance of the C-terminal residues in the maturation of RgpB from *Porphyromonas gingivalis* reveal a novel mechanism for protein export in a subgroup of Gram-Negative bacteria? J. Bacteriol. **189:**833-843.
22. **Pate, J. L., and L.-Y. E. Chang.** 1979. Evidence that gliding motility in prokaryotic cells is driven by rotary assemblies in the cell envelopes. Curr. Microbiol. **2:**59-64.
23. **Pate, J. L., S. J. Petzold, and L.-Y. E. Chang.** 1979. Phages for the gliding bacterium *Cytophaga johnsonae* that infect only motile cells. Curr. Microbiol. **2:**257-262.
24. **Rhodes, R. G., S. S. Nelson, S. Pochiraju, and M. J. McBride.** 2011. *Flavobacterium johnsoniae sprB* is part of an operon spanning the additional gliding motility genes *sprC*, *sprD*, and *sprF*. J. Bacteriol. **193:**599-610.
25. **Rhodes, R. G., H. G. Pucker, and M. J. McBride.** 2011. Development and use of a gene deletion strategy for *Flavobacterium johnsoniae* to identify the redundant motility genes *remF*, *remG*, *remH*, and *remI*. J. Bacteriol. **193:**2418-2428.
26. **Rhodes, R. G., M. N. Samarasam, A. Shrivastava, J. M. van Baaren, S. Pochiraju, S. Bollampalli, and M. J. McBride.** 2010. *Flavobacterium johnsoniae gldN* and *gldO* are partially redundant genes required for gliding motility and surface localization of SprB. J. Bacteriol. **192:**1201-1211.

27. **Rhodes, R. G., M. N. Samarasam, E. J. Van Groll, and M. J. McBride.** 2011. Mutations in *Flavobacterium johnsoniae sprE* Result in Defects in Gliding Motility and Protein Secretion. J. Bacteriol. **193:**5322-5327.
28. **Ridgway, H. F.** 1977. Source of energy for gliding motility in *Flexibacter polymorphus*: effects of metabolic and respiratory inhibitors on gliding movement. J. Bacteriol. **131:**544-556.
29. **Saiki, K., and K. Konishi.** 2007. Identification of a *Porphyromonas gingivalis* novel protein Sov required for the secretion of gingipains. Microbiol. Immunol. **51:**483-491.
30. **Sato, K., M. Naito, H. Yukitake, H. Hirakawa, M. Shoji, M. J. McBride, R. G. Rhodes, and K. Nakayama.** 2010. A protein secretion system linked to bacteroidete gliding motility and pathogenesis. Proc. Natl. Acad. Sci. USA **107:**276-281.
31. **Sato, K., E. Sakai, P. D. Veith, M. Shoji, Y. Kikuchi, H. Yukitake, N. Ohara, M. Naito, K. Okamoto, E. C. Reynolds, and K. Nakayama.** 2005. Identification of a new membrane-associated protein that influences transport/maturation of gingipains and adhesins of *Porphyromonas gingivalis* J. Biol. Chem. **280:**8668-8677.
32. **Sato, K., H. Yukitake, Y. Narita, M. Shoji, M. Naito, and K. Nakayama.** 2013. Identification of *Porphyromonas gingivalis* proteins secreted by the Por secretion system. FEMS microbiology letters **338:**68-76.
33. **Seers, C. A., N. Slakeski, P. D. Veith, T. Nikolof, Y. Y. Chen, S. G. Dashper, and E. C. Reynolds.** 2006. The RgpB C-terminal domain has a role in attachment of RgpB to the outer membrane and belongs to a novel C-terminal-domain family found in *Porphyromonas gingivalis*. J. Bacteriol. **188:**6376-6386.
34. **Shoji, M., K. Sato, H. Yukitake, Y. Kondo, Y. Narita, T. Kadowaki, M. Naito, and K. Nakayama.** 2011. Por secretion system-dependent secretion and glycosylation of *Porphyromonas gingivalis* hemin-binding protein 35. PLOS One **6:**e21372.
35. **Shrivastava, A., R. G. Rhodes, S. Pochiraju, D. Nakane, and M. J. McBride.** 2012. *Flavobacterium johnsoniae* RemA is a mobile cell-surface lectin involved in gliding. J. Bacteriol. **194:**3678-3688.
36. **Slakeski, N., C. A. Seers, K. Ng, C. Moore, S. M. Cleal, P. D. Veith, A. W. Lo, and E. C. Reynolds.** 2011. C-terminal domain residues important for secretion and attachment of RgpB in *Porphyromonas gingivalis*. J. Bacteriol. **193:**132-142.
37. **Stanier, R. Y.** 1947. Studies on non-fruiting myxobacteria. I. *Cytophaga johnsonae*, N. Sp., A chitin-decomposing myxobacterium. J. Bacteriol. **53:**297-315.
38. **Vieria, J., and J. Messing.** 1982. The pUC plasmids, an M13mp7-derived system for insertion mutagenesis and sequencing with synthetic universal primers. Gene **19:**259-268.

39. **Wolkin, R. H., and J. L. Pate.** 1985. Selection for nonadherent or nonhydrophobic mutants co-selects for nonspreading mutants of *Cytophaga johnsonae* and other gliding bacteria. J. Gen. Microbiol. **131:**737-750.

Chapter 4. Untangling *Flavobacterium johnsoniae* gliding motility and protein secretion

Abstract

Flavobacterium johnsoniae is a gliding member of the phylum *Bacteroidetes*. Nineteen *F. johnsoniae* genes, mutants of which are deficient in gliding, have been discovered. Eight of these genes, *gldK*, *gldL*, *gldM*, *gldN*, *sprA*, *sprE, sprF* and *sprT* encode proteins of the Type IX bacterial protein secretion system (T9SS). The T9SS is required for surface localization of the motility adhesins SprB and RemA. The gliding proteins GldA, GldB, GldD, GldF, GldG, GldH, GldI and GldJ are essential for secretion but they are not thought to be components of the T9SS. The *F. johnsoniae* T9SS and gliding motility apparatus appear to be intertwined. Here we provide the first experimental evidence that separates motility from secretion. Previous results suggested that GldJ is unstable in strains with mutations in *gldA*, *gldB*, *gldD*, *gldF*, *gldG*, *gldH* or *gldI*. Here we demonstrate that GldK levels are dramatically reduced in cells lacking GldJ. The absence of the T9SS protein GldK may explain the secretion defects of cells with mutations in *gldJ*, or in any of the genes required for stability of GldJ protein. *F. johnsoniae* cells with a truncated GldJ, lacking 14 amino acids from the C-terminus had almost wild type levels of GldK. Presence of SprB on the cell surface and the ability to digest chitin indicated that the T9SS was functional in this strain. However, no SprB movement was observed. This indicates that the GldJ C-terminal region is important for movement of SprB. Cells with mutations in the ATP binding site of the ABC transporter protein GldA also had dramatically reduced levels of GldJ and GldK. These

results are important first steps towards untangling the *F. johnsoniae* gliding motility machinery from the T9SS.

Introduction

F. johnsoniae gliding involves mobile cell-surface adhesins SprB and RemA that interact with glass, agar and exopolysaccharide-coated surfaces (22). These interactions produce the friction that enables *F. johnsoniae* to crawl. Type IX bacterial protein secretion system (T9SS) proteins, GldK, GldL, GldM, GldN, SprA, SprE and SprT have recently been shown to be involved in secretion of SprB, RemA and an extracellular chitinase (19-21) and Shrivastava et al. in review. Besides these T9SS proteins, GldA, GldB, GldD, GldF, GldG, GldH, GldI and GldJ are also required for gliding (2-7, 10, 11, 15, 16). These proteins may be involved in movement of SprB and RemA. However, strains with mutations in *gldA*, *gldB*, *gldD*, *gldF*, *gldG*, *gldH*, *gldI* or *gldJ* also appear to have protein secretion defects. These mutants are defective in chitin utilization and exhibit complete resistance to previously reported *F. johnsoniae* bacteriophages (2-7, 10, 11, 15, 16). These phages are thought to use proteins such as SprB and RemA, that are secreted by the T9SS, as receptors. These results suggest that cells with mutations in *gldA*, *gldB*, *gldD*, *gldF*, *gldG*, *gldH, gldI* and *gldJ* have T9SS defects. Here we provide evidence that the secretion defects of these mutants may be a consequence of instability of the T9SS protein GldK. We also demonstrate that expression of truncated GldJ that is not functional for motility stabilizes GldK and allows T9SS function. This indicates that GldJ may have a direct role in movement of SprB, in addition to its role in stabilizing the T9SS apparatus.

Materials and Methods

Bacterial strains, plasmids, and growth conditions. *F. johnsoniae* ATCC 17061 strain UW101, was the wild-type strain used in this study. *F. johnsoniae* strains were grown in Casitone-yeast extract (CYE) medium at 30^{o}C, as previously described (12). To observe colony spreading, *F. johnsoniae* was grown at 25^{o}C on PY2 medium supplemented with 10 g of agar per L (2). Motility medium (MM) was used to observe movement of individual cells in wet mounts (9). Strains and plasmids used in this study are listed in Table 10, and primers used in this study are listed in Table 11. The plasmids used for complementation were all derived from pCP1 and have copy numbers of approximately 10 in *F. johnsoniae* (2, 8, 12). Antibiotics were used at the following concentrations when needed: ampicillin, 100 μg/ml; cefoxitin, 100 μg/ml; erythromycin, 100 μg/ml; kanamycin, 35 μg/ml; and tetracycline, 20 μg/ml.

Construction of truncated GldJ mutant. pMM317, pAB31 and pMM318 (Table 10) were transferred into UW102-55 which contains a frameshift mutation after amino acid 29 of GldJ (figure 43). pMM317 and pMM318 carry *gldJ* sequence that results in truncated versions of GldJ, with the 1st 337 and 547 amino acids respectively (4). To generate the plasmid pAB31, *gldJ* was amplified using Phusion DNA polymerase (New England Biolabs, Ipswich, MA) and primer 1360 (introducing a BamHI site) and primer 1361 (introducing TAA sequence and a SphI site after 1626 bp of *gldJ*). The product was digested with BamHI and SphI and inserted into pCP23 that had been digested with the same enzymes. GldJ point mutant UW102-81 and UW102-55 carrying pAB31 encode the same length of GldJ.

Immunodetection of GldA, GldJ and GldK. Wild type and mutant cells of *F. johnsoniae* were grown to mid-log phase in CYE at 25°C. Cells were washed twice in distilled water by centrifugation at 4,000 x g, and were lysed by incubation for 5 min at 100°C in SDS-PAGE loading buffer. Proteins (15 μg per lane) were separated by SDS–PAGE and Western blotting was performed as described previously (19).

Analysis of wild type and mutant cells for production and secretion of SprB Cells were grown to mid exponential phase in CYE medium at 25°C. Secretion of SprB was examined essentially as previously described (19, 22). Briefly, cells were grown to mid exponential phase in MM medium at 25°C. Purified anti-SprB (1 μl of a 1:10 dilution of a 300-mg/L stock), 0.5-mm-diameter Protein G-coated polystyrene spheres (1 μl of a 0.1% stock preparation; Spherotech Inc., Libertyville, IL), and bovine serum albumin (BSA) (1 μl of a 1% solution) were added to 7 μl of cells (approximately 5 x 10^8 cells per ml) in MM. The cells were introduced into a tunnel slide and examined by phase-contrast microscopy at 25°C. Samples were examined 2 min after spotting, and images were recorded for 30 s to determine the % of cells that had anti-SprB-coated spheres attached to them.

Measurement of chitin utilization. The ability of *F. johnsoniae* to utilize chitin was assayed as described previously (19). *F. johnsoniae* cells were grown overnight in MM media without shaking at 25°C. 2 μl of cells were spotted on MYA-chitin containing appropriate antibiotics and plates were incubated for 2.5 days.

Results

Disruption of *gldA*, *gldB*, *gldD*, *gldF*, *gldG*, *gldH*, *gldI* and *gldJ* results in dramatically reduced levels of GldK. Bioinformatics analysis shows that *gldA*, *gldD* *gldF*, *gldG*, *gldI* and *gldJ* genes are not present in most nonmotile members of the phylum *Bacteroidetes* (14). Some of these nonmotile bacteriodetes, such as *P. gingivalis* have functional T9SSs. The presence of GldA, GldD, GldF, GldG, GldI and GldJ in motile members of the phylum *Bacteroidetes* hints at their involvement in the process of gliding motility. GldB and GldH are present in all motile, some non motile and also in some members of the phylum *Bacteroidetes* which do not have T9SSs (14) and Figure 7 chapter 1. It is possible that GldB and GldH have different roles than GldA, GldD, GldF, GldG, GldI and GldJ. *F. johnsoniae* GldA, GldB, GldD, GldF, GldG, GldH, GldI and GldJ are required for motility, chitin utilization and for infection by bacteriophages. Since mutations in known T9SS genes result in the same phenotypes, this suggests that GldA, GldB, GldD, GldF, GldG, GldH, GldI and GldJ are needed for T9SS function. Why these motility proteins are important for T9SS function has been a mystery. Levels of T9SS proteins GldK, GldL, GldM and GldN were examined by immunodetection in wild type and mutant cells. GldK levels were dramatically reduced in cells with mutations in *gldA*, *gldB*, *gldD*, *gldF*, *gldG*, *gldH*, *gldI* or *gldJ* (Figure 40A). GldL and GldM levels were found to be the same as wild type in these strains (Figure 40B, C). Since *gldL* and *gldM* are cotranscribed with *gldK* (Shrivastava et al. in review) this indicates that the reduced GldK levels are not the result of decreased transcription of the *gldKLMN* operon. GldN levels were partially reduced as compared to the wild type (Figure 40D). Decreased GldN

levels were previously reported for *gldK* mutants (Figure 21, chapter 3, and Shrivastava et al. in review) and are thought to be the result of instability of GldN in the absence of GldK.

GldJ levels are dramatically reduced in *gldA*, *gldB*, *gldD*, *gldF*, *gldG*, *gldH* and *gldI* mutant cells (4). In contrast, mutations in *gldK*, *gldL*, *gldM* or *gldN* have no effect on GldJ levels (3). The *gldJ* mRNA levels in cells with mutations in *gldA*, *gldB*, *gldD*, *gldF*, *gldG*, *gldH* and *gldI* were similar to those in wild type cells (4). For these reasons it was proposed that GldA, GldB, GldD, GldF, GldG, GldH and GldI are required for the stability of GldJ. *gldK* mRNA was detected in a *gldJ* mutant (data not shown). The dramatically reduced levels of GldK and low levels of GldN in *gldA*, *gldB*, *gldD*, *gldF*, *gldG*, *gldH*, *gldI* and *gldJ* mutant strains suggest a domino effect in which GldJ is required for the stability of GldK, which is required for full stability of GldN.

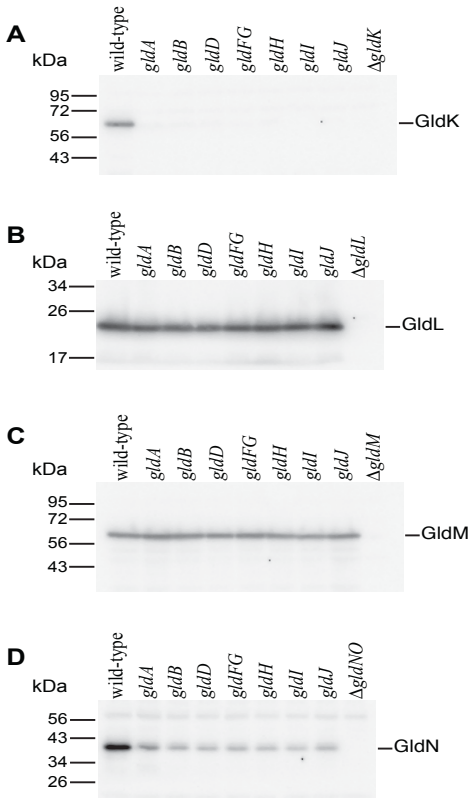

Figure 40. Immunodetection of GldK (A), GldL (B), GldM (C) and GldN (D) in cells of wild-type and mutant *F. johnsoniae* strains. Cell extracts (15 μg of protein) of wild type (CJ1356), *gldA* mutant (UW101-288), *gldB* mutant (CJ569), *gldD* mutant (CJ282), *gldFG* double mutant (CJ787), *gldH* mutant (CJ1043), *gldI* mutant (UW102-41) and *gldJ* mutant (UW102-80). *gldK* mutant (CJ2122), *gldL* mutant (CJ2157), *gldM* mutant (CJ2262) and *gldN* mutant (CJ2090) were used as controls in panel A, B, C and D respectively.

Point mutations that alter the active site of GldA lead to loss of GldK protein and defects in secretion. *gldA* is predicted to encode the ATP binding component of an ATP-binding-cassette (ABC) transporter. The membrane proteins GldF and GldG are also components of this putative transporter (3). Knockout mutants in *gldA* are completely deficient in motility and secretion (1). The exact role of this complex in

motility is not known. It may transport some molecule across the cytoplasmic membrane, into or out of the cell.

F. johnsoniae strains with spontaneous and chemically induced point mutations in *gldA* were examined to determine whether GldA has a central role in motility, in protein secretion, or both. We found two nonmotile mutants (UW102-168 and UW102-9) that had point mutations in *gldA* and made wild-type levels of full length GldA as detected by western blotting. UW102-9 has a **G40R** substitution in the highly conserved predicted ATP binding site whereas UW102-168 has a **R136C** mutation in the conserved ABC transporter signature sequence (LSGG motif). GldA has the sequence **LSKGYRQR** which is described as the ABC transporter signature sequence based on NCBI BLAST analysis**. R136** is highlighted in red and is conserved in some sequences while in others it is replaced by another positively charged amino acid, **K.** Both mutants (UW102-168 and UW102-9) were nonmotile. GldA protein was present at the same level as wild-type in both mutants but GldJ and GldK levels were dramatically reduced (Figure 41). These results suggest that not only is GldA protein required to stabilize GldJ and GldK, but the function of GldA is also necessary for the stability of GldJ and GldK. We do not yet know what the relevant function of GldA is, but it presumably binds to and hydrolyzes ATP, and disruption of this activity results in defects in gliding and in protein secretion.

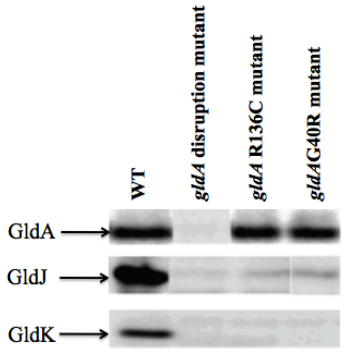

Figure 41. Immunodetection of GldA, GldJ and GldK in wild-type cells and in cells of strains with mutations in *gldA*. Lane1, WT UW101. Lane2, *gldA* disruption mutant CJ288. Lane3, *gldA* R136C mutant UW102-9. Lane4, *gldA* G40R mutant UW102-168.

GldK is present in cells expressing a C-terminal truncated version of GldJ.

To study the role of GldJ in the stability of GldK, strains with truncated GldJ were generated. Plasmid pAB31 which carries a DNA fragment that encodes the 1st 542 amino acids of GldJ was generated. pAB31 and UW102-81 (*gldJ* point mutant) encode the same length GldJ (Figure 42). Plasmid pMM317 and pMM318 which carry the sequence to encode the 1st 337 and 547 amino acids of GldJ respectively have been described previously (4). pAB31, pMM317 and pMM318 were transferred by conjugation into the *gldJ* null mutant, UW102-55.

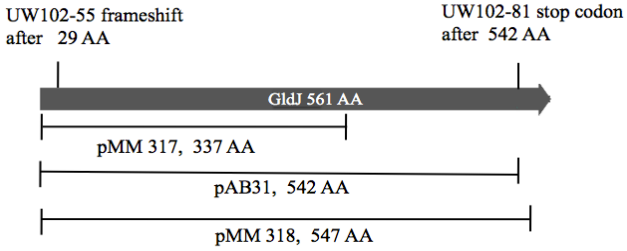

Figure 42. Map of GldJ. plasmids pMM317, pAB31 and pMM318 encode 337, 542 and 547 amino acids of GldJ respectively.

Strains with truncated GldJ were examined for the presence of GldJ and GldK. Immunoblot analysis showed that GldJ and GldK levels were dramatically reduced in cells of UW102-55 and UW102-81 as compared to the wild type. Similarly, UW102-55 cells carrying pMM317 and pAB31, which should make truncated versions of GldJ of 337 and 542 amino acids respectively, also had little if any detectable GldJ and GldK. In contrast, almost wild type levels of GldJ and GldK were observed for UW102-55 carrying pMM318 (Figure 43 and data not shown). pMM318 carries a *gldJ* sequence that encodes 5 more amino acids than pAB31. It appears that these 5 amino acids are important for stabilizing both GldJ and GldK.

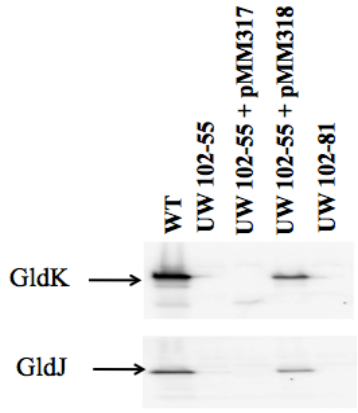

Figure 43. Immunodetection of GldJ and GldK in wild-type cells and in cells of strains with truncated GldJ.

Cells expressing C-terminal truncated versions of GldJ are competent for protein secretion but not for motility. Restoration of GldK to near wild type levels in UW102-55 carrying pMM318 indicated that secretion via the T9SS might be restored in this strain. Anti-SprB antisera-coated polystyrene spheres attached to cells of UW102-55

carrying pMM318 indicating that SprB was on the cell-surface (Figure 44A). Cells of UW102-55 carrying pMM318 were also able to digest chitin (Figure 44C). These results indicate a functional T9SS. However, contrary to the wild type strain the bound anti-SprB antisera-coated polystyrene spheres did not move along the cell surface (data not shown). Also, UW102-55 carrying pMM318 did not form spreading colonies when plated on PY2 agar. These results indicate that the C-terminal 14 amino acids of GldJ are important for movement of SprB on the cell surface, and thus for gliding motility.

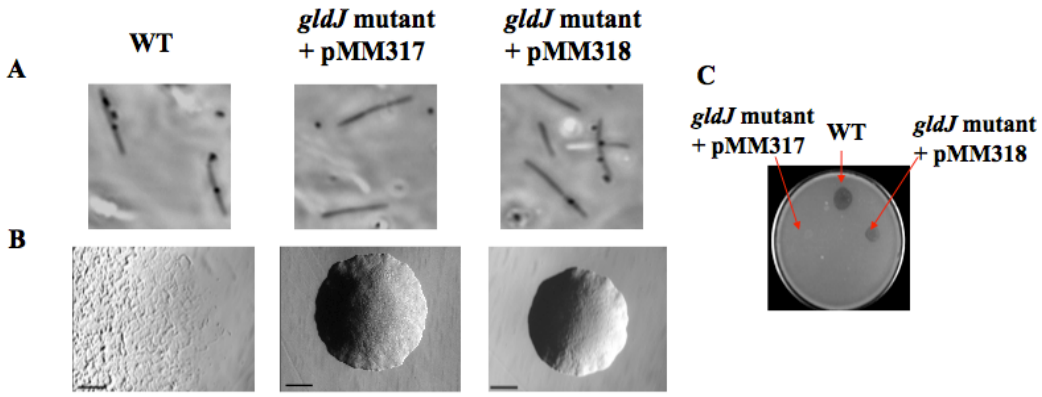

Figure 44. Effect of truncated GldJ on secretion and motility. (A) Microscopic images of cells showing binding of anti-SprB-coated polystyrene spheres. Wild type cells bound and propelled the spheres from pole to pole at 2-4 µm/sec. Cells of *gldJ* mutant UW102-55 (not shown), and cells of UW102-55 with truncated GldJ (1st 337 amino acids expressed from pMM317) failed to bind the spheres, indicating that SprB was not on the cell surface. Cells with UW102-55 with truncated GldJ, expressing the 1st 547 amino acids (pMM318) bound the spheres but did not propel them. SprB was on the cell surface but the motility machinery was not functional.

(B) Colony pictures showing spreading on PY2 agar; incubated 36 h at 25°C. Bar = 0.5 mm. Wild type cells form spreading colonies while cell of the the *gldJ* mutant UW102-55 carrying either pMM317 or pMM318 form non spreading colonies.

(C) Cells of the *gldJ* mutant UW102-55 with truncated GldJ (1st 547 amino acids of GldJ expressed from pMM318) utilize chitin while cells of UW102-55 with pMM317 do not utilize chitin. Approximately 10^6 cells were spotted on chitin agar and incubated at 25°C for 48 h.

Bioinformatic analysis of the C-terminal region of *gldJ*. Comparative analysis of GldJ across 22 members of the phylum *Bacteroidetes* shows that it has a highly conserved 'IGFRCAM' sequence near the C-terminus. pMM318 encodes the 1st 547 amino acids of GldJ including the 'IGFRCAM' sequence while pAB31 encodes the 1st 542 amino acids of GldJ terminating after 'IGF' which disrupts this region. The nonmotile mutant UW102-81, which does not produce stable GldJ protein, has a stop codon that terminates GldJ after 'IGF' (Figure 42 and 45). This indicates that the 'IGFRCAM' sequence may be important for the stability of both GldJ and GldK in the cell. In the C-terminal region of GldJ, V549, G550, K557 and R560 are also highly conserved and these amino acids might play important roles in the movement of SprB on the cell surface (Figure 45).

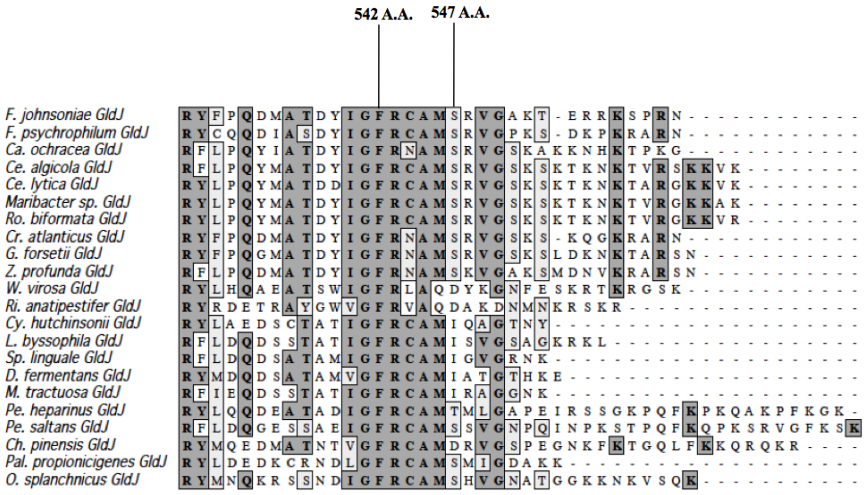

Figure 45. ClustalW alignment of C-terminal regions of GldJ proteins from 22 members of the phylum *Bacteroidetes*.

Discussion

The *F. johnsoniae* gliding motility and T9SSs appear to be intertwined. Our results suggest that GldA, GldB, GldD, GldF, GldG, GldH and GldI stabilize GldJ which in turn stabilizes GldK (Figure 46). Our results also show that the ATP binding site of GldA is important for the stability of GldJ and GldK. The function of GldA in motility is not entirely known. *F. johnsoniae* movement is dependent on the proton motive force (17) and Nakane et al unpublished, so it is unlikely that GldA performs a 'motor' function. It is possible that its entire role in motility is to stabilize GldJ. Recently it has been shown that two members of the phylum *Bacteroidetes*, *Cellulophaga algicola* and *Maribacter* sp. HTCC2170, do not have the gliding motility related ABC transporter proteins GldA, GldF and GldG. Both *C. algicola* and *Maribacter sp.* have the ability to glide (14). The ability of these two bacteria to glide without GldA, GldF and GldG can be explained in two ways. The first possibility is that *F. johnsoniae* GldA, GldF and GldG transport currently unknown cargo that is required to stabilize GldJ and GldK, but that in *C. algicola* and *Maribacter* sp. HTCC2170 GldJ is stable without this assistance. Alternatively, *C. algicola* and *Maribacter* sp. HTCC2170 might have proteins that replace the missing GldA, GldF and GldG. Both *C. algicola* and *Maribacter* sp. HTCC2170 have genes that encode other ABC transporters. It is possible that one of these transporters plays a role in stabilizing GldJ and the T9SS. Besides transporting unknown cargo, GldA, GldF and GldG might also have structural roles in stabilizing GldJ. It is possible that GldA, GldB, GldD, GldF, GldG, GldH and GldI interact with GldJ to form a complex that is involved in the movement of SprB and in gliding. Loss of

any of the interacting partners might expose GldJ to unknown proteases that result in GldJ instability. Our results show that the C-terminal region of GldJ is critical for movement of SprB and for motility. Our results also show that GldJ is needed to stabilize the T9SS protein GldK and that GldK is needed to stabilize GldN. This domino effect may explain the pleiotropic effects that result from mutations in *gldA, gldB, gldD, gldF, gldG, gldH, gldI* and *gldJ* and explain the link between motility and secretion.

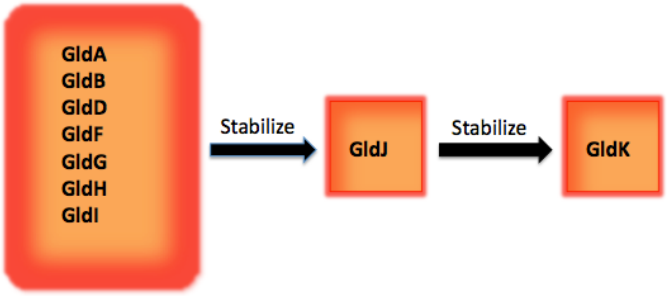

Figure 46. Proposed effect of Gld proteins for stability of GldJ and GldK

Table 10. Strains and plasmids used in this study.

Strains	**Genotype and Description**[a]	**Source or reference**
UW101 (ATCC 17061)	Wild type	(10, 13)
UW102-55	*gldJ* mutant	(4)
UW102-81	*gldJ* mutant	(4)
CJ288	*gldA* mutant	(2)
UW102-9	*gldA* mutant	(2)
UW102-168	*gldA* mutant	(19)
CJ569	*gldB* mutant	(4)
CJ282	*gldD* mutant	(4)
CJ787	*gldFG* double mutant	(4)
CJ1043	*gldH* mutant	(4)
UW102-41	*gldI* mutant	(4)
UW102-80	*gldJ* mutant	(4)
CJ1827	*rpsL2*; (Sm^r) 'wild-type' strain used in construction of deletion mutants	(18)
CJ2122	*rpsL2* Δ*gldK*	Shrivastava et al. in review
CJ2157	*rpsL2* Δ*gldL*	Shrivastava et al. in review

CJ2262	*rpsL2* Δ*gldM*	Shrivastava et al. in review
CJ2090	*rpsL2* Δ*gldNO*	(22)
Plasmids		
pCP11	*E. coli-F. johnsoniae* shuttle plasmid; Ap^r (Em^r)	(4)
pCP23	*E. coli-F. johnsoniae* shuttle plasmid; Ap^r $(Tc)^r$	(2)
pMM317	Fragment encoding the 1st 337 amino acids of GldJ inserted in pCP11; Ap^r (Em^r)	(4)
pMM318	Fragment encoding the 1st 547 amino acids of GldJ inserted in pCP11; Ap^r (Em^r)	(4)
pAB31	Fragment encoding the 1st 542 amino acids of GldJ inserted in pCP23. Primer 1360/1361 were used to construct pAB31; Ap^r (Tc^r)	This study

[a]Antibiotic resistance phenotypes: ampicillin, Ap^r; erythromycin, Em^r; streptomycin, Sm^r; tetracycline, Tc^r. Unless indicated otherwise, the antibiotic resistance phenotypes are those expressed in *E. coli*. The antibiotic resistance phenotypes given in parentheses are those expressed in *F. johnsoniae* but not in *E. coli*.

Table 11. Primers used in this study.

Primer	Sequence and description
1360	5' GCTAGGGATCCGAAGCGGAAACCATCTCCTG 3', used to construct pAB31. BamHI site underlined.
1361	5' GCTAGGCATGCTTAGAAACCTATGTAATCAGTTGCCAT 3', used to construct pAB31. SphI site underlined.

References

1. **Agarwal, S., D. W. Hunnicutt, and M. J. McBride.** 1997. Cloning and characterization of the Flavobacterium johnsoniae (Cytophaga johnsonae) gliding motility gene, gldA. Proc Natl Acad Sci U S A **94:**12139-12144.
2. **Agarwal, S., D. W. Hunnicutt, and M. J. McBride.** 1997. Cloning and characterization of the *Flavobacterium johnsoniae* (*Cytophaga johnsonae*) gliding motility gene, *gldA*. Proc. Natl. Acad. Sci. USA **94:**12139-12144.
3. **Braun, T. F., M. K. Khubbar, D. A. Saffarini, and M. J. McBride.** 2005. *Flavobacterium johnsoniae* gliding motility genes identified by *mariner* mutagenesis. J. Bacteriol. **187:**6943-6952.
4. **Braun, T. F., and M. J. McBride.** 2005. *Flavobacterium johnsoniae* GldJ is a lipoprotein that is required for gliding motility. J. Bacteriol. **187:**2628-2637.
5. **Hunnicutt, D. W., M. J. Kempf, and M. J. McBride.** 2002. Mutations in *Flavobacterium johnsoniae gldF* and *gldG* disrupt gliding motility and interfere with membrane localization of GldA. J. Bacteriol. **184:**2370-2378.
6. **Hunnicutt, D. W., and M. J. McBride.** 2001. Cloning and characterization of the *Flavobacterium johnsoniae* gliding motility genes *gldD* and *gldE*. J. Bacteriol. **183:**4167-4175.
7. **Hunnicutt, D. W., and M. J. McBride.** 2000. Cloning and characterization of the *Flavobacterium johnsoniae* gliding motility genes, *gldB* and *gldC.* J. Bacteriol. **182:**911-918.
8. **Kempf, M. J., and M. J. McBride.** 2000. Transposon insertions in the *Flavobacterium johnsoniae ftsX* gene disrupt gliding motility and cell division. J. Bacteriol. **182:**1671-1679.
9. **Liu, J., M. J. McBride, and S. Subramaniam.** 2007. Cell-surface filaments of the gliding bacterium *Flavobacterium johnsoniae* revealed by cryo-electron tomography. J. Bacteriol. **189:**7503-7506.
10. **McBride, M. J., and T. F. Braun.** 2004. GldI is a lipoprotein that is required for *Flavobacterium johnsoniae* gliding motility and chitin utilization. J. Bacteriol. **186:**2295-2302.
11. **McBride, M. J., T. F. Braun, and J. L. Brust.** 2003. *Flavobacterium johnsoniae* GldH is a lipoprotein that is required for gliding motility and chitin utilization. J. Bacteriol. **185:**6648-6657.
12. **McBride, M. J., and M. J. Kempf.** 1996. Development of techniques for the genetic manipulation of the gliding bacterium *Cytophaga johnsonae*. J. Bacteriol **178:**583-590.
13. **McBride, M. J., G. Xie, E. C. Martens, A. Lapidus, B. Henrissat, R. G. Rhodes, E. Goltsman, W. Wang, J. Xu, D. W. Hunnicutt, A. M. Staroscik, T. R. Hoover, Y. Q. Cheng, and J. L. Stein.** 2009. Novel features of the polysaccharide-digesting gliding bacterium *Flavobacterium johnsoniae* as revealed by genome sequence analysis. Appl. Environ. Microbiol. **75:**6864-6875.

14. **McBride, M. J., and Y. Zhu.** 2013. Gliding motility and Por secretion system genes are widespread among members of the phylum *Bacteroidetes*. J. Bacteriol. **195:**270-278.
15. **Nelson, S. S., S. Bollampalli, and M. J. McBride.** 2008. SprB is a cell surface component of the *Flavobacterium johnsoniae* gliding motility machinery. J. Bacteriol. **190:**2851-2857.
16. **Nelson, S. S., P. P. Glocka, S. Agarwal, D. P. Grimm, and M. J. McBride.** 2007. *Flavobacterium johnsoniae* SprA is a cell-surface protein involved in gliding motility. J. Bacteriol. **189:**7145-7150.
17. **Pate, J. L., and L.-Y. E. Chang.** 1979. Evidence that gliding motility in prokaryotic cells is driven by rotary assemblies in the cell envelopes. Curr. Microbiol. **2:**59-64.
18. **Rhodes, R. G., H. G. Pucker, and M. J. McBride.** 2011. Development and use of a gene deletion strategy for *Flavobacterium johnsoniae* to identify the redundant motility genes *remF*, *remG*, *remH*, and *remI*. J. Bacteriol. **193:**2418-2428.
19. **Rhodes, R. G., M. N. Samarasam, A. Shrivastava, J. M. van Baaren, S. Pochiraju, S. Bollampalli, and M. J. McBride.** 2010. *Flavobacterium johnsoniae gldN* and *gldO* are partially redundant genes required for gliding motility and surface localization of SprB. J. Bacteriol. **192:**1201-1211.
20. **Rhodes, R. G., M. N. Samarasam, E. J. Van Groll, and M. J. McBride.** 2011. Mutations in *Flavobacterium johnsoniae sprE* Result in Defects in Gliding Motility and Protein Secretion. Journal of bacteriology **193:**5322-5327.
21. **Sato, K., M. Naito, H. Yukitake, H. Hirakawa, M. Shoji, M. J. McBride, R. G. Rhodes, and K. Nakayama.** 2010. A protein secretion system linked to bacteroidete gliding motility and pathogenesis. Proc. Natl. Acad. Sci. USA **107:**276-281.
22. **Shrivastava, A., R. G. Rhodes, S. Pochiraju, D. Nakane, and M. J. McBride.** 2012. *Flavobacterium johnsoniae* RemA is a mobile cell-surface lectin involved in gliding. J. Bacteriol. **194:**3678-3688.

Appendix 1. PorX, PorY and PorQ have no apparent roles in gliding motility or T9SS mediated secretion of *F. johnsoniae*.

P. gingivalis PorX is predicted to be a bacterial two component response regulator and has a CheY like domain. *P. gingivalis* PorY is predicted to be a bacterial two-component sensor and has a Histidine Kinase A domain. *P. gingivalis* PorX and PorY are thought to be 'orphan' signal transduction proteins because the expected cognate partners do not appear to be encoded by nearby genes in either case. It is thought that PorX and PorY function together as a two-component signal transduction system. Microarray and qRT-PCR analysis showed that T9SS genes were downregulated in *P. gingivalis* strains with mutations in either *porX* or *porY* (2). It is not known whether *F. johnsoniae* T9SS and gliding motility machinery are regulated by a two-component signal transduction system. In fact, nothing is known regarding regulation of motility or T9SS genes in *F. johnsoniae*. Homologs of *P. gingivalis porX* (Fjoh_2906) and *porY* (Fjoh_1592) are present in *F. johnsoniae* but the functions of these genes are not known.

P. gingivalis PorQ is a putative T9SS protein. *P. gingivalis* strains with mutations in *porQ* are partially defective in T9SS mediated gingipain secretion (2). A homolog of *P. gingivalis porQ* (Fjoh_2755) is present in the *F. johnsoniae* genome. Fjoh_2755 also has about 26% identity with Fjoh_0288 which is a gene upstream of a large polysaccharide biosynthetic cluster. However, *P. gingivalis porQ* and Fjoh_0288 do not have regions of similarity.

To probe the function of *F. johnsoniae porX, porY* and *porQ*, strains with in-frame deletions were generated using a gene deletion method described previously (1). Briefly,

approximately 2 kbp regions upstream and downstream of *porX* were amplified by primer pairs 1081/1082 and 1083/1084 respectively and ligated into BamHI-SalI digested pRR51 to generate pAB13. pAB13 was transferred into streptomycin resistant wild-type strain CJ1827 by triparental conjugation, and the *porX* deletion mutant was isolated as described previously (1). *F. johnsoniae porY* and *porQ* were deleted in a similar way using the plasmids and primers listed in Tables 12 and 13.

F. johnsoniae Δ*porX,* Δ*porY* and Δ*porQ* strains were analysed for their ability to move on agar and glass surfaces. Δ*porX,* Δ*porY* and Δ*porQ* strains formed thin spreading colonies on PY2 agar similar to wild-type *F. johnsoniae* (Figure 47). Cells of Δ*porX,* Δ*porY* and Δ*porQ* strains also attached to and moved on glass surfaces similar to wild-type cells (data not shown).

F. johnsoniae Δ*porX,* Δ*porY* and Δ*porQ* strains were also assayed for their ability to utilize chitin. Δ*porX,* Δ*porY* and Δ*porQ* strains were able to digest chitin similar to wild-type *F. johnsoniae* (Figure 48).

Since no defects in motility or secretion were observed for Δ*porX,* Δ*porY* and Δ*porQ* strains, it appears that *F. johnsoniae* PorX and PorY might not regulate expression of T9SS or motility genes. Also, it appears that *F. johnsoniae* PorQ does not have a significant role in motility or T9SS mediated protein secretion.

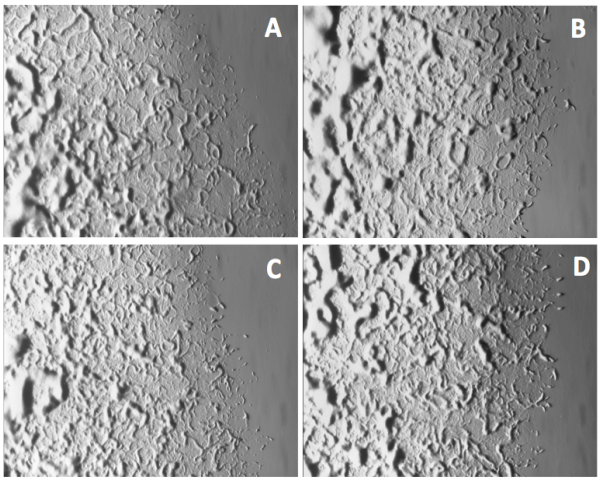

Figure 47. Photomicrographs of *F. johnsoniae* colonies. Colonies were incubated at 25°C on PY2 agar for 36 h. Photomicrographs were taken with a Photometrics Cool-SNAPcf ^{2} camera mounted on an Olympus IMT-2 phase-contrast microscope. (A) Wild-type *F. johnsoniae* CJ1827 (B) CJ2039 (Δ*porX*) (C) CJ2020 (Δ*porY*) (D) CJ2092 (Δ*porQ*)

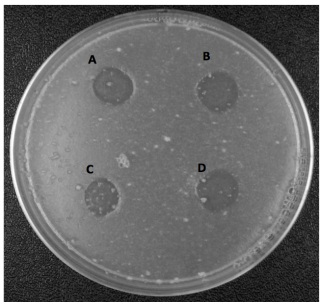

Figure 48. PorX , PorY and PorQ are not required for chitin utilization. Approximately 4 x 10^7 cells of *F. johnsoniae* were spotted on MYA-chitin medium and incubated at 25°C for 36 h. (A) Wild-type *F. johnsoniae* UW101 (B) CJ2039 (Δ*porX*) (C) CJ2020 (Δ*porY*) (D) CJ2092 (Δ*porQ*)

Table 12. Strains and plasmids used in this study.

***F. johnsoniae* Strains**	**Genotype and Description**	**Source or reference**
CJ1827	*rpsL2*; (Sm^r) 'wild-type' strain used in construction of deletion mutants	(1)
CJ2039	*rpsL2* Δ*porX*; (Sm^r)	This study
CJ2020	*rpsL2* Δ*porY*; (Sm^r)	This study
CJ2092	*rpsL2* Δ*porQ*; (Sm^r)	This study
Plasmids		
pRR51	*rpsL*-containing suicide vector; Ap^r (Em^r)	(1)
pAB08	1.6 kbp region upstream of *porY* amplified with primer pair 1045-1046 and cloned into BamHI-XbaI site of pRR51	This study
pAB09	1.8 kbp region downstream of *porY* amplified with primer pair 1047-1048 and cloned into XbaI-SphI site of pRR51	This study
pAB10	Construct to delete *porY*. 1.6 kbp region upstream of *porY* cut from pAB08 and cloned into BamHI-XbaI site of pAB09	This study
pAB12	2.1 kbp region upstream of *porX* was amplified with primer pair 1081-1082 and cloned into BamHI-XbaI site of pRR51	This study
pAB13	Construct to delete *porX*. 1.9 kbp region upstream of *porX* was amplified with primer pair 1083-1084 and cloned into XbaI-SalI site of pAB12	This study
pAB14	1.8 kbp region upstream of *porQ* was amplified with primer pair 1106-1107 and cloned into BamHI-XbaI site of pRR51	This study
pAB15	Construct to delete *porQ*. 1.8 kbp region downstream of *porQ* was amplified with primer pair 1108-1109 and cloned into XbaI-SalI site of pAB12	This study

Table 13. Primers used in this study

Primers	Sequence and Description
1045	5’ GCTAGGGATCCCCGCTCTGGATCTAAATCGC 3’ primer used to construct pAB08. BamHI site underlined
1046	5’ GCTAGTCTAGATATTTCTACTTTCAGAAAAGCGCAT 3’ primer used to construct pAB08. XbaI site underlined
1047	5’ GCTAGTCTAGAGGAAAAGGAACTACGTTTCAGATT 3’ primer used to construct pAB08. XbaI site underlined
1048	5’ GCTAGGCATGCCCAGAAGCCAAACTGGCAG 3’ primer used to construct pAB08. SphI site underlined
1081	5’ GCTAGGGATCCCGTTGCCAATCTGTGGCAC 3’ primer used to construct pAB12. BamHI site underlined
1082	5’ GCTAGTCTAGAGACCCAAAGTATTCTTATCTTATCCAT 3’ primer used to construct pAB12. XbaI site underlined
1083	5’ GCTAGTCTAGACCGTTTTTGGTATTTAACCCTAAATAA 3’ primer used to construct pAB13. XbaI site underlined
1084	5' GCTAGGTCGACTACAGCTGGATAAGAACCATCTTCATC 3' primer used to construct pAB13. SalI site underlined
1106	5’ GCTAGGGATCCAACCATTCAGGAAGAATTGGG 3’ primer used to construct pAB14. BamHI site underlined
1107	5’ GCTAGTCTAGAAACATAGTGTTTTAACATTCGTTTTGG 3’ primer used to construct pAB14. XbaI site underlined
1108	5’ GCTAGTCTAGAGGGTTGGTTTTAAACCTTCAATAA 3’ primer used to construct pAB15. XbaI site underlined
1109	5’ GCTAGGTCGACCTTGTGAAATCGACATAATAATAGTCG 3’ primer used to construct pAB15. SalI site underlined

References

1. **Rhodes, R. G., H. G. Pucker, and M. J. McBride.** 2011. Development and use of a gene deletion strategy for *Flavobacterium johnsoniae* to identify the redundant motility genes *remF*, *remG*, *remH*, and *remI*. J. Bacteriol. **193:**2418-2428.
2. **Sato, K., M. Naito, H. Yukitake, H. Hirakawa, M. Shoji, M. J. McBride, R. G. Rhodes, and K. Nakayama.** 2010. A protein secretion system linked to bacteroidete gliding motility and pathogenesis. Proc. Natl. Acad. Sci. USA **107:**276-281.

Appendix 2. Construction of *F. johnsoniae* polysaccharide biosynthesis/transport gene mutants

F. johnsoniae cells with transposon mediated mutations in the genes that encode for polysaccharide biosynthesis and export proteins RemC, Wza and Wzc are defective in cell-aggregation (3) and (Figure 18 chapter 2). Interaction between cell-surface adhesin RemA and exopolysaccharide causes cell-aggregation (3). Cells with mutations in *remC*, *wza* and *wzc* in a Δ*sprBCD* background are defective in motility as compared with the parent Δ*sprBCD* strain. However, cells with mutations in *remC*, *wza* and *wzc* in a wild-type background do not exhibit motility defects (1). Also, the phage phenotype of cells with mutations in *remC*, *wza* and *wzc* in a wild-type background is similar to that of wild-type cells (1).

remC was disrupted in wild-type CJ1827 and in Δ*sprB* background strains of *F. johnsoniae* (Table 1). Cells of *remC* disruption in Δ*sprB* background are almost nonmotile on glass (data not shown). Δ*sprB* mutant cells are sensitive to infection by *F. johnsoniae* bacteriophages ϕCj28, ϕCj29, ϕCj42, ϕCj48 and ϕCj54. *remC* disruption mutant cells in Δ*sprB* background were resistant to infection by bacteriophages ϕCj28 and ϕCj29 (data not shown). The motility defect and phage pattern of the Δ*sprB remC* strain was similar to what was previously reported for a strain with a *remC* transposon insertion a in Δ*sprBCD* background (3). To probe if RemC plays a role in cell-surface localization of RemA, *remC* disruption mutant in a *remA-myc-tag-1* background was generated (Table 14). Anti-myc antibody-coated polystyrene spheres were used to probe the presence of RemA on the cell surface. Anti-myc antibody-coated polystyrene spheres

attached to cells indicating the presence of RemA on the cell surface. The spheres moved rapidly along the cell surface, indicating that RemA was propelled by the motility machinery in the mutant, just as it is in wild type cells (data not shown). Similarly, *wzc* was also deleted in various mutant backgrounds. More experiments are needed to study the phenotype of strains with *wzc* mutants.

Table 14. Strains and plasmid used in this study

Strain	Description	Reference
CJ1827	*rpsL2*; (Sm^r) 'wild-type' strain used in construction of deletion mutants	(2)
CJ1922	*rpsL2* Δ*sprB*; (Sm^r)	(2)
CJ2083	*rpsL2 remA::myc-tag-1*; (Sm^r)	(3)
CJ1999	*rpsL2* Δ*wzc* (Sm^r)	This study
CJ2072	*rpsL2* Δ*sprB* in CJ2083 background (Sm^r)	This study
CJ2261	*remC* disruption in CJ1827 background (Em^r Sm^r)	This study
CJ2264	*remC* disruption in CJ1922 background (Em^r Sm^r)	This study
CJ2259	*remC* disruption in CJ2083 background (Em^r Sm^r)	This study
CJ2142	*rpsL2* Δ*remA* Δ*wzc* (Sm^r)	This study
CJ2143	*rpsL2* Δ*remA* Δ*sprB* Δ*wzc* (Sm^r)	This study
CJ2144	*rpsL2* Δ*remA* Δ*sprB* Δ*fjoh_803-806* Δ*wzc* (Sm^r)	This study
CJ2111	Δ*wzc* in CJ2083 background (Sm^r)	This study
CJ2118	Δ*wzc* in CJ2072 background (Sm^r)	This study

References.

1. **Bollampalli, S.** 2011. Role of cell surface polysaccharides and proteins in Flavobacterium johnsoniae gliding motility
   Bollampalli, Sreelekha. PhD Thesis. University of Wisconsin-Milwaukee, Milwaukee.
2. **Rhodes, R. G., H. G. Pucker, and M. J. McBride.** 2011. Development and use of a gene deletion strategy for *Flavobacterium johnsoniae* to identify the redundant motility genes *remF*, *remG*, *remH*, and *remI*. J. Bacteriol. **193:**2418-2428.
3. **Shrivastava, A., R. G. Rhodes, S. Pochiraju, D. Nakane, and M. J. McBride.** 2012. *Flavobacterium johnsoniae* RemA is a mobile cell-surface lectin involved in gliding. J. Bacteriol. **194:**3678-3688.

CURRICULUM VITAE

Personal :

Name : Abhishek Shrivastava
Address : Department of Biological Sciences,
UW-Milwaukee, 3209 N. Maryland ave,
Milwaukee, WI – 53211.

Education :

PhD : Molecular Microbiology : 2008-2013.
Department of Biological Sciences, University of Wisconsin-Milwaukee

Masters degree in Biochemistry : 2006-2008.
Department of Biochemistry, The Maharaja Sayajirao University of Baroda, Gujarat, India

Undegraduate degree : 2003-2006
Major : Biotechnology
Sardar Patel University, Gujarat, India.

Publications :

1. *Flavobacterium johnsoniae* RemA is a mobile cell surface lectin involved in gliding.
Shrivastava A, Rhodes R.G., Nakane D, Pochiraju S and McBride M.J.
Journal of Bacteriology, 2012 Jul; 194(14):3678-88.

2. *Flavobacterium johnsoniae gldN* and *gldO* are partially redundant genes required for gliding motility and surface localization of SprB.
Rhodes R.G., Samarasan M.N., Shrivastava A, van Barren J.M., Pochiraju S, Bolampalli S and McBride M.J. **Journal of Bacteriology**, 2010 Mar; 192(5):1201-11.

3. *Flavobacterium johnsoniae* GldK, GldL, GldM, and SprA are required for secretion of the cell-surface gliding motility adhesins SprB and RemA
Shrivastava A, van Barren J.M., Johnston J.J. and McBride M.J. In review

4. Untangling *Flavobacterium johnsoniae* gliding motility and protein secretion

Shrivastava A, Johnston J.J. and McBride M.J. Manuscript in preparation.

5. Role of Polysaccharides in gliding motility of *Flavobacterium johnsoniae*.
Bollampalli S, Shrivastava A and McBride M.J. Manuscript in preparation.

Poster Presentations :

1. *Flavobacterium johnsoniae* RemA is a mobile cell surface adhesin involved in gliding.
Gordon Research Conference on Bacterial Cell Surface and Motility. June 2012.
Shrivastava A, Rhodes R.G., Nakane D, Pochiraju S and McBride M.J.

2. Novel Protein Secretion and gliding motility machineries of *Flavobacterium johnsoniae*.
Gordon Research Conference on Bacterial Cell Surface and Motility. June 2012.
Shrivastava A, Kharade S, Rhodes R.G., van Baaren J.M. and McBride M.J.

3. GldJ and GldK provide a link between Novel motility and protein secretion system of *Flavobacterium johnsoniae.*
American Society for Microbiology (ASM) 110th General meeting, May 2010.
Shrivastava A, van Baaren J.M. and McBride M.J.

4. Function of GldK as a component of PorSS of *Flavobacterium johnsoniae*.
Shrivastava A, van Baaren J.M. and McBride M.J. UW-Milwaukee Bio Sci symposium. 2010.

Invited Lectures :

1. Novel motility and protein secretion system of *Flavobacterium johnsoniae.*
Milwaukee Microbiology Society Seminar Series at Great Lakes Water Institute, UW-Milwaukee. 2012.

Awards/honors :

1. UW-Milwaukee Ruth Walker Grant in aid award. 2012, 2010
2. UW-Milwaukee Chancellors Graduate award. 2008-2012.
3. UW-Milwaukee Graduate School Travel award. 2012, 2010
5. UW-Milwaukee Department of Bio Science travel award. 2010.
6. Junior Research Fellowship and National Eligibility Test (JRF/NET) from Council for Scientific and Industrial Research (CSIR), India. 2008.

Teaching and Organizational Experience :

Trained 4 undergraduate students in independent research and mentored new graduate students at UW-Milwaukee.
Graduate Teaching Assistant, UW-Milwaukee. Courses taught :
BIO SCI 383 : General Microbiology lab. Spring 2008, Fall 2009, Fall 2010.
BIO SCI 698 : Independent Study in Microbiology. Spring 2010.
President UW-Milwaukee Badminton Club. 2010-2012
Have been actively involved in organizing and taking part in various co-curricular and sports related activities.